

# Behavior Of Bright-Dark Solitons Under Trapping Potentials

Shreya Dilipkumar Shah

In partial fulfilment of the requirements for the  
Degree of Master of Science

Department of Physics,  
National University of Singapore  
2010

# Acknowledgement

I am very much thankful to my supervisor, Prof. Li Baowen, Department of Physics, National University of Singapore, for giving me such a nice opportunity to work with him. His ideas, suggestions and encouragement have helped me a lot for doing research work and writing and preparing this project work.

I am also very much thankful to Prof. Gong Jiangbin and Dr. Xiong Bo, Department of Physics, National University of Singapore as they have given good guidance for my project work.

I am thankful to my friends Juzar and Bijay for helping me regarding computational work. I am also thankful to all my lab mates and dear friends for giving moral support during my stay at Singapore.

I am very much thankful to my parents and loving brother Archit for supporting me in my Master Project. I am also very much thankful to my grandfather for believing in me.

And at last how can I forget the Department of Physics, National University of Singapore for giving me the opportunity to do Master course. My thanks are also to all the faculty members of the department.

# Abstract

We investigate the vector-soliton solutions of two-species Bose-Einstein condensates with arbitrary scattering lengths. The results show that, for quasi-one-dimension homogeneous systems, exact solutions exist even in the regime where the nonlinear system is non-integrable. In addition, these vector solitons can be dynamically stable in the presence of soft trapping potentials. If trapping potentials are strong, then these vector solitons can be dynamically unstable. In this case, Bright and Dark solitons will be destroyed.

## Index

Chapter 1	Introduction	3
Chapter 2		
2.1	What is Soliton?	6
2.2	Solutions for Bright and Dark Solitons	8
2.3	Numerical Method to study Dynamics and Dynamical Stability for Bright and Dark Solitons	12
Chapter 3	Results and Discussion	14
3.1	Density Profiles for Different Trapping Potentials	16
3.2	Density Profiles for Special cases	54
3.3	Density Profiles for Different $b_{12}$ values	61
Chapter 4	Conclusion	74
	Scope for the future work	75

Appendix A Gross-Pitaevskii Equation	75
Appendix B Thomas-Fermi Approximation	76
References	78

# Chapter-1

## Introduction:

A Bose-Einstein condensate (BEC) is a state of matter of a dilute gas of weakly interacting bosons confined in an external potential and cooled to temperatures very near to absolute zero (0 K or -273.15° C or -459.67 ° F) [1]. Under such conditions, a large fraction of the bosons occupy the lowest quantum state of the external potential, at which point quantum effects become apparent on a macroscopic scale.

This state of matter was first predicted by Satyendra Nath Bose and Albert Einstein in 1925. Seventy years later, the first gaseous condensate was produced by Eric Cornell and Carl Wieman in 1995 at the University of Colorado at Boulder NIST-JILA lab, using a gas of Rubidium atoms cooled to 170 nanokelvin (nK). For their achievements Cornell, Wieman and Wolfgang Ketterle at MIT received the 2001 Noble Prize in Physics.

Bose-Einstein Condensates in dilute atomic gases, which were first realized experimentally in 1995 for Rubidium [2], Sodium [3], and Lithium [4], provide unique opportunities for exploring quantum phenomena on a macroscopic scale. The particle density at the centre of a Bose-Einstein condensed atomic cloud is typically  $10^{13}$ - $10^{15}$  cm<sup>-3</sup>. By contrast, the density of molecules in air at room temperature and atmospheric pressure is about  $10^{19}$  cm<sup>-3</sup>. In liquids and solids the density is of order  $10^{22}$  cm<sup>-3</sup>, while the density of nucleons in atomic nuclei is about  $10^{38}$  cm<sup>-3</sup>.

To observe quantum phenomena in such low-density systems, the temperature must be of order  $10^{-5}$  K or less. This may be contrasted with the temperatures at which quantum phenomena occur in solids and liquids. In solids, quantum effects become strong for electrons in metals below the Fermi temperature, which is typically  $10^4$ - $10^5$  K, and for phonons below the Debye temperature, which is typically of order  $10^2$  K. For the helium liquids, the temperatures required for observing quantum phenomena are of order 1 K. Due to the much higher particle density in atomic nuclei, the corresponding degeneracy temperature is about  $10^{11}$  K.

The path that led in 1995 to the first realization of Bose-Einstein condensation in dilute gases exploited the powerful methods developed over the past quarter of a century for cooling alkali metal atoms by using lasers. Since laser cooling alone cannot produce sufficiently high densities and low temperature for condensation, it is followed by an evaporative cooling stage, in which more energetic atoms are removed from the trap, thereby cooling the remaining atoms. Cold gas clouds have many advantages

for investigations of quantum phenomena. A major one is that in the Bose-Einstein condensate, essentially all atoms occupy the same quantum state, and the condensate may be described very well in terms of a mean-field theory. Although the gases are dilute, interactions play an important role because temperatures are so low, and they give rise to collective phenomena related to those observed in solids, quantum liquids and nuclei. Experimentally, the systems are attractive ones to work with, since they may be manipulated by the use of lasers and magnetic fields. In addition, interactions between atoms may be varied either by using different atomic species, or, for species that have a Feshbach resonance, by changing the strength of an applied magnetic or electric field. A further advantage is that, because of low density, 'microscopic' length scales are so large that the structure of the condensate wave function may be investigated directly by optical means. Finally, real collision processes play little role, and therefore these systems are ideal for studies of interference phenomena and atom optics.

Since the first realization of BEC, a tremendous amount of research has been taken place in this interdisciplinary field [2, 3, 4, 5]. One specific topic of wide interest is multi-component BECs, which possess complicated quantum phases [6] and might provide a candidate model for quantum simulations. Theoretical [7-9] and experimental [10-12] studies have shown that inter-species interaction plays crucial roles in these systems. Recently two-species BECs with tunable interspecies interaction were successfully produced [13, 14]. This important progress motivates further explorations to understand and utilize the peculiar of two-species BECs.

One important aspect of BEC dynamics is matter wave solitons described by nonlinear Schrodinger equations [5, 15-17]. Solitons represent a highly nonlinear wave phenomenon with unique propagation features and have attracted great interests from many different fields, e.g., nonlinear optics [18]. Because the equations of motion for matter-wave solitons are similar to those for solitons in other contexts, well-established understanding of solitons can be applied to BEC systems to achieve better control of matter waves. In return, BEC systems make it possible to study the formation of solitons under some circumstances that cannot be realized in other field.

In my project work, interesting behaviour of vector-soliton in two-species condensates with arbitrary scattering lengths has been studied. It is found that exact solutions exist even in the non-integrable regime and maintain their dynamic stability in the presence of soft trapping potentials. Density profiles for Bright and Dark solitons have been obtained.

My project work contains four chapters. In first chapter, general introduction for BECs has been given. Numerical method to study density profile for Bright and Dark solitons has been given in second

chapter. Third chapter contains results for various cases having different trapping potentials. And fourth chapter will show conclusion, limitations and future scope of this work.



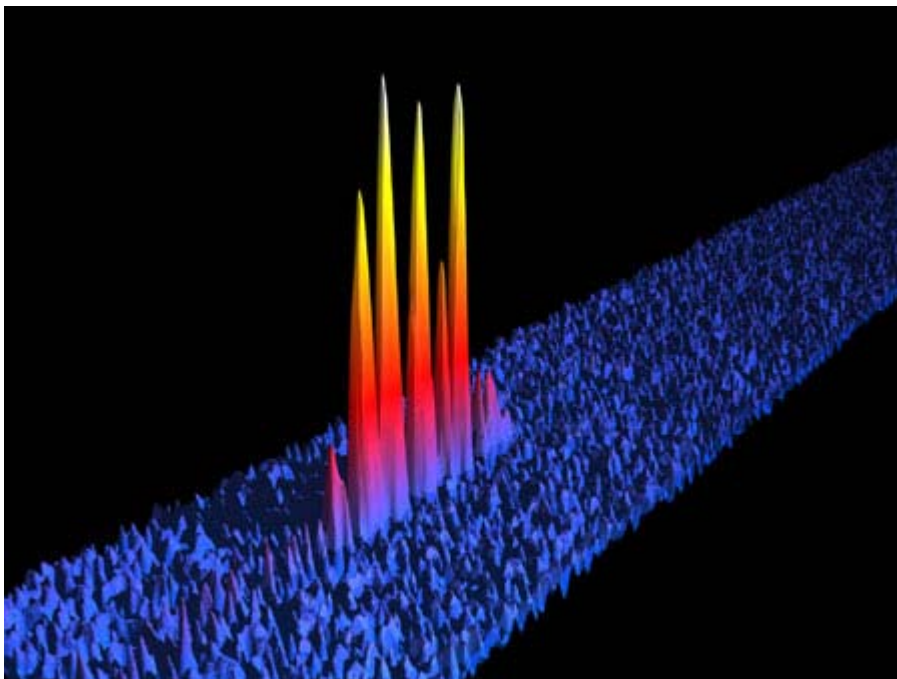
## Chapter-2

### 2.1 What is Soliton?

A soliton is a self-reinforcing solitary wave (a wave packet or pulse) that maintains its shape while it travels at constant speed [19]. Solitons are caused by a cancellation of nonlinear and dispersive effects in the medium. The term “dispersive effects” refers to a property of certain systems where the speed of the waves varies according to frequency. Solitons arise as the solutions of a widespread class of weakly nonlinear dispersive partial differential equations describing physical systems. The soliton phenomenon was first described by John Scott Russell who observed a solitary wave in the Union Canal in Scotland. He produced the phenomenon in a wave tank and named it the “Wave of Translation”.

Thus,

- 1) Solitons are of permanent form;
- 2) Solitons are localised within a region;
- 3) Solitons can interact with other solitons, and emerge from the collision unchanged, except for a phase shift.



Bright and Dark are two types of solitons. Bright solitons are associated with self-focusing or self-attractive waves while Dark solitons are associated with self-defocusing or self-repulsive waves.

In the case of self-focusing, the fundamental bright soliton has the following general form:

$$u(z, x) = a \operatorname{sech} \left[ a(x - vz) \right] \exp \left[ i v x + \frac{i(a^2 - v^2)z}{2} \right], \quad \text{--- (2.1)}$$

where,  $a$  is the soliton amplitude and  $v$  is the velocity. For spatial solitons,  $v$  represents the transverse velocity of solitons propagating at an angle to the  $z$  axis.

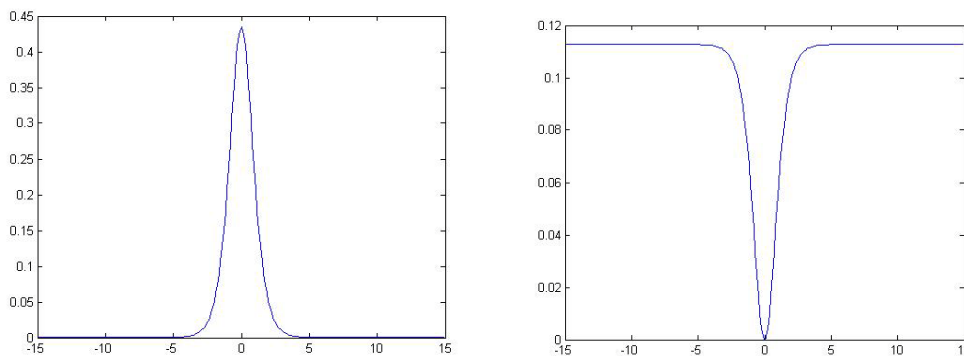
In the case of self-defocusing, the fundamental dark soliton has the following general form:

$$u(z, x) = u_0 \left\{ B \tanh[u_0 B(x - Au_0 z)] + iA \right\} \exp \left[ -i u_0^2 z \right], \quad \text{--- (2.2)}$$

where, the parameters  $A$  and  $B$  are connected by the relation  $A^2 + B^2 = 1$ .

An important difference between the bright and dark solitons is that the speed of a dark soliton depends on its amplitude. In contrast with bright solitons, which have a constant phase, the phase of a dark soliton changes across its width.

Thus, by analogy, the word dark is used to describe solitons that correspond to density depressions. This category of solitons is further divided into black ones, for which the minimum density is zero, and grey ones, for which it is greater than zero. Solitons with a density maximum are referred to as bright.



Bright Soliton and Dark Soliton

## 2.2 Solutions for Bright and Dark Solitons:

Our main aim is to show the interesting behaviour of vector-soliton in two-species condensates with arbitrary scattering lengths [20]. It is found that exact solutions exist even in the non-integrable regime and maintain their dynamic stability in the presence of soft trapping potentials. Different types of vector-solitons can be realized and transformed to each other when the atom-atom interaction strength is tuned via Feshbach resonance. This opens up new possibilities in the quantum control of multi-component BECs and other related complex systems.

The mean-field dynamics of a two-species BEC is governed by the following equations [reference]:

$$i\hbar \frac{\partial \tilde{\Psi}_1}{\partial t} = \left[ -\frac{\hbar^2 \nabla^2}{2m_1} + V_1 + U_{11} |\Psi_1|^2 + U_{12} |\Psi_2|^2 \right] \Psi_1 , \quad \text{--- (2.3)}$$

$$i\hbar \frac{\partial \tilde{\Psi}_2}{\partial t} = \left[ -\frac{\hbar^2 \nabla^2}{2m_2} + V_2 + U_{21} |\Psi_1|^2 + U_{22} |\Psi_2|^2 \right] \Psi_2 , \quad \text{--- (2.4)}$$

where, the condensate wave functions are normalized by particle numbers

$$N_i = \int |\Psi_i|^2 d^3r,$$

and intra- and inter- species interaction strengths are given as,

$$U_{ii} = 4\pi \hbar^2 a_{ii} / m_i,$$

$$U_{12} = U_{21} = 2\pi \hbar^2 a_{12} / m$$

respectively, with  $a_{ij}$  being the corresponding scattering lengths and  $m$  being the reduced mass. The trapping potentials are assumed to be

$$V_i = m_i [\omega_{ix}^2 x^2 + \omega_{iT}^2 (y^2 + z^2)] / 2 ,$$

Further assuming  $\omega_{iT} \gg \omega_{ix}$  such that transverse motion of the condensates are frozen to the ground state of the transverse harmonic trapping potential, the system becomes quasi-one-dimensional. Integrating out the transverse coordinates, the resulting equations for the axial wave functions  $\tilde{\Psi}_{1,2}(\mathbf{x})$  in dimensionless form can be written as,

$$i \frac{\partial \tilde{\Psi}_1}{\partial t} = \left[ -\frac{1}{2} \frac{\partial^2}{\partial x^2} + \frac{\lambda_1^2 x^2}{2} + b_{11} |\tilde{\Psi}_1|^2 + b_{12} |\tilde{\Psi}_2|^2 \right] \tilde{\Psi}_1, \quad \text{--- (2.5)}$$

$$i \frac{\partial \tilde{\Psi}_2}{\partial t} = \left[ -\frac{\kappa}{2} \frac{\partial^2}{\partial x^2} + \frac{\lambda_2^2 x^2}{2\kappa} + b_{21} |\tilde{\Psi}_1|^2 + b_{22} |\tilde{\Psi}_2|^2 \right] \tilde{\Psi}_2, \quad \text{--- (2.6)}$$

Here, we have chosen  $\sqrt{\hbar/(m_1 \omega_{1T})}$  and  $2\pi/\omega_{1T}$  to be the units for length and time, respectively; and  $\tilde{\Psi}_{1,2}$  is normalized such that  $\int |\tilde{\Psi}_1|^2 dx = 1$  and

$$\int |\tilde{\Psi}_2|^2 dx = N_2/N_1,$$

Other parameters in equations (2.5) and (2.6) are defined as following:

$$b_{11} = 2 a_{11} N_1,$$

$$b_{12} = b_{21} = 2 m_1 a_{12} \frac{N_1}{[(1+\gamma)m]},$$

$$b_{22} = 2 m_1 a_{22} \frac{N_1 \gamma}{m_2},$$

$$\gamma = \omega_{2T}/\omega_{1T},$$

$$\lambda_1 = \omega_{1x}/\omega_{1T},$$

$$\lambda_2 = \omega_{2x}/\omega_{1T},$$

$$\kappa = m_1/m_2.$$

When the longitudinal trapping potential is neglected ( $\lambda_i = 0$ ), Equations (2.3) and (2.4) are perfectly integrable under the condition  $\kappa = 1$  (i.e.  $m_1 = m_2$ ) and  $b_{11} = b_{12} = b_{21} = b_{22}$  [21], allowing for a general procedure to construct two-component vector-soliton solutions in the form of "dark-dark" [22], "bright-dark" [23] and "bright-bright" [24] solitons.

When integrability is destroyed, different studies have shown that distorted versions of soliton solutions exist, but closed form can only be given for special cases. Remarkably, we show here that even when the above-mentioned integrability condition is violated, there still exists, in general a specific class of exact vector-soliton solutions for arbitrary interaction strengths, so long as  $b_{12}^2 \neq b_{11} b_{22}$ .

The vector-soliton solutions can be found by inserting an appropriate ansatz into Equations (2.5) and (2.6). Defining the following two quantities:

$$C_1 \equiv (b_{22} - \kappa b_{12}) / (b_{12}^2 - b_{11}b_{22}), \quad \text{--- (2.7)}$$

$$C_2 \equiv (b_{12} - \kappa b_{11}) / (b_{12}^2 - b_{11}b_{22}), \quad \text{--- (2.8)}$$

The conditions under which various vector-soliton solutions exist are found to be as following:

$C_1 > 0, C_2 < 0$  : Bright – Bright (BB),

$C_1 > 0, C_2 > 0$  : Bright – Dark (BD),

$C_1 < 0, C_2 > 0$  : Dark – Dark (DD),

$C_1 < 0, C_2 < 0$  : Dark – Bright (DB).

Explicit expressions for these vector-solitons are then found from the ansatz we use. In particular, the BB solution (i.e., bright soliton for species 1 and bright soliton for species 2; analogous convention applies to all other solutions) is given by,

$$\tilde{\Psi}_{1B} = \eta \sqrt{C_1} \operatorname{sech}(\eta x - \eta v t) e^{i(vx + \frac{(\eta^2 - v^2)t}{2})}, \quad \text{--- (2.9a)}$$

$$\tilde{\Psi}_{2B} = \eta \sqrt{-C_2} \operatorname{sech}(\eta x - \eta v t) e^{i(\frac{vx}{\kappa} + \frac{(\kappa\eta^2 - v^2)t}{2})}, \quad \text{--- (2.9b)}$$

The BD solution is given by,

$$\tilde{\Psi}_{1B} = \eta \sqrt{C_1} \operatorname{sech}(\eta x - \eta v t) e^{i(vx + f_1 t)}, \quad \text{--- (2.10a)}$$

$$\tilde{\Psi}_{2D} = [iv\sqrt{C_2}/\kappa + \eta\sqrt{C_2} \tanh(\eta x - \eta v t)] e^{if_2 t}, \quad \text{--- (2.10b)}$$

$$\text{with } f_1 = \frac{\eta^2 - v^2}{2} - b_{12}C_2(\eta^2 + \frac{v^2}{\kappa^2}) \text{ AND } f_2 = -b_{22}C_2(\eta^2 + \frac{v^2}{\kappa^2}),$$

The DD solutions is found to be,

$$\tilde{\Psi}_{1D} = [iv\sqrt{-C_1} + \eta\sqrt{-C_1} \tanh(\eta x - \eta v t)] e^{if_1 t}, \quad \text{--- (2.11a)}$$

$$\tilde{\Psi}_{2D} = [iv\sqrt{C_2}/\kappa + \eta\sqrt{C_2} \tanh(\eta x - \eta v t)] e^{if_2 t}, \quad \text{--- (2.11b)}$$

with  $f_1 = -\eta^2 - v^2(-b_{11}C_1 + \frac{b_{12}C_2}{\mu^2})$  AND  $f_2 = -\mu\eta^2 - v^2(-b_{21}C_1 + \frac{b_{22}C_2}{\mu^2})$ ,

Finally, the DB solution can be obtained from the BD solution (2.8) by exchanging indices 1 and 2, and let  $C_{1,2} \rightarrow -C_{1,2}$ .

In all these cases, the parameter  $\eta$  determines the width of the soliton and can be found by the normalization condition for  $\tilde{\Psi}_{1,2}$ . The parameter  $v$  gives the velocity of the soliton.

Here, we take  ${}^7\text{Li}$  as species 1 and  ${}^{23}\text{Na}$  as species 2, with fixed and realistic intra-species interaction strength  $b_{11} < 0$ ,  $b_{22} > 0$  and variable inter-species interaction strength  $b_{12}$ . Figure [1] depicts the “phase diagram” for different regimes of vector solitons as  $b_{12}$  is varied.

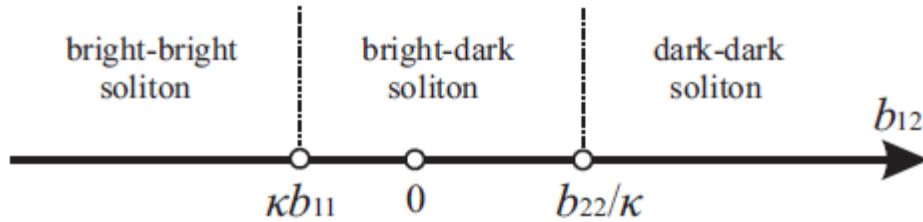


FIG. 1: Phase diagram of vector solitons vs. inter-species interaction  $b_{12}$  for the system with  $b_{11} < 0$  and  $b_{22} > 0$ . In the examples shown later in the paper, we assume that the two species experience the same trapping frequency:  $\omega_{1\perp} = \omega_{2\perp} = 2\pi \times 710\text{Hz}$ . The number of atoms in the first species ( ${}^7\text{Li}$ ) is assumed to be 5000, which results in the dimensionless intra-species interaction strength  $b_{11} = -1.47$  and  $b_{22} = 5.89$ . The two critical values of the inter-species interaction strength are therefore  $\kappa b_{11} = -0.45$  and  $b_{22}/\kappa = 19.35$ .

As is indicated in Figure [1], the system supports BB ( $b_{12} < \kappa b_{11}$ ), BD ( $\kappa b_{11} < b_{12} < b_{22}/\kappa$ ) and DD ( $b_{12} > b_{22}/\kappa$ ) vector soliton, while the condition for DB soliton can never be satisfied for this particular  ${}^7\text{Li}$ - ${}^{23}\text{Na}$  system.

Here we are trying to study dynamical stability for Bright-Dark (BD) solitons. Dynamical stability of the vector-soliton solutions can be confirmed by direct numerical simulations of Equations (2.5) and (2.6). In our simulations, a harmonic trapping potential is added along the longitudinal direction to make the simulations more realistic. The trapping potential is weak such that its variation across the soliton scale is negligible. Such a soft trapping potential spatially confines the solitons without affecting their

essential properties. For initial condition, we use the exact solution of Equation (2.10a) for the bright component, while we multiply Equation (2.10b) by a Thomas-Fermi profile to simulate the dark component (Appendix B).

## 2.3 Numerical Method to study Dynamics and Dynamical Stability for Bright and Dark Solitons:

We use an explicit, unconditionally stable and spectrally accurate numerical method to solve the GPE (2.5) and (2.6) for dynamics of BEC. Due to the external trapping potential  $V_1$  and  $V_2$ , the solution  $\Psi(x,t)$  of (2.5) and (2.6) decays to zero exponentially fast when  $|x| \rightarrow \infty$ . So we have to choose boundary condition to truncate this problem.

Here, we will use Time-Splitting Pseudospectral method to study behaviour of Bright and Dark solitons. First we use Time-Splitting method. We choose a time step  $\Delta t > 0$ . For  $n = 0, 1, 2, \dots$  from time  $t = t_n = n\Delta t$  to  $t = t_{n+1} = t_n + \Delta t$ , the GPEs (2.5) and (2.6) are solved in two splitting steps as following:

- First, consider following equations:

$$i \frac{\partial \tilde{\Psi}_1}{\partial t} = \left[ -\frac{1}{2} \frac{\partial^2}{\partial x^2} + \frac{\lambda_1^2 x^2}{2} + b_{11} |\tilde{\Psi}_1|^2 + b_{12} |\tilde{\Psi}_2|^2 \right] \tilde{\Psi}_1, \quad \text{--- (2.5)}$$

$$i \frac{\partial \tilde{\Psi}_2}{\partial t} = \left[ -\frac{\kappa}{2} \frac{\partial^2}{\partial x^2} + \frac{\lambda_2^2 x^2}{2\kappa} + b_{21} |\tilde{\Psi}_1|^2 + b_{22} |\tilde{\Psi}_2|^2 \right] \tilde{\Psi}_2, \quad \text{--- (2.6)}$$

- To decouple linearity and nonlinearity, we consider first kinetic energy terms:

$$i \frac{\partial \tilde{\Psi}_1}{\partial t} = \left[ -\frac{1}{2} \frac{\partial^2 \tilde{\Psi}_1}{\partial x^2} \right], \quad \text{--- (2.12)}$$

$$i \frac{\partial \tilde{\Psi}_2}{\partial t} = \left[ -\frac{\kappa}{2} \frac{\partial^2 \tilde{\Psi}_2}{\partial x^2} \right], \quad \text{--- (2.13)}$$

- Next we take potential energy and nonlinear terms as following:

$$i \frac{\partial \tilde{\Psi}_1}{\partial t} = \left[ \frac{\lambda_1^2 x^2}{2} + b_{11} |\tilde{\Psi}_1|^2 + b_{12} |\tilde{\Psi}_2|^2 \right] \tilde{\Psi}_1 , \quad \dots (2.14)$$

$$i \frac{\partial \tilde{\Psi}_2}{\partial t} = \left[ \frac{\lambda_2^2 x^2}{2\kappa} + b_{21} |\tilde{\Psi}_1|^2 + b_{22} |\tilde{\Psi}_2|^2 \right] \tilde{\Psi}_2 , \quad \dots (2.15)$$

- For time  $t \in [t_n, t_{n+1}]$ , Equations (2.14) and (2.15) leave  $|\tilde{\Psi}_1(x, t)|$  and  $|\tilde{\Psi}_2(x, t)|$  invariant in time  $t$ , and thus it can be integrated exactly and we can get  $\tilde{\Psi}_1(x, t)$  and  $\tilde{\Psi}_2(x, t)$  as,

$$\tilde{\Psi}_1(x, t) = \tilde{\Psi}_1(x - t_n) \text{Exp}[-i \left( \frac{\lambda_1^2 x^2}{2} + b_{11} |\tilde{\Psi}_1|^2 + b_{12} |\tilde{\Psi}_2|^2 \right) (t - t_n)] , \quad \dots (2.16)$$

AND

$$\tilde{\Psi}_2(x, t) = \tilde{\Psi}_2(x - t_n) \text{Exp}[-i \left( \frac{\lambda_2^2 x^2}{2\kappa} + b_{21} |\tilde{\Psi}_1|^2 + b_{22} |\tilde{\Psi}_2|^2 \right) (t - t_n)] , \quad \dots (2.17)$$

- These equations (2.16) and (2.17) will be used to solve equations (2.12) and (2.13) for generating wave functions to evaluate Density profiles [25, 26] for Bright and Dark solitons.



## Chapter - 3

### Results and Discussion:

In this chapter dynamics of vector solitons inside a longitudinal trap have been discussed.

Consider following equations,

$$i \frac{\partial \tilde{\Psi}_1}{\partial t} = \left[ -\frac{1}{2} \frac{\partial^2}{\partial x^2} + \frac{\lambda_1^2 x^2}{2} + b_{11} |\tilde{\Psi}_1|^2 + b_{12} |\tilde{\Psi}_2|^2 \right] \tilde{\Psi}_1 , \quad \text{--- (2.3)}$$

$$i \frac{\partial \tilde{\Psi}_2}{\partial t} = \left[ -\frac{\kappa}{2} \frac{\partial^2}{\partial x^2} + \frac{\lambda_1^2 x^2}{2\kappa} + b_{21} |\tilde{\Psi}_1|^2 + b_{22} |\tilde{\Psi}_2|^2 \right] \tilde{\Psi}_2 , \quad \text{--- (2.4)}$$

for Bright and Dark solitons respectively.

As shown in chapter 2, the Bright-Dark [BD] solution is given as,

$$\tilde{\Psi}_{1B} = \eta \sqrt{C_1} \operatorname{sech}(\eta x - \eta v t) e^{i(vx + f_1 t)} , \quad \text{--- (2.8a)}$$

$$\tilde{\Psi}_{2D} = [iv\sqrt{C_2}/\kappa + \eta\sqrt{C_2} \tanh(\eta x - \eta v t)] e^{if_2 t} , \quad \text{--- (2.8b)}$$

$$\text{with } f_1 = \frac{\eta^2 - v^2}{2} - b_{12} C_2 \left( \eta^2 + \frac{v^2}{\kappa^2} \right) \text{ AND } f_2 = -b_{22} C_2 \left( \eta^2 + \frac{v^2}{\kappa^2} \right) ,$$

To study the stability analysis for Bright-Dark solitons, we will change trapping potential  $\lambda_1$  and  $\lambda_2$  for Bright and Dark solitons respectively. Trapping potential for both solitons are not equal in all cases. While keeping  $\lambda_2$  constant for Dark soliton,  $\lambda_1$  will change having values 0, 0.2, 0.4, 0.6, 0.8 and 1.0. For example, if  $\lambda_2$  is zero and  $\lambda_1$  will go as 0, 0.2, 0.4, 0.6, 0.8 and 1.0 respectively.  $\lambda_2$  will be changed as 0, 0.2, 0.4, 0.6, 0.8 and 1.0.

## 3.1: Density Profile for Different Trapping Potentials

Here plots are shown for following six cases:

3.1.1:  $\lambda_2 = 0$  for  $\lambda_1 = 0, 0.2, 0.4, 0.6, 0.8$  and  $1.0$

3.1.2:  $\lambda_2 = 0.2$  for  $\lambda_1 = 0, 0.2, 0.4, 0.6, 0.8$  and  $1.0$

3.1.3:  $\lambda_2 = 0.4$  for  $\lambda_1 = 0, 0.2, 0.4, 0.6, 0.8$  and  $1.0$

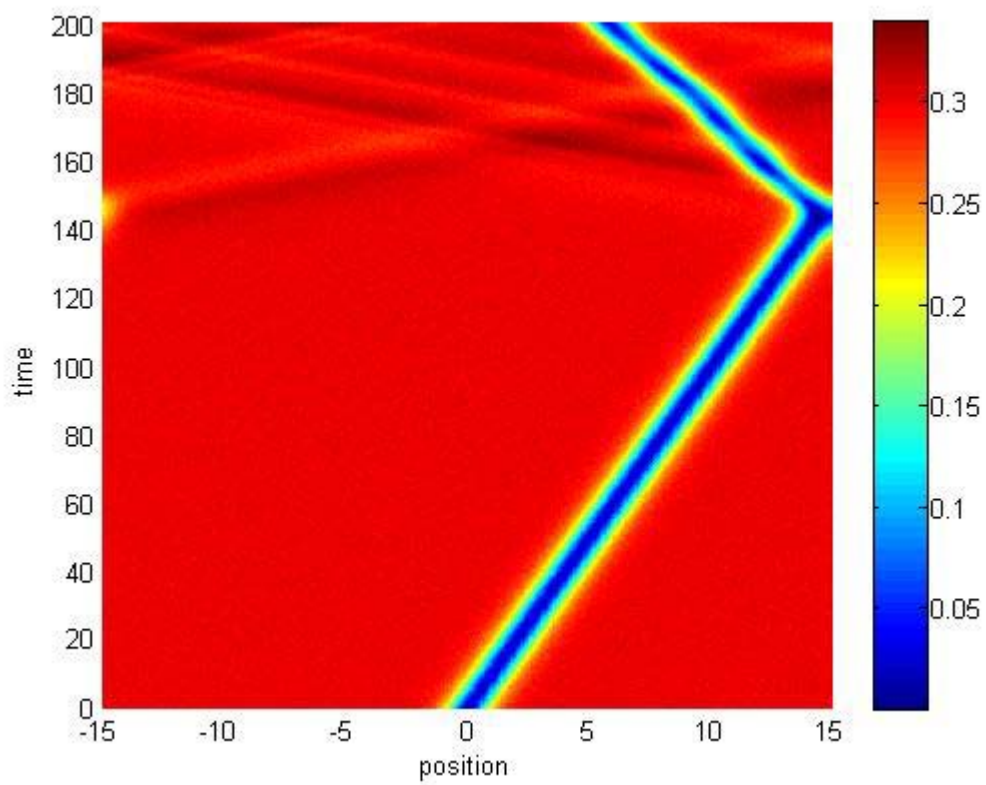
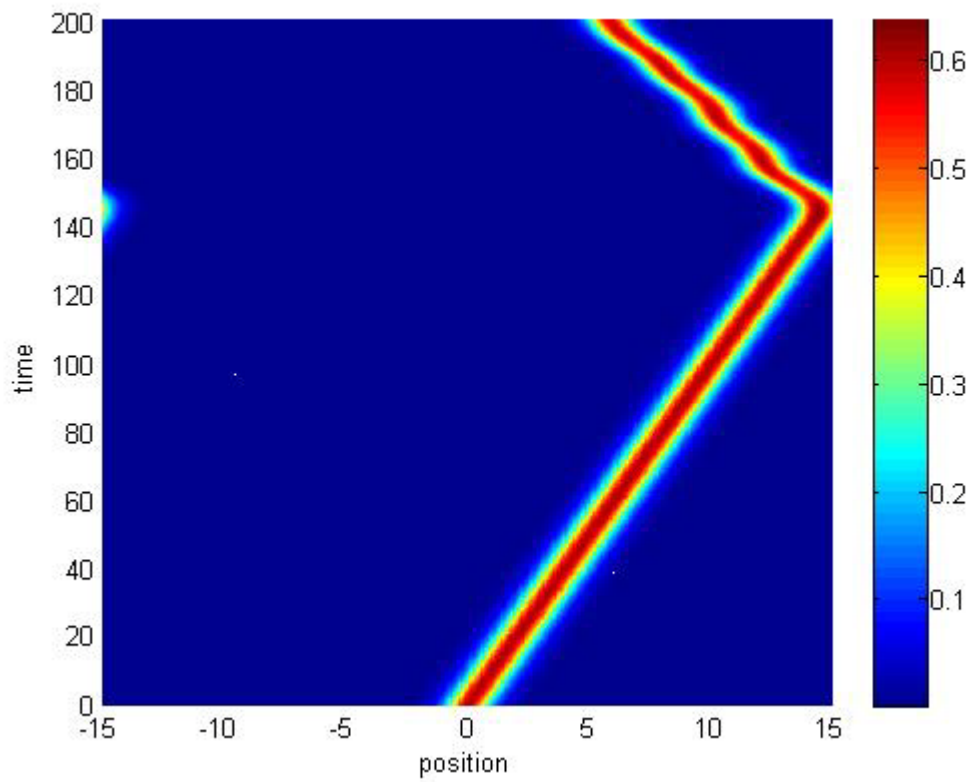
3.1.4:  $\lambda_2 = 0.6$  for  $\lambda_1 = 0, 0.2, 0.4, 0.6, 0.8$  and  $1.0$

3.1.5:  $\lambda_2 = 0.8$  for  $\lambda_1 = 0, 0.2, 0.4, 0.6, 0.8$  and  $1.0$

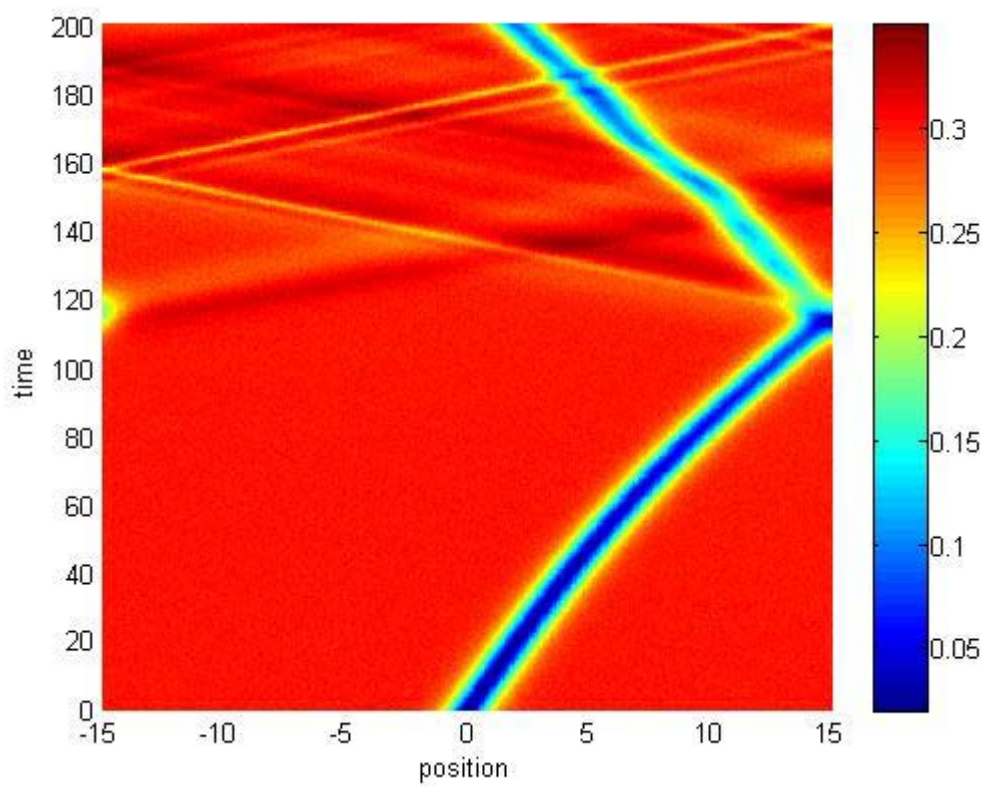
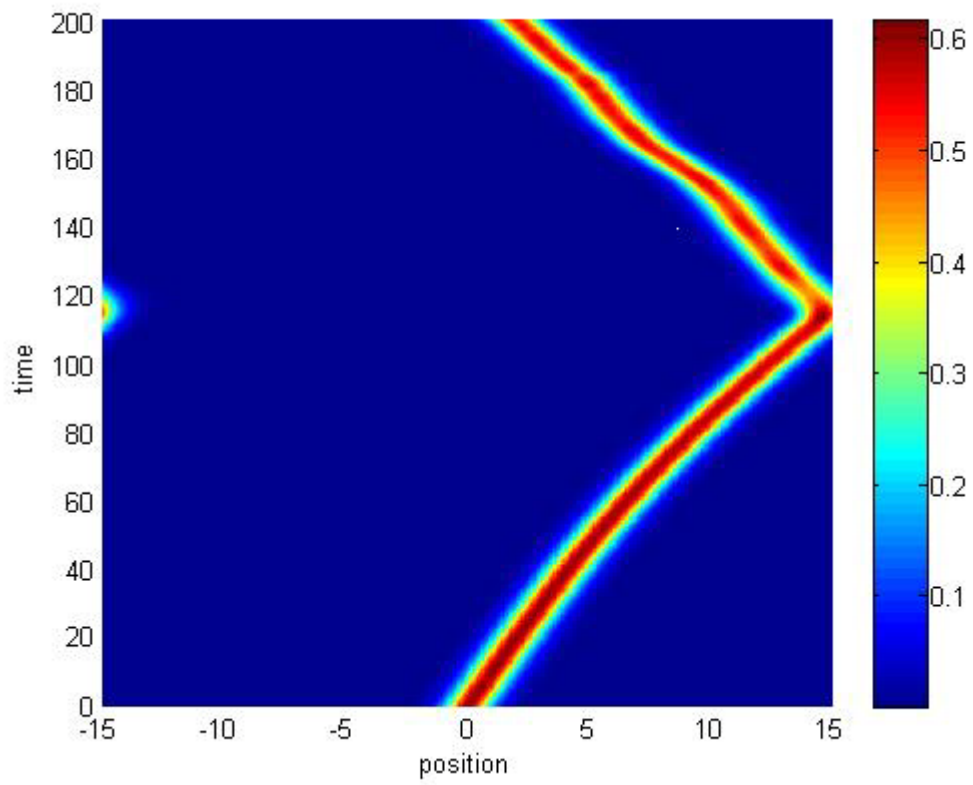
3.1.6:  $\lambda_2 = 1.0$  for  $\lambda_1 = 0, 0.2, 0.4, 0.6, 0.8$  and  $1.0$

Here different density plots are shown for different values of  $\lambda_1$  and  $\lambda_2$ . Also, some plots are shown for special cases for Bright and Dark solitons.

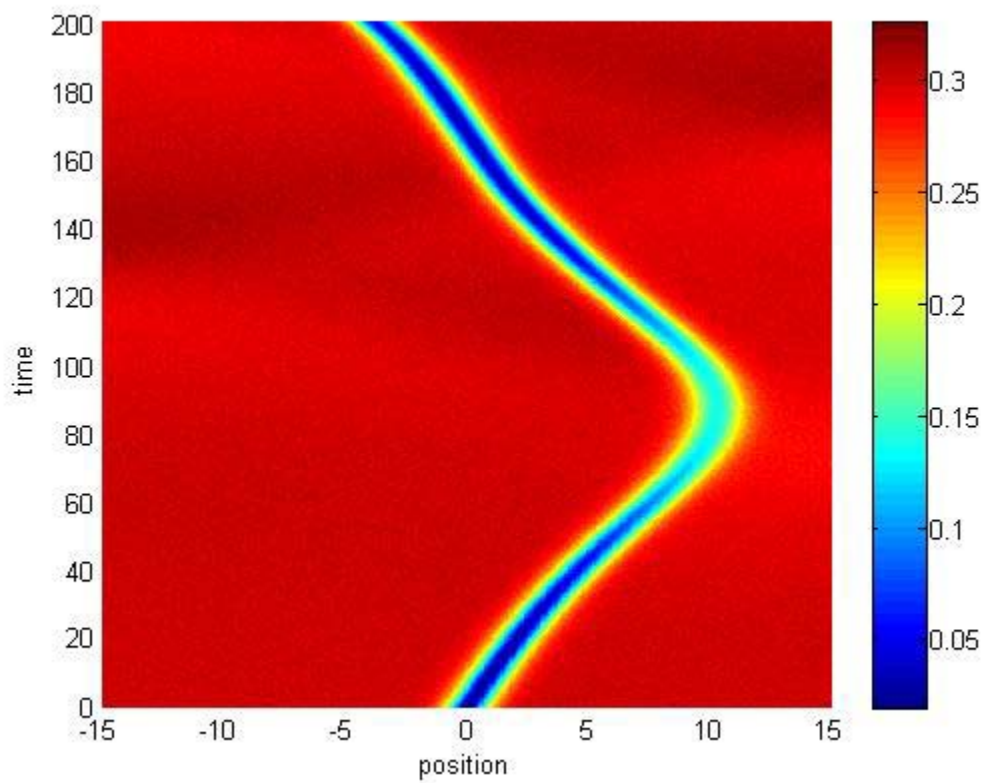
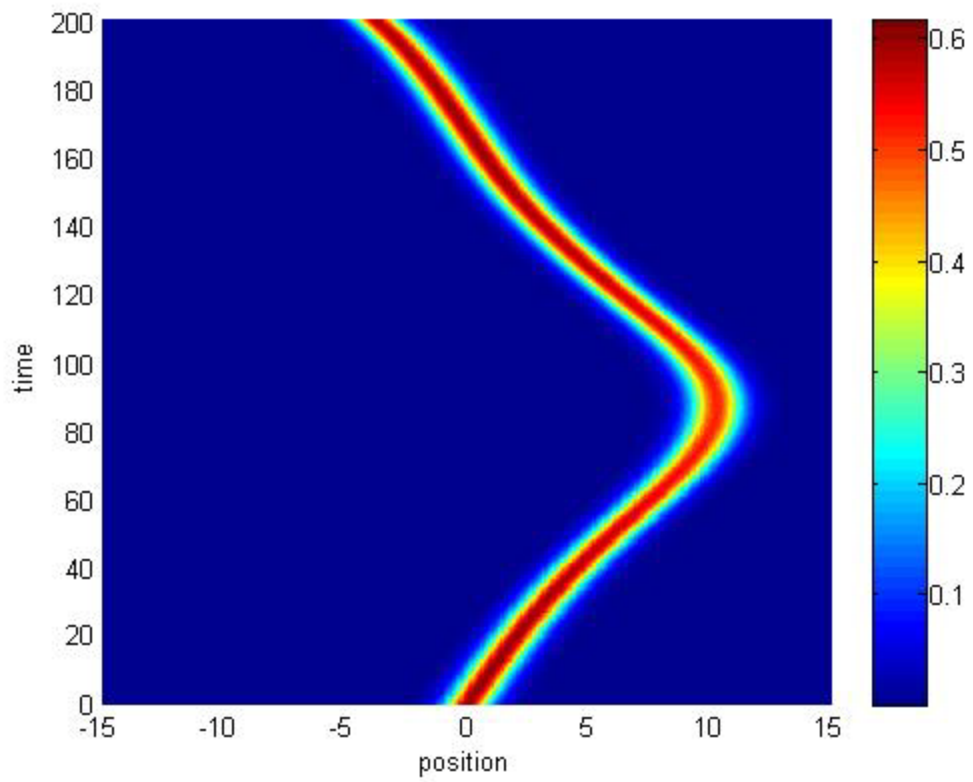
As discussed in chapter 2, for Bright-Dark solitons, the condition is  $C_1 > 0$  and  $C_2 > 0$ . To achieve this condition, values for different parameters are taken as  $b_{11} = -1.47$ ,  $b_{22} = 5.89$  and  $b_{12} = b_{21} = 2$ . These values are quite reasonable for getting Bright and Dark solitons as shown in the Phase Diagram in chapter 2. Velocity  $v$  is taken as  $0.1$ . In figures, upper figure shows density profile for Bright soliton while lower figure shows density profile for Dark soliton.



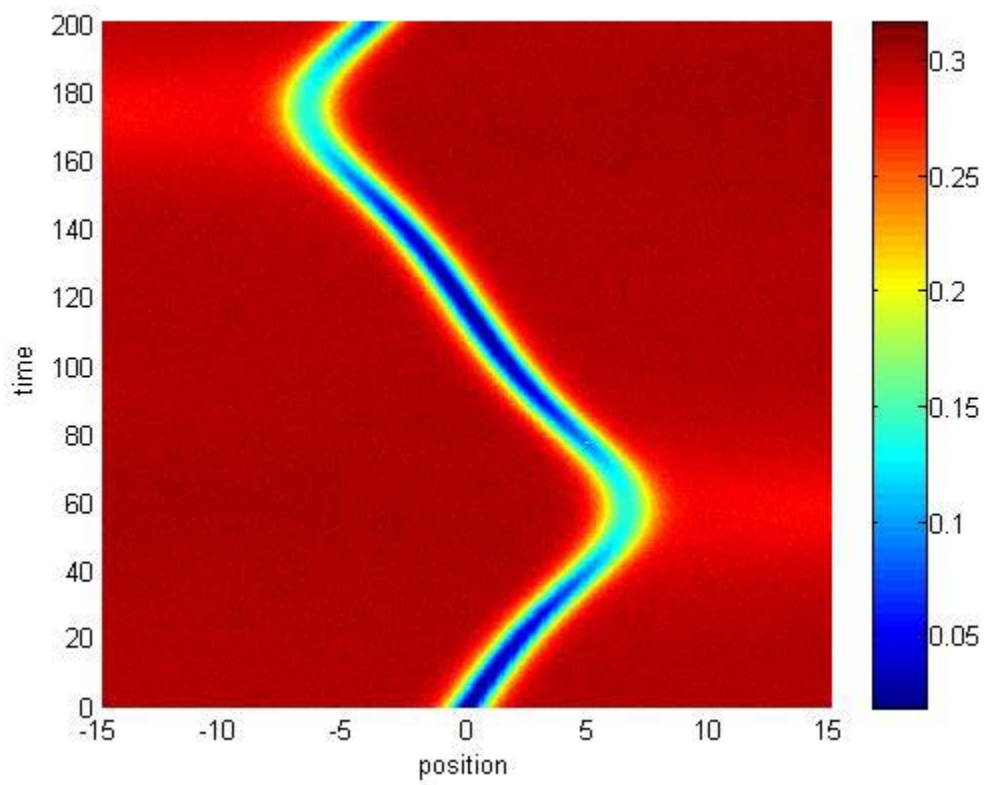
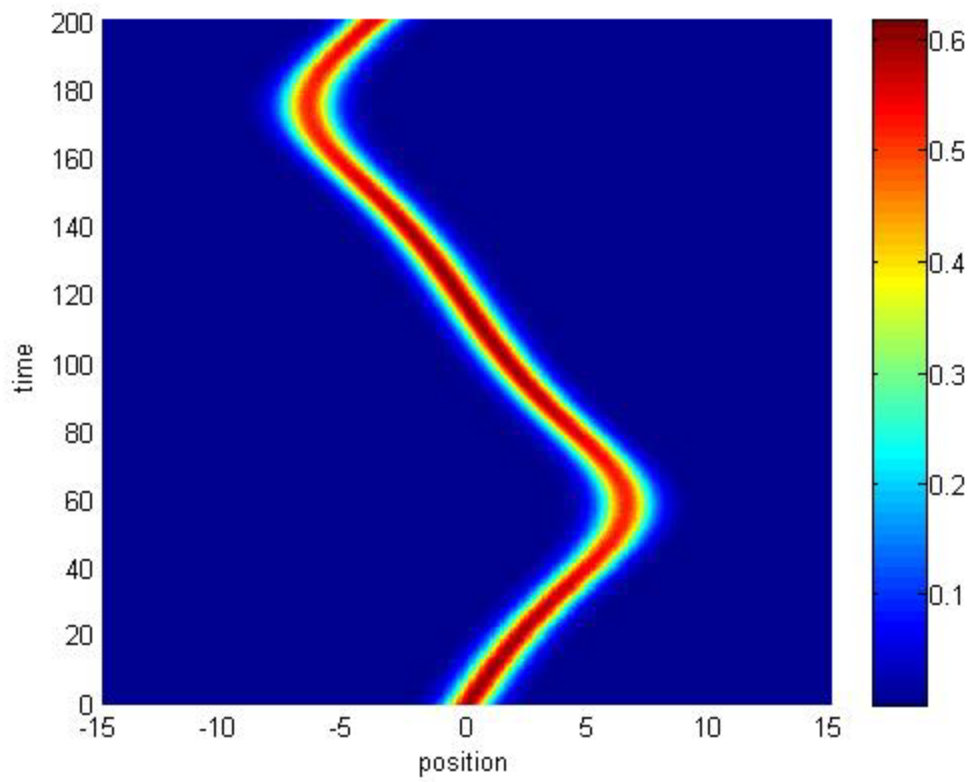
3.1.1.1 Density Profile for  $\lambda_1 = 0$  and  $\lambda_2 = 0$



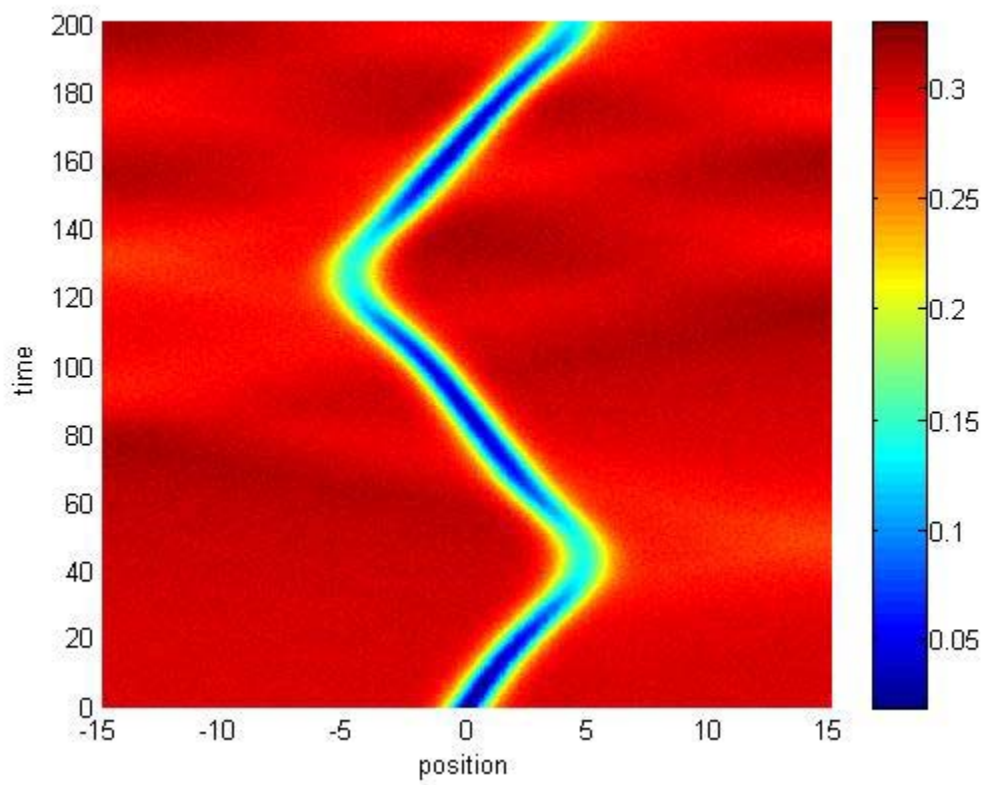
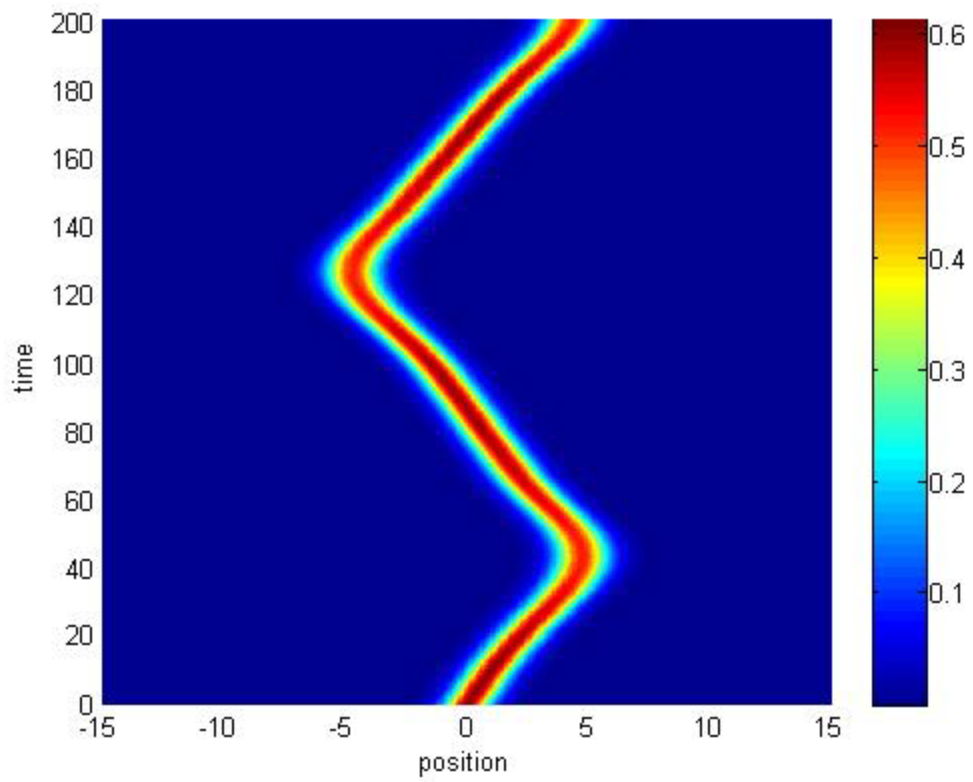
3.1.1.2 Density Profile for  $\lambda_1 = 0.02$  and  $\lambda_2 = 0$



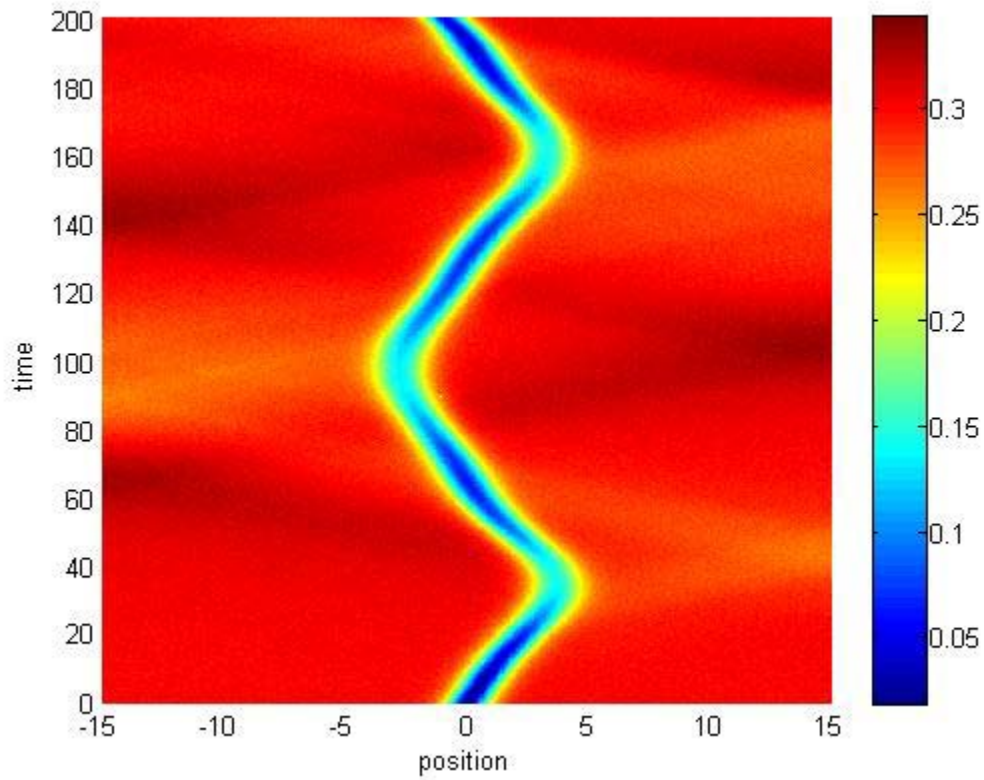
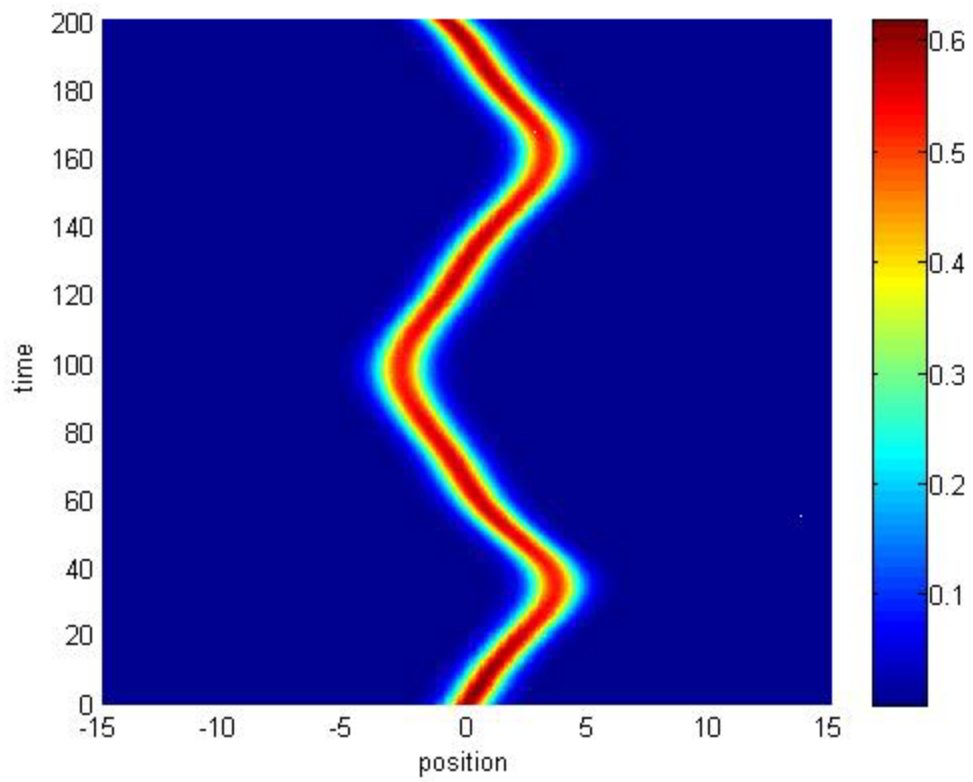
3.1.1.3 Density Profile for  $\lambda_1 = 0.04$  and  $\lambda_2 = 0$



3.1.1.4 Density Profile for  $\lambda_1 = 0.06$  and  $\lambda_2 = 0$

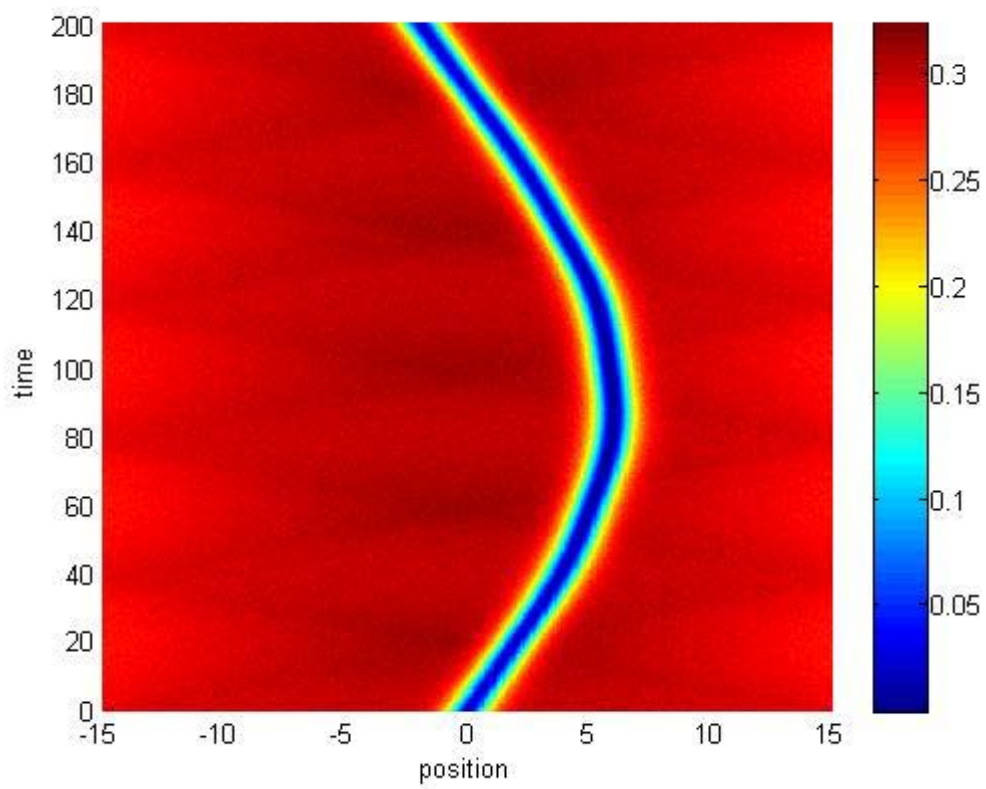
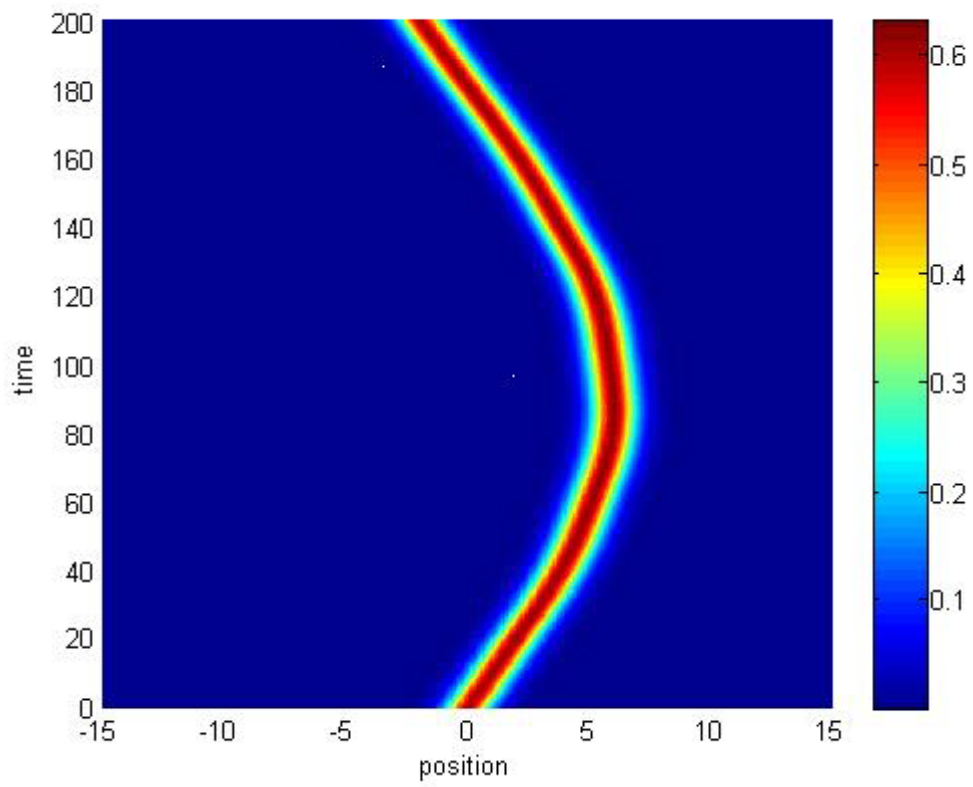


3.1.1.5 Density Profile for  $\lambda_1 = 0.08$  and  $\lambda_2 = 0$

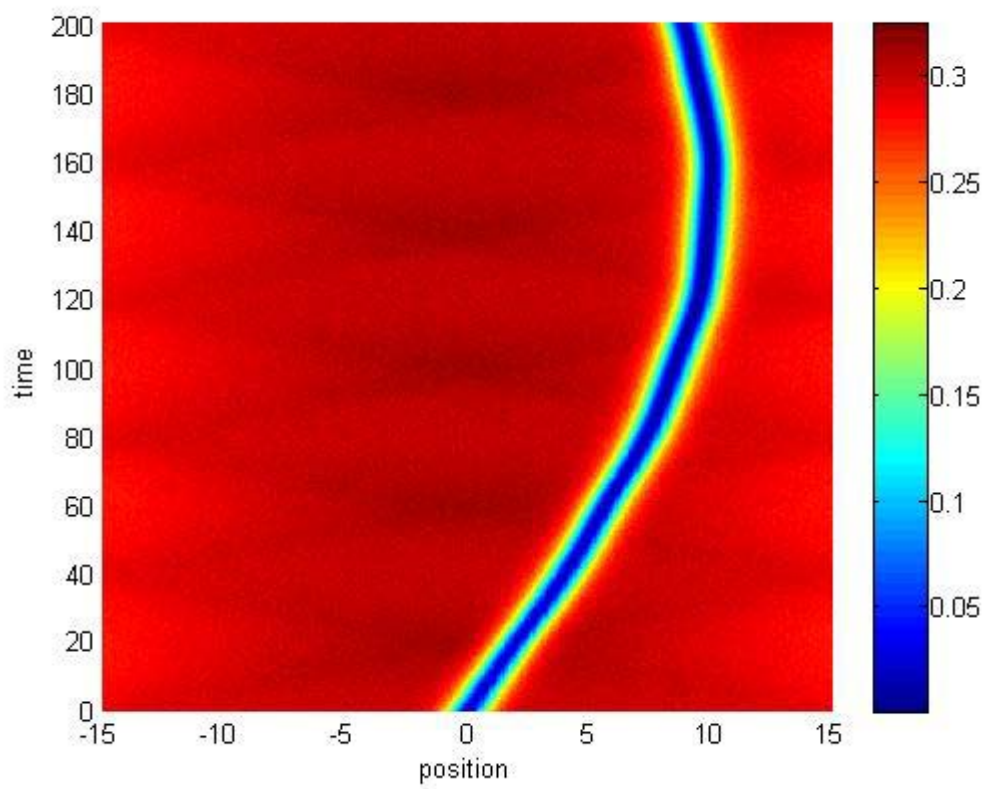
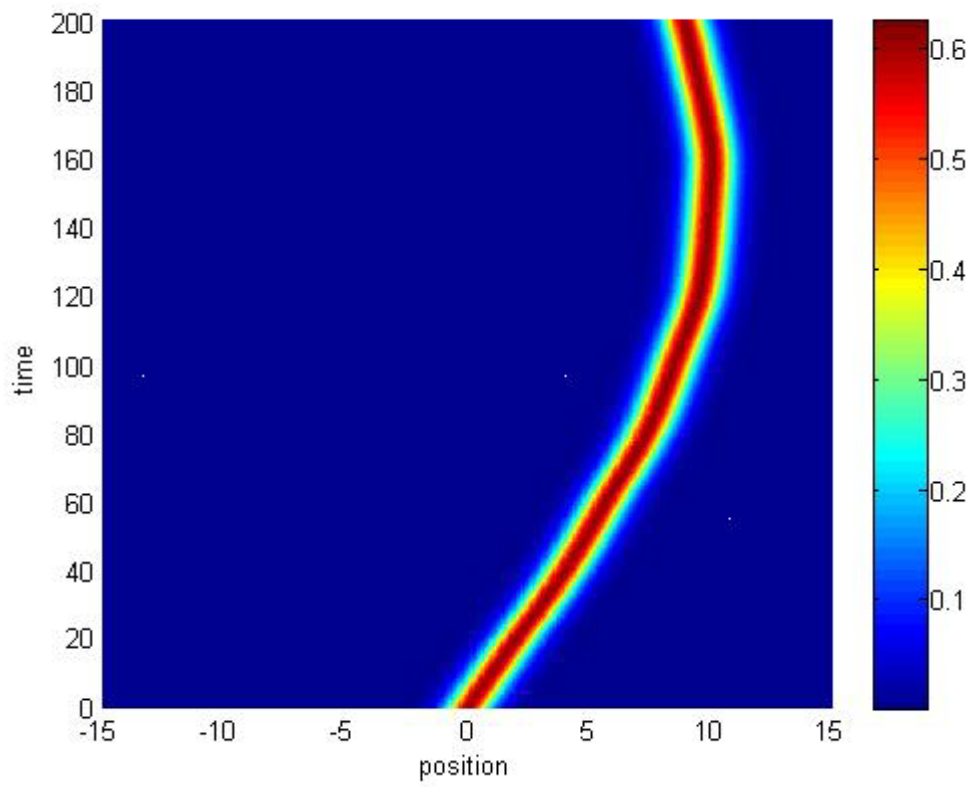


3.1.1.6 Density Profile for  $\lambda_1 = 0.1$  and  $\lambda_2 = 0$

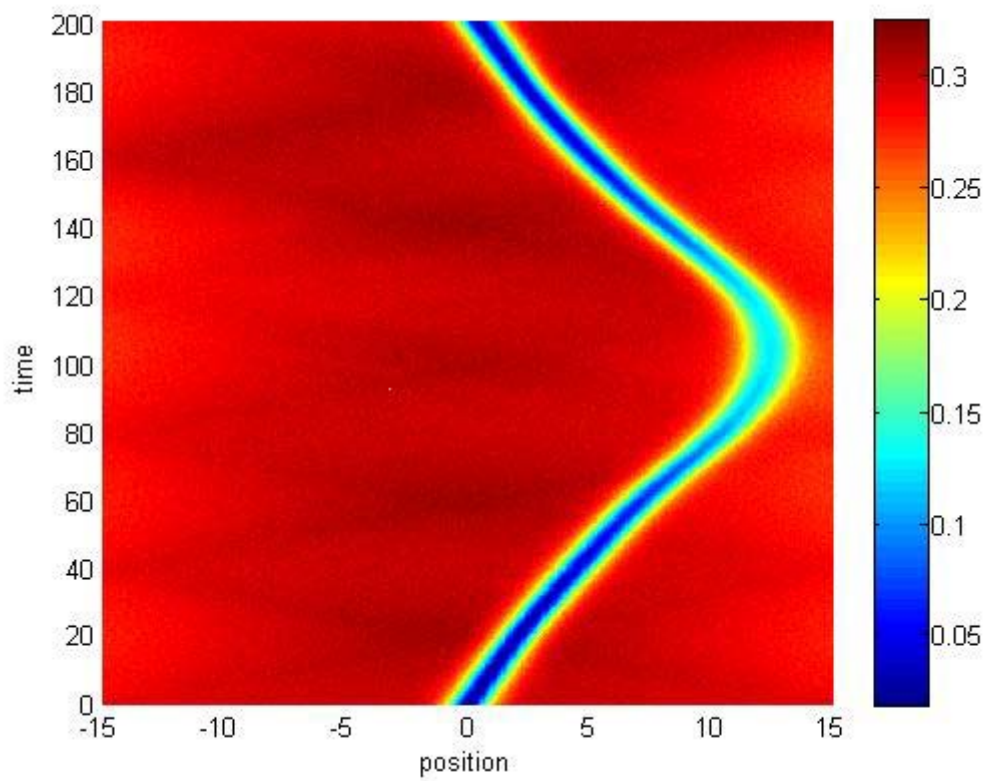
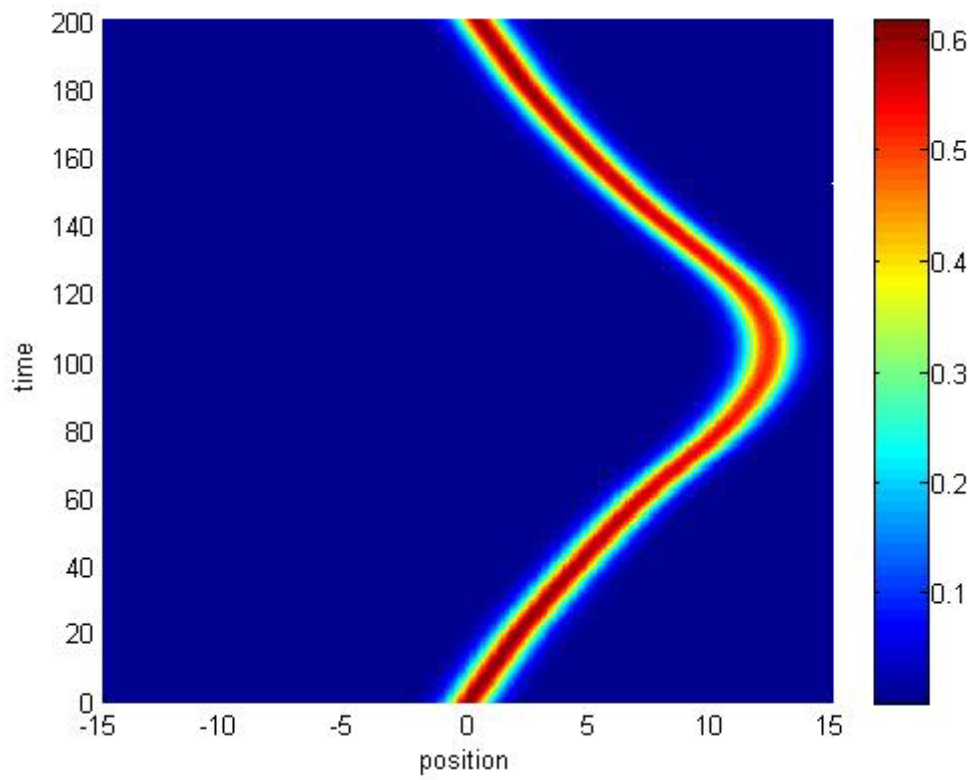




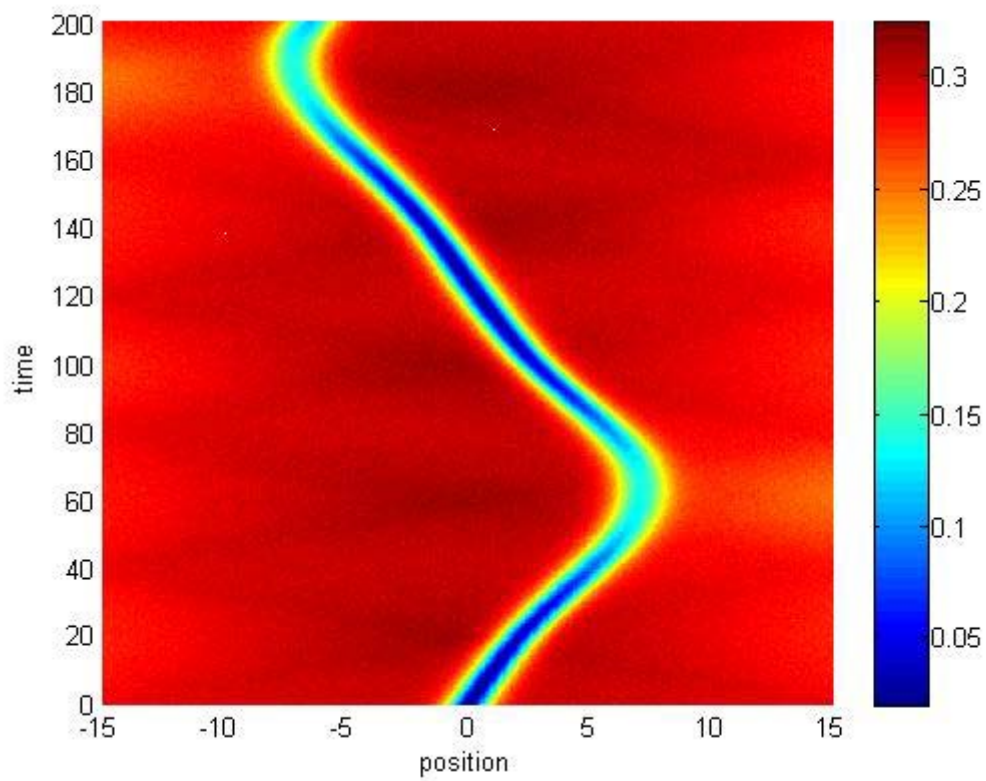
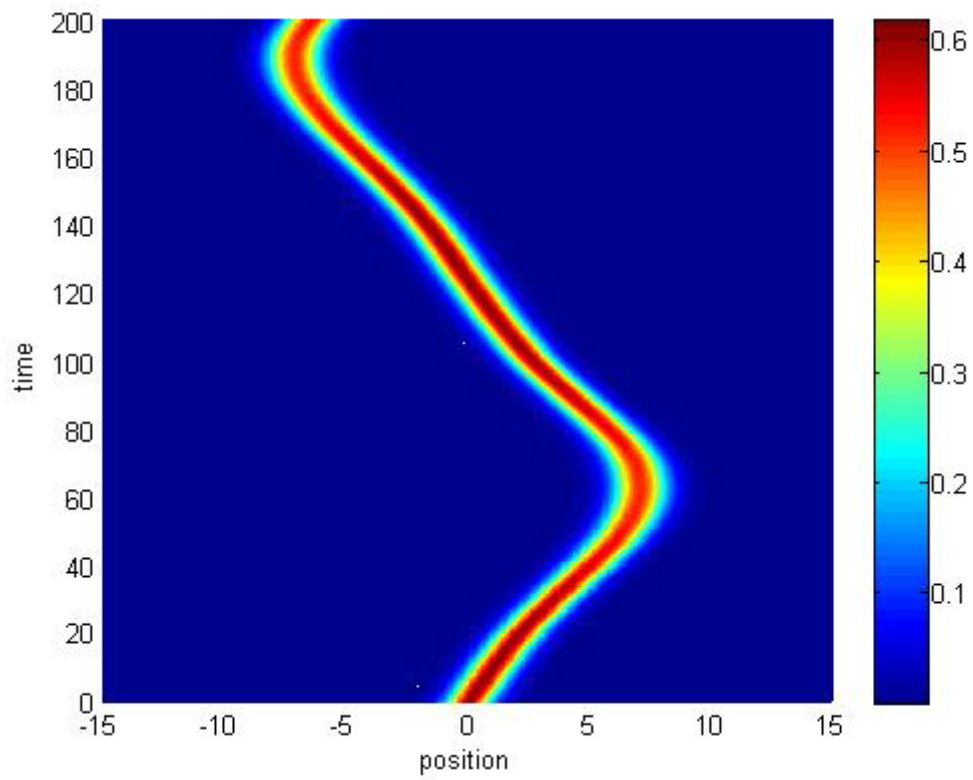
3.1.2.1 Density Profile for  $\lambda_1 = 0$  and  $\lambda_2 = 0.02$



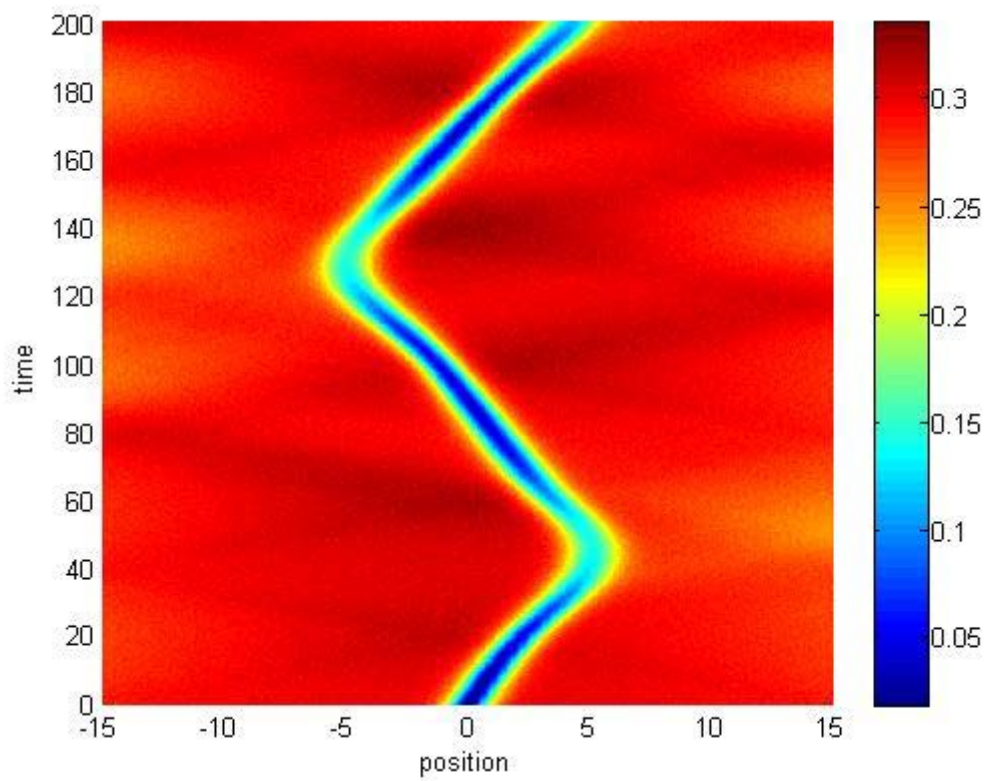
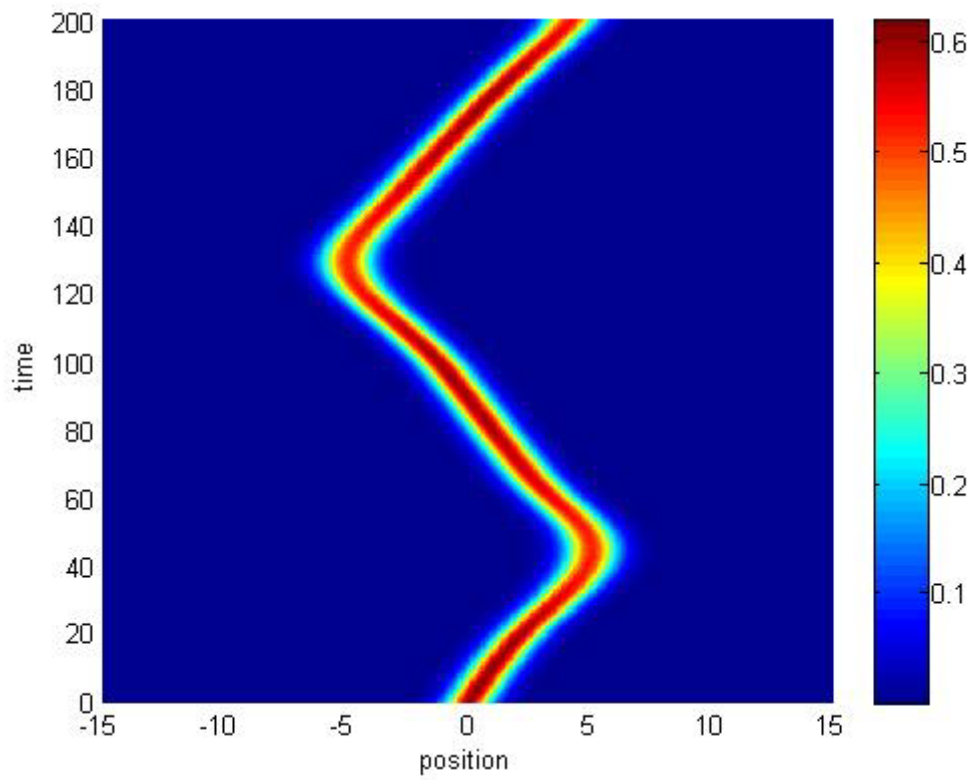
3.1.2.2 Density Profile for  $\lambda_1 = 0.02$  and  $\lambda_2 = 0.02$



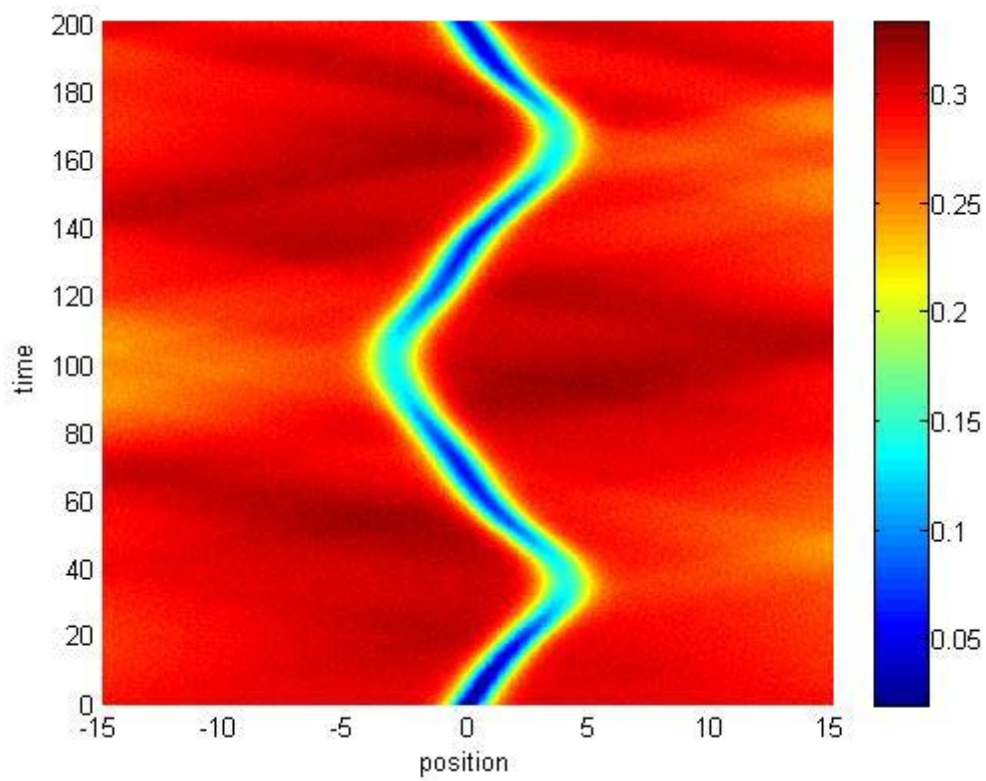
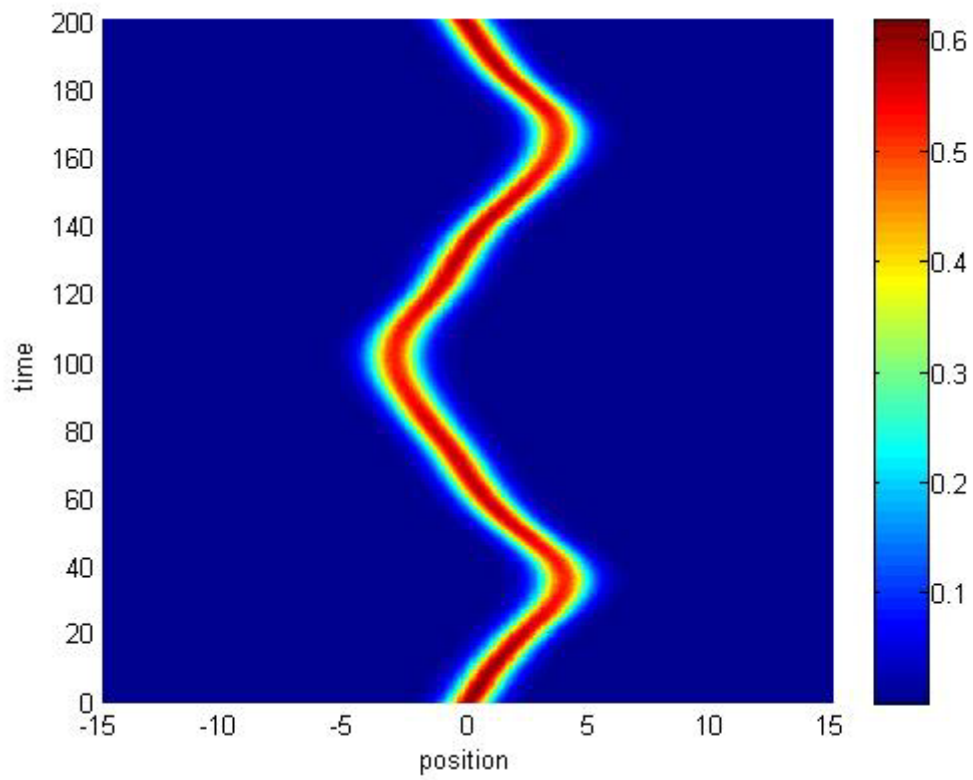
3.1.2.3 Density Profile for  $\lambda_1 = 0.04$  and  $\lambda_2 = 0.02$



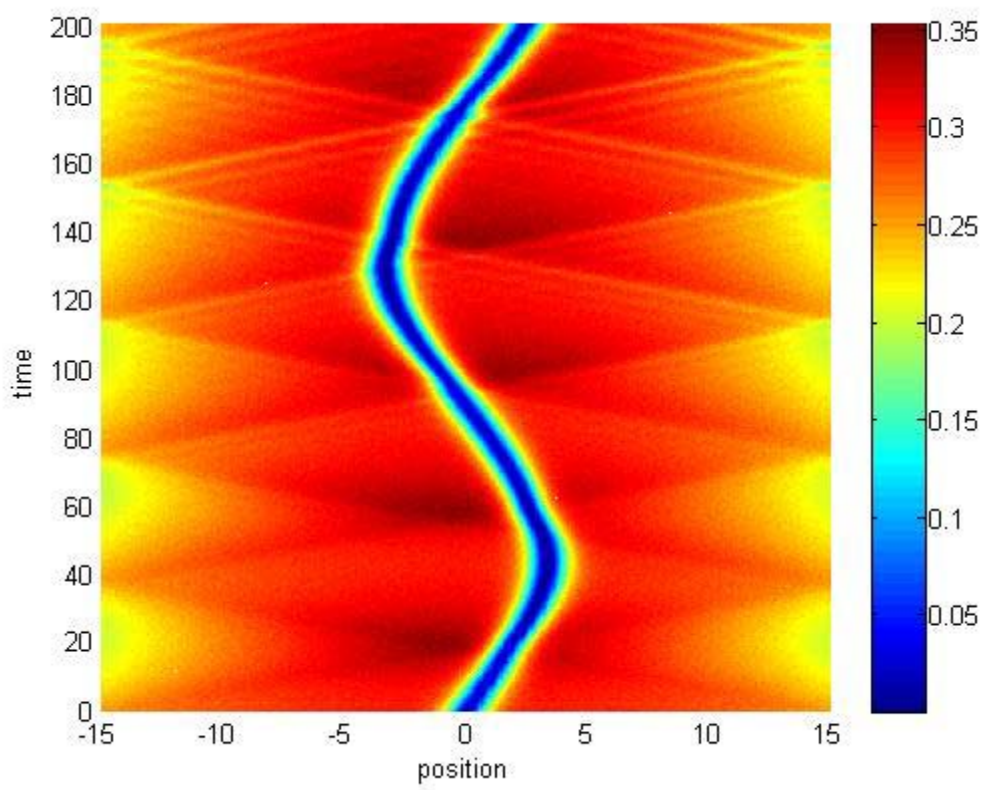
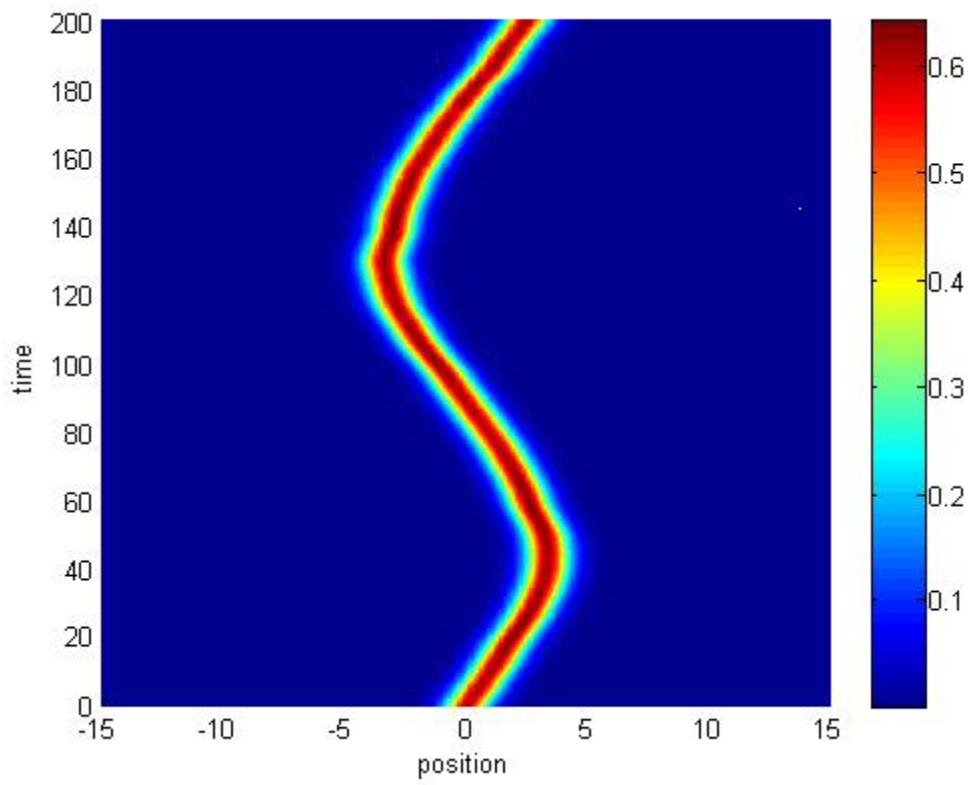
3.1.2.4 Density Profile for  $\lambda_1 = 0.06$  and  $\lambda_2 = 0.02$



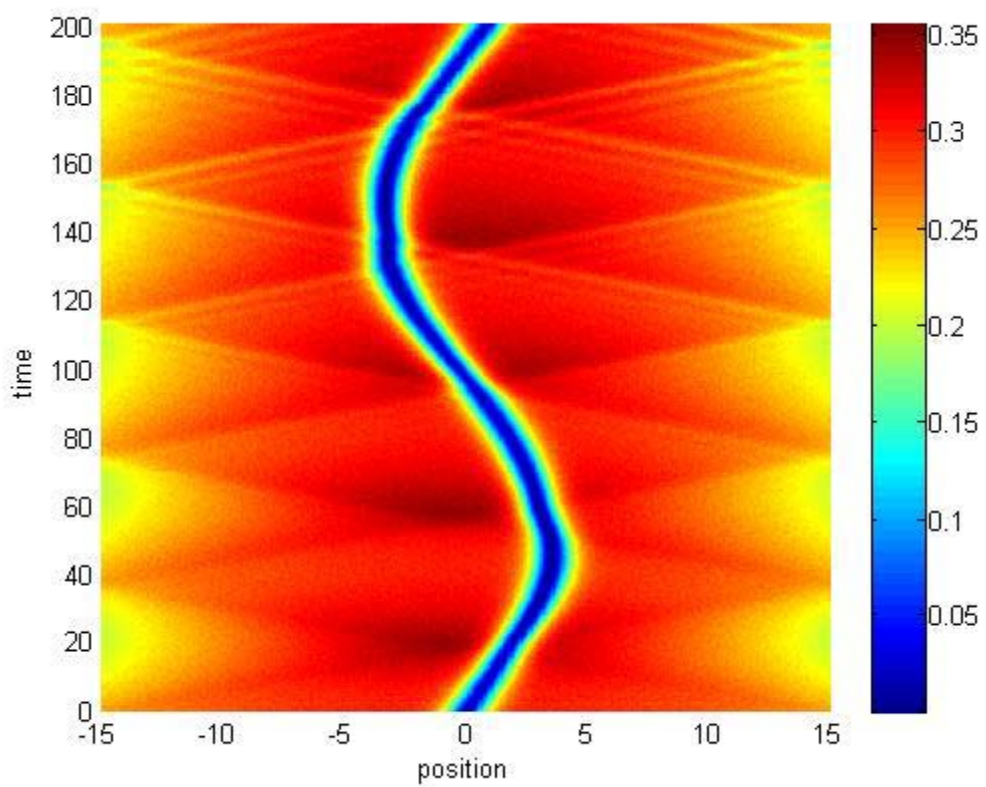
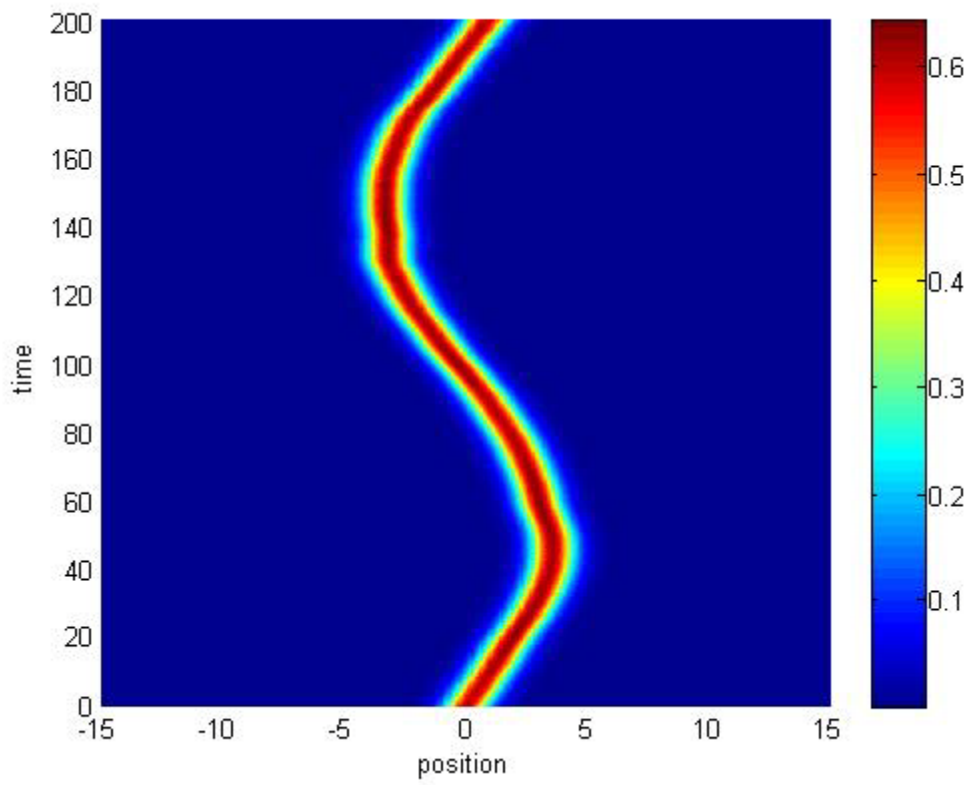
3.1.2.5 Density Profile for  $\lambda_1 = 0.08$  and  $\lambda_2 = 0.02$



3.1.2.6 Density Profile for  $\lambda_1 = 0.1$  and  $\lambda_2 = 0.02$

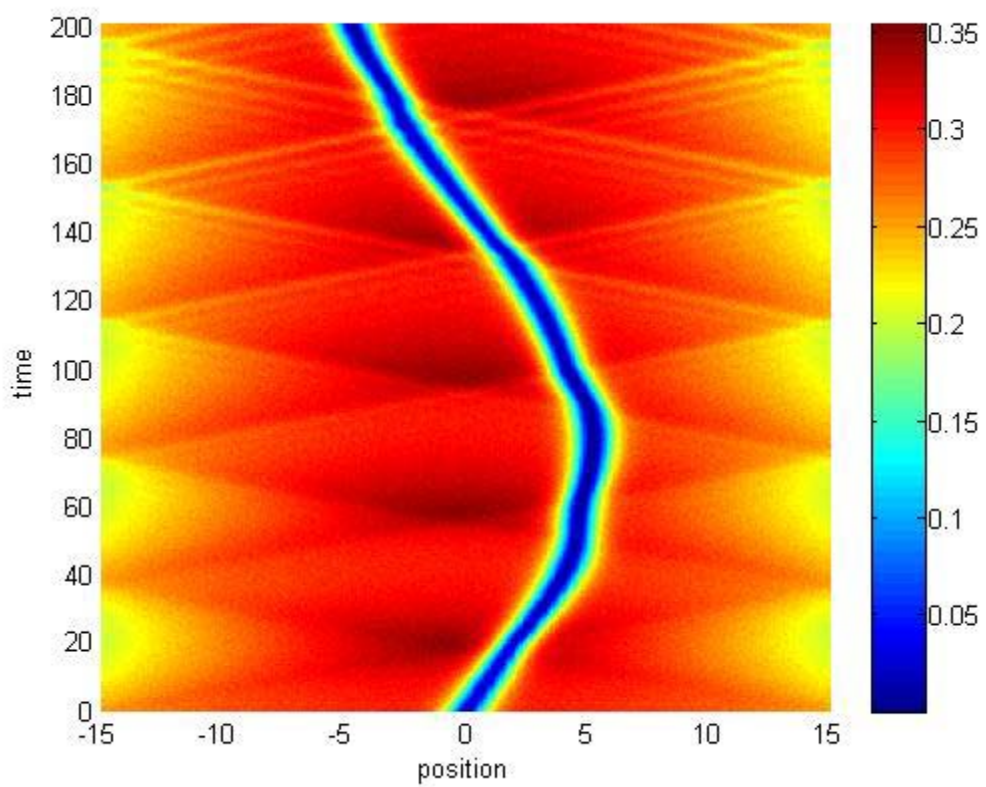
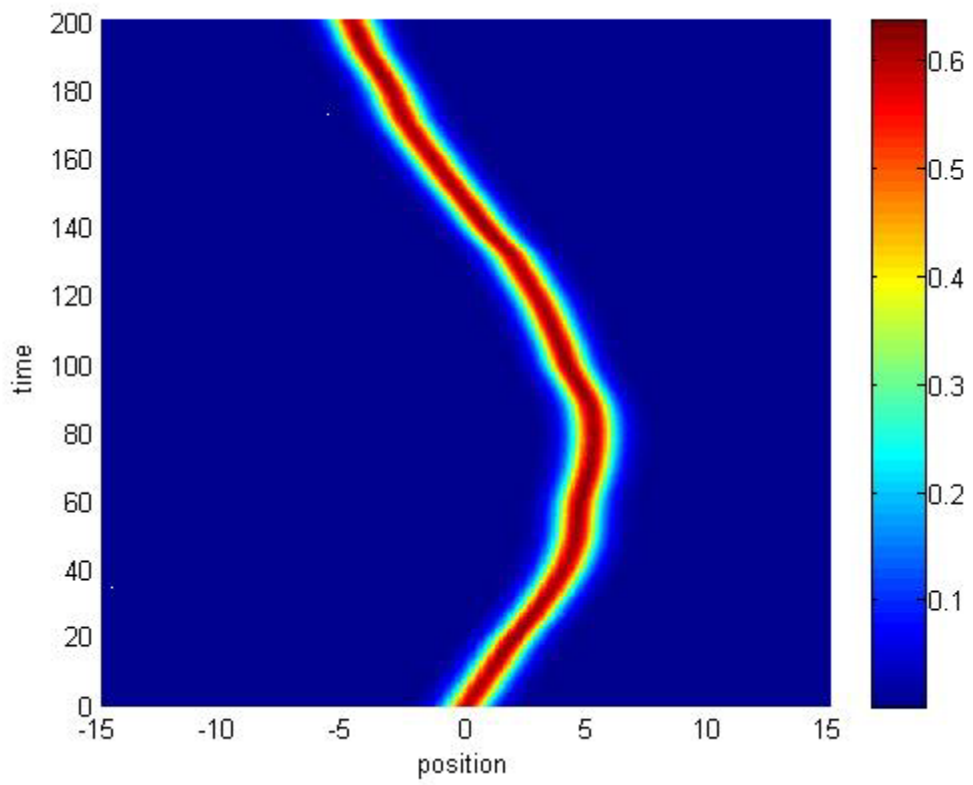


3.1.3.1 Density Profile for  $\lambda_1 = 0$  and  $\lambda_2 = 0.04$

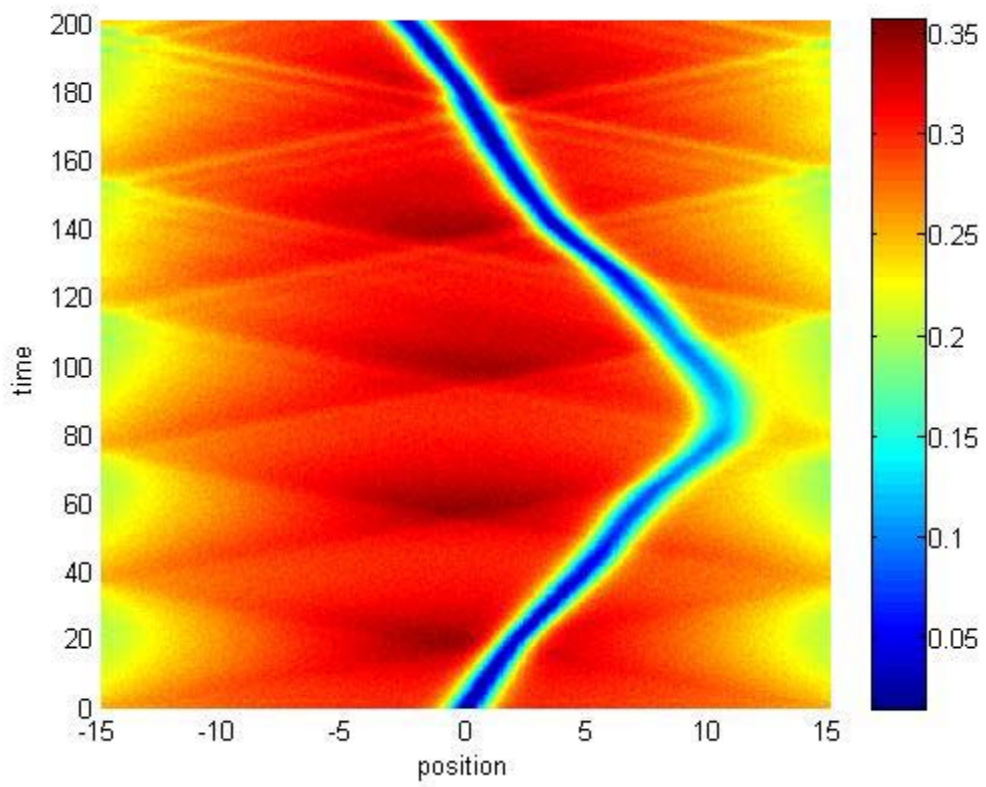
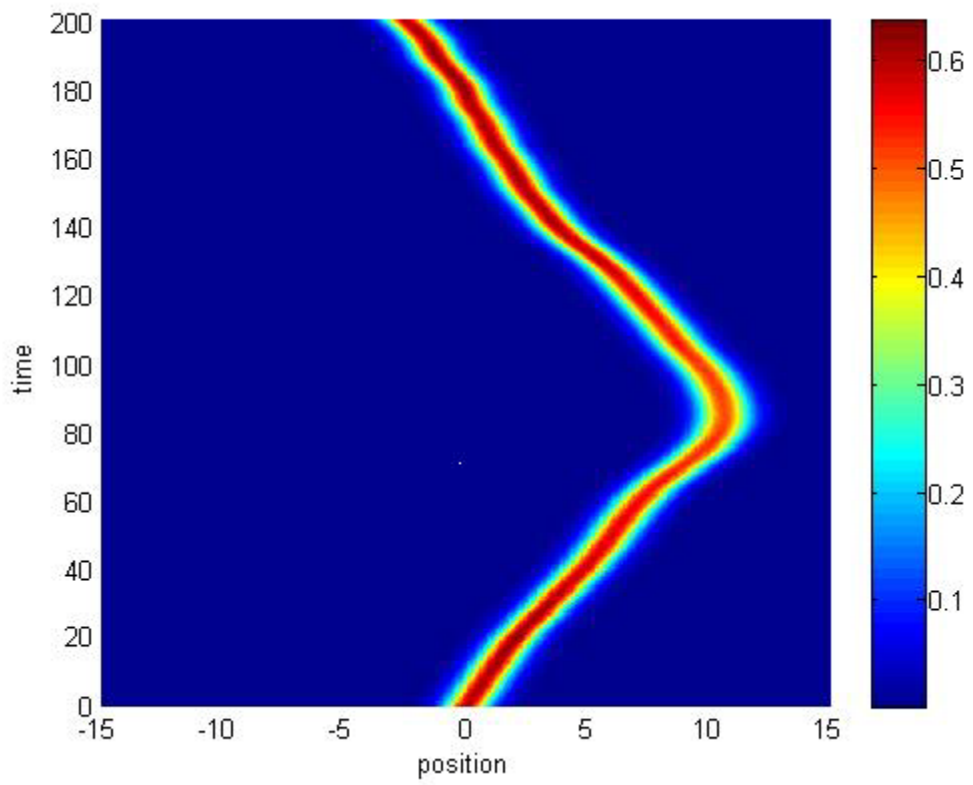


3.1.3.2 Density Profile for  $\lambda_1 = 0.02$  and  $\lambda_2 = 0.04$

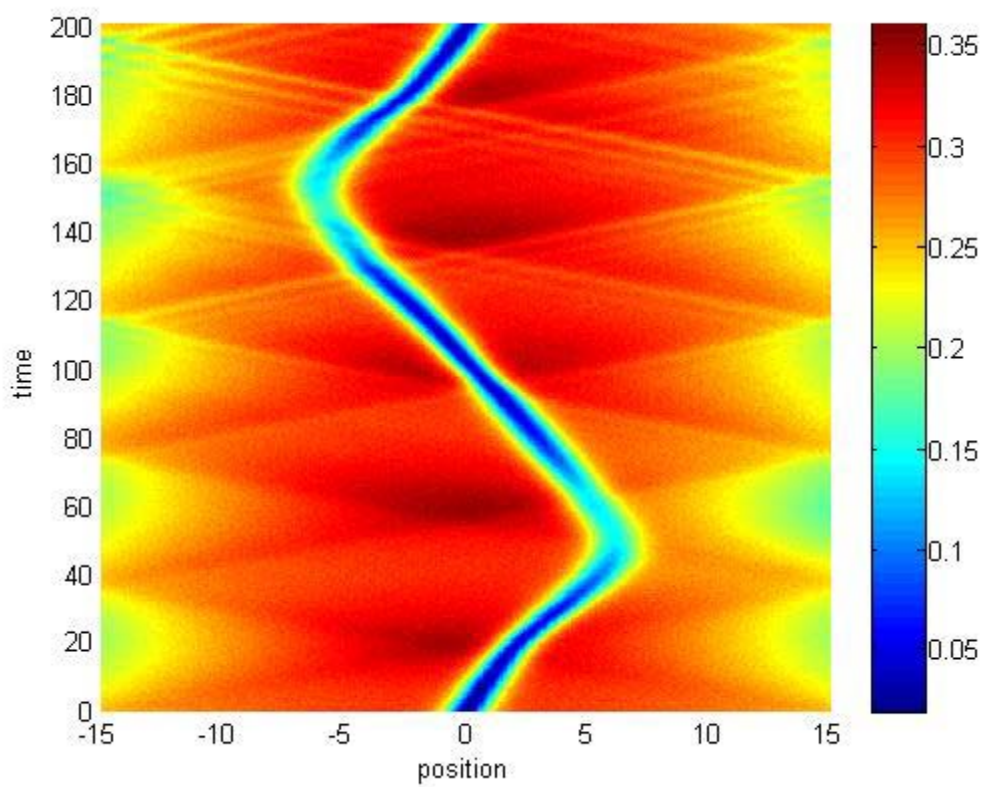
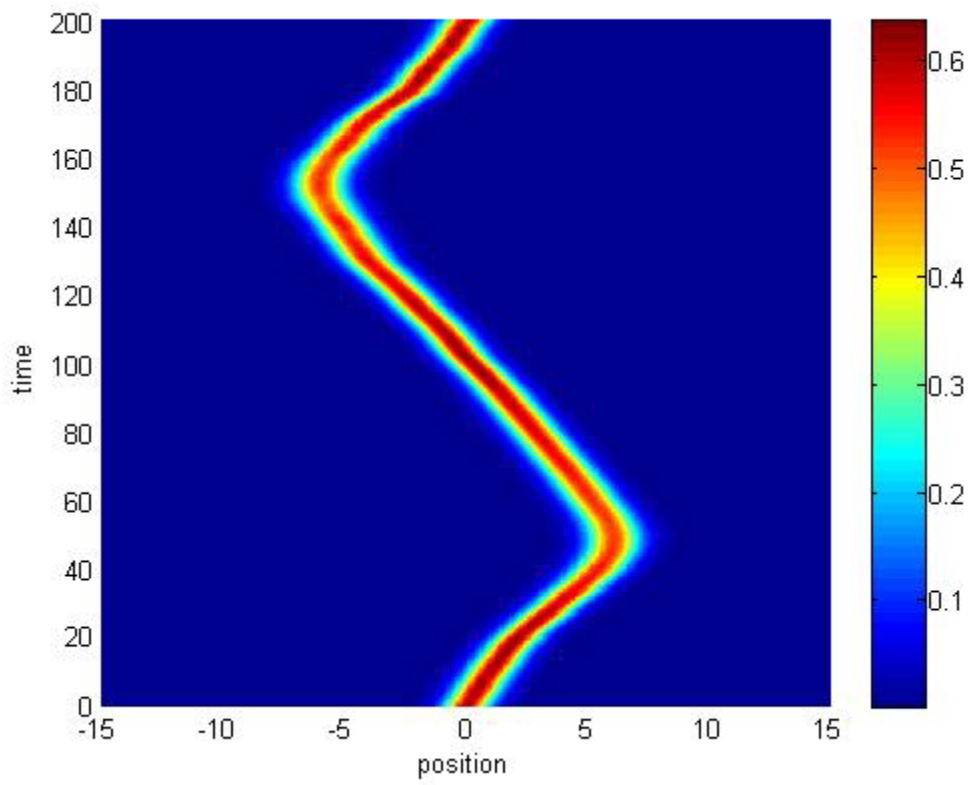




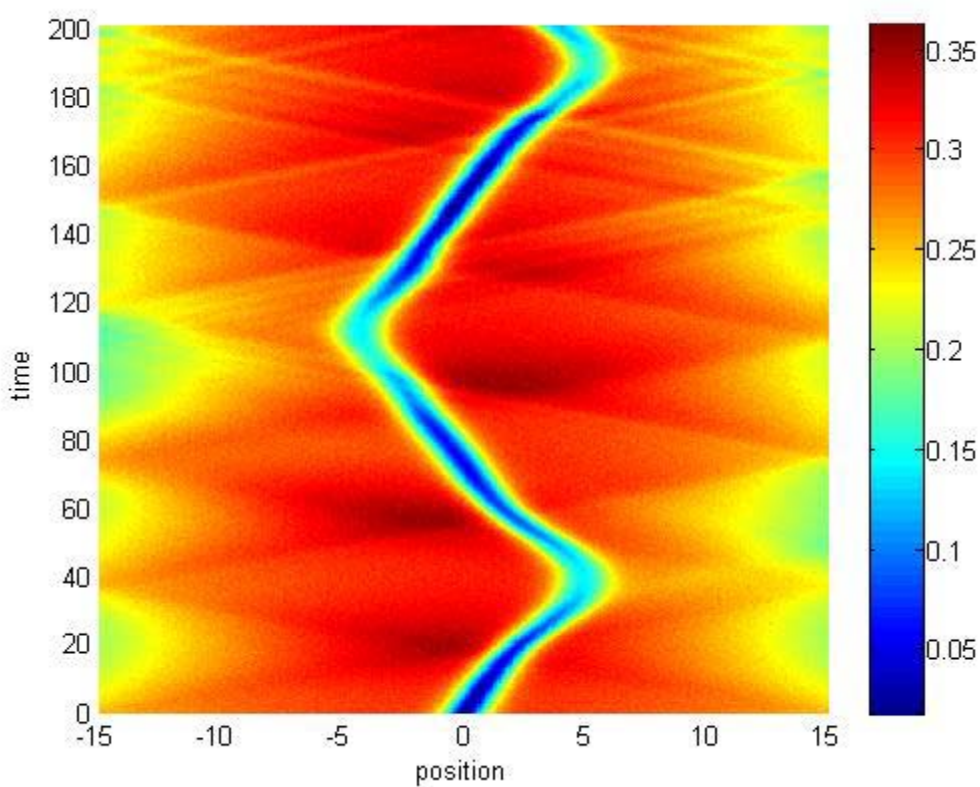
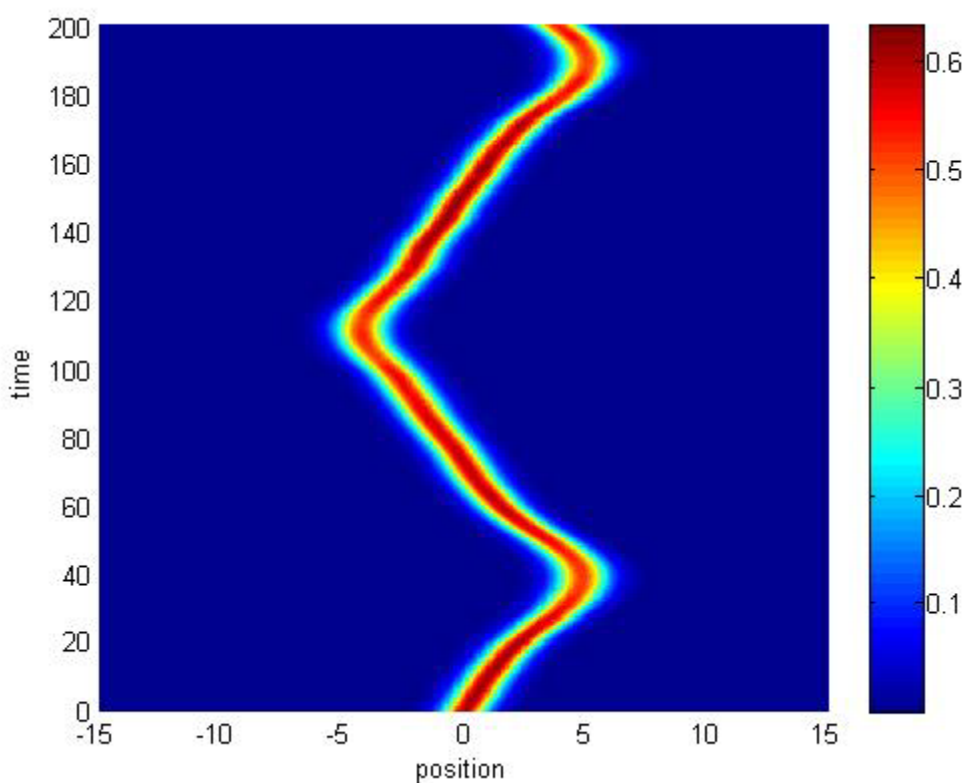
3.1.3.3 Density Profile for  $\lambda_1 = 0.04$  and  $\lambda_2 = 0.04$



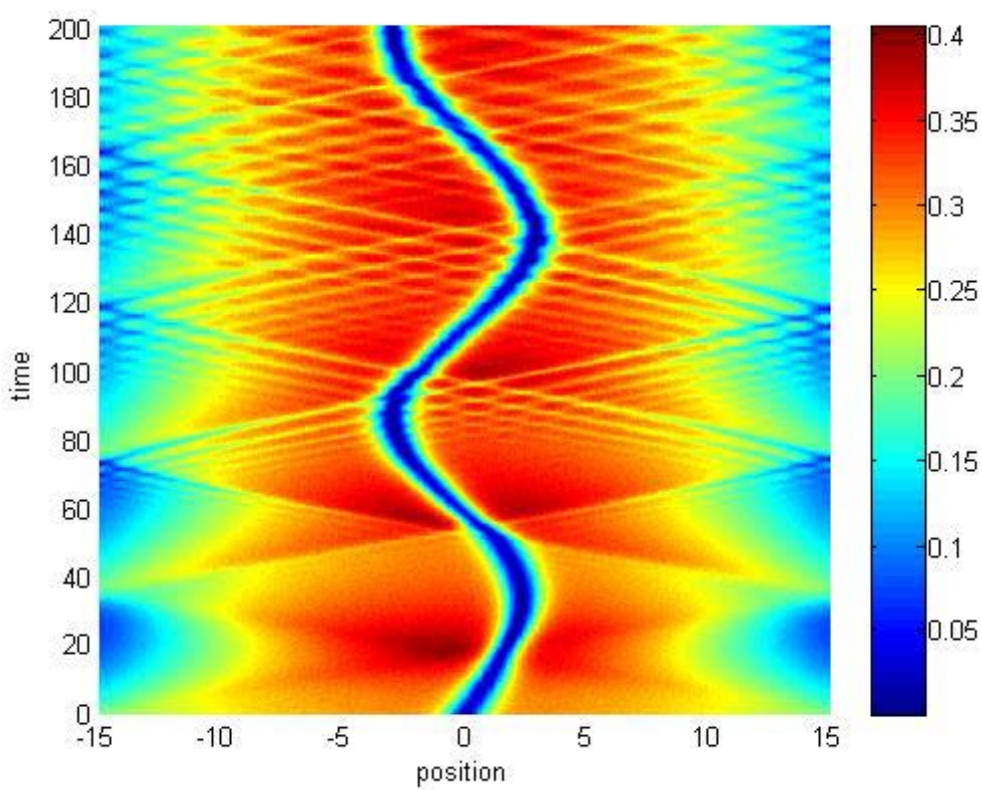
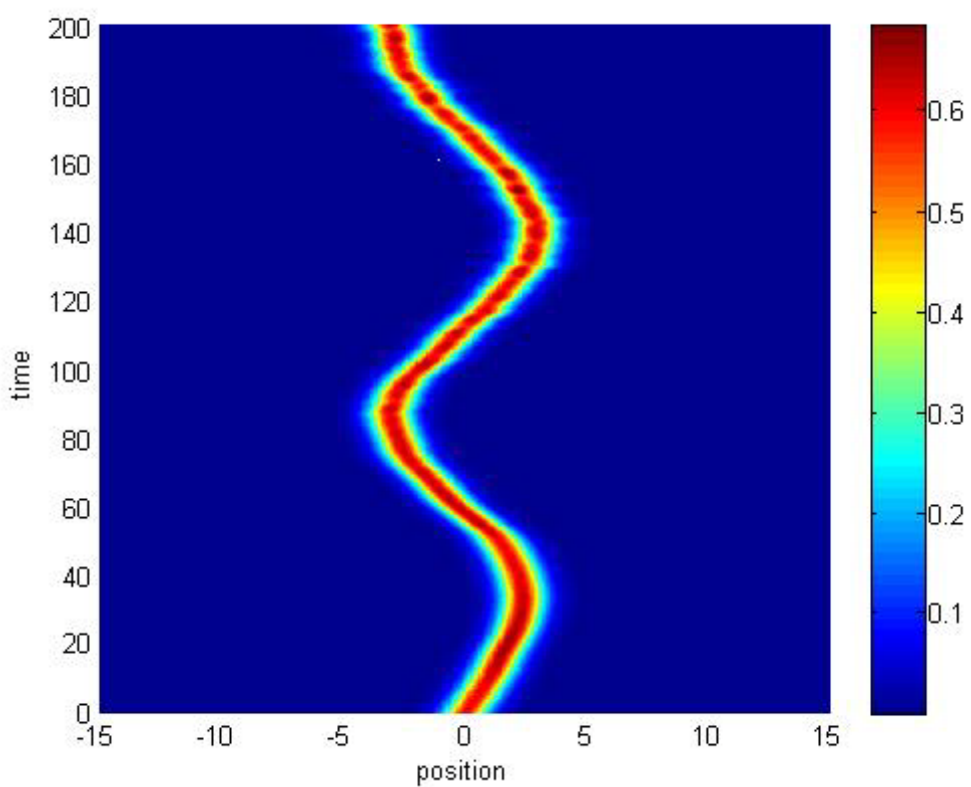
3.1.3.4 Density Profile for  $\lambda_1 = 0.06$  and  $\lambda_2 = 0.04$



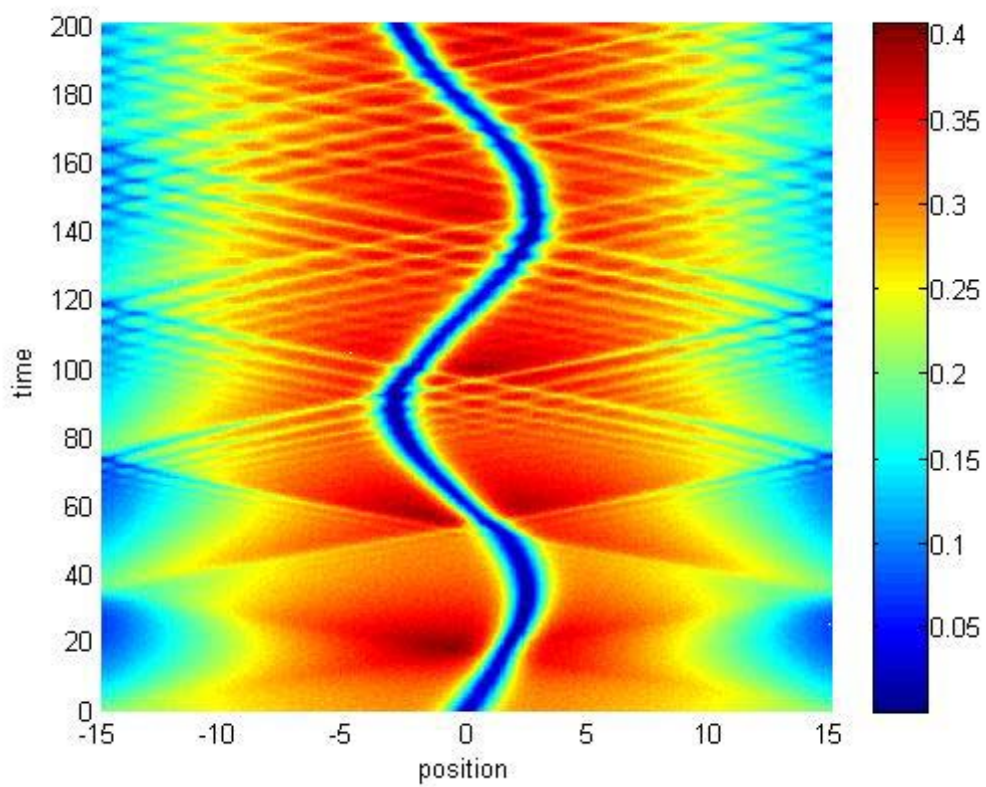
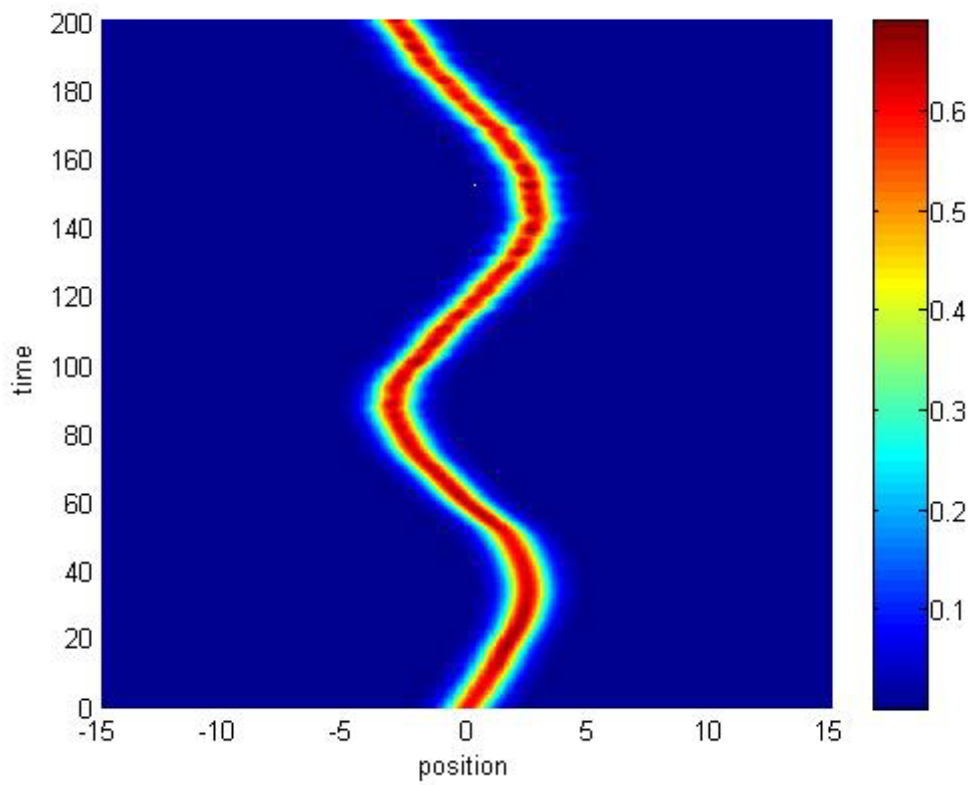
3.1.3.5 Density Profile for  $\lambda_1 = 0.08$  and  $\lambda_2 = 0.04$



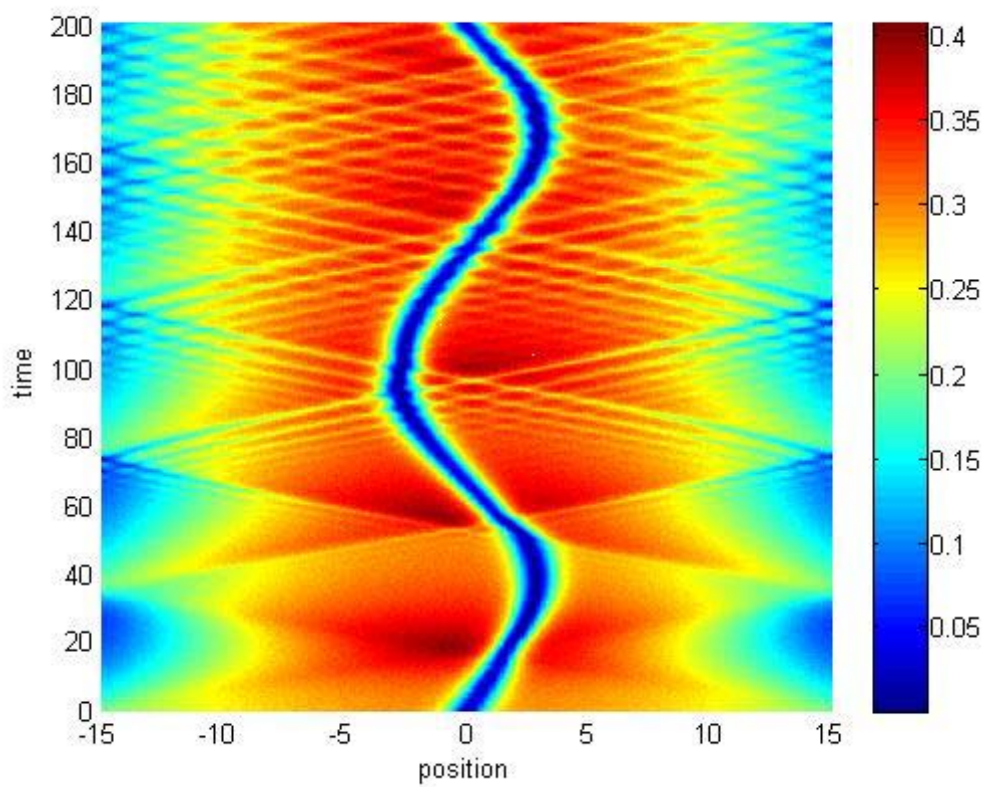
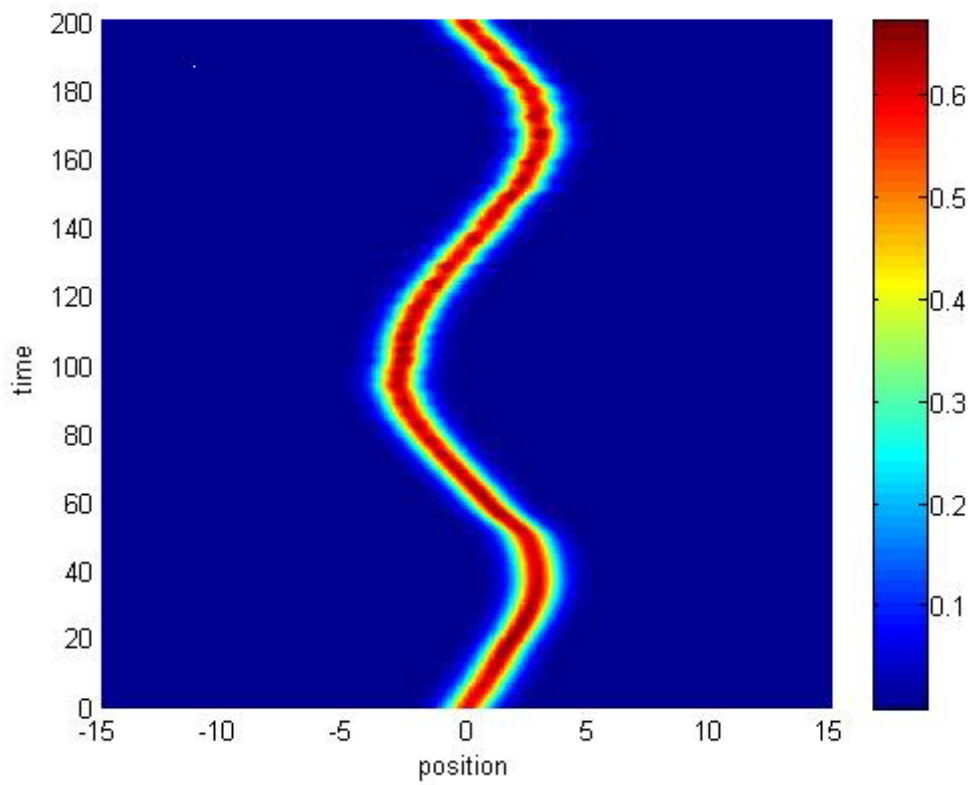
3.1.3.6 Density Profile for  $\lambda_1 = 0.1$  and  $\lambda_2 = 0.04$



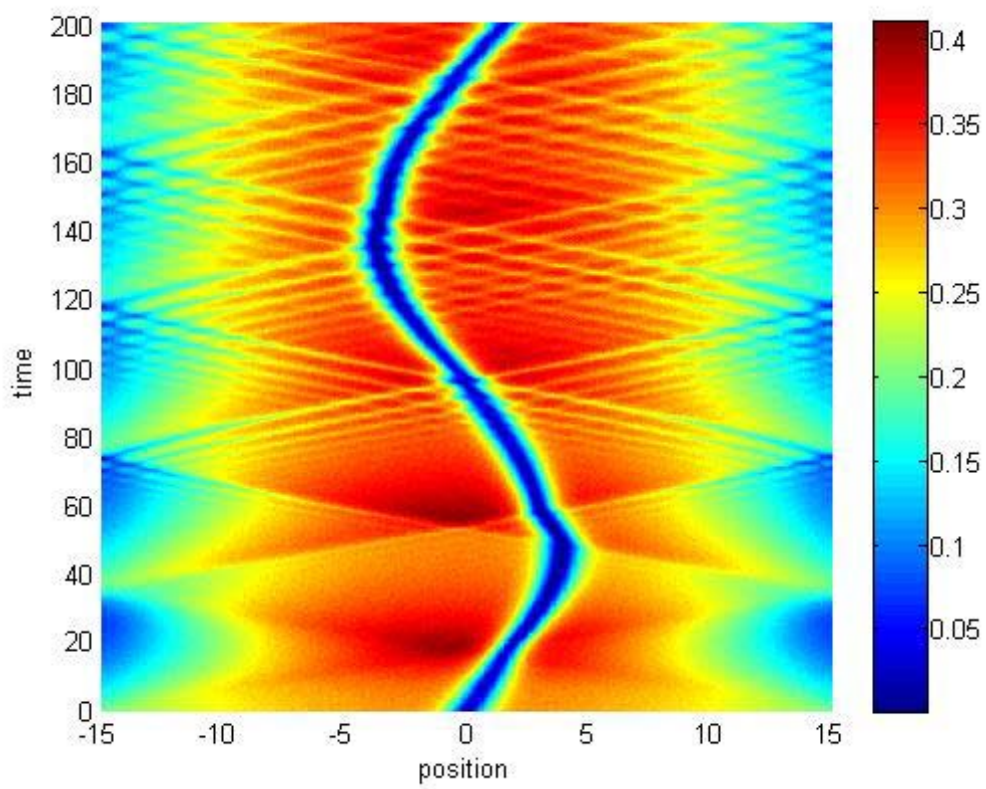
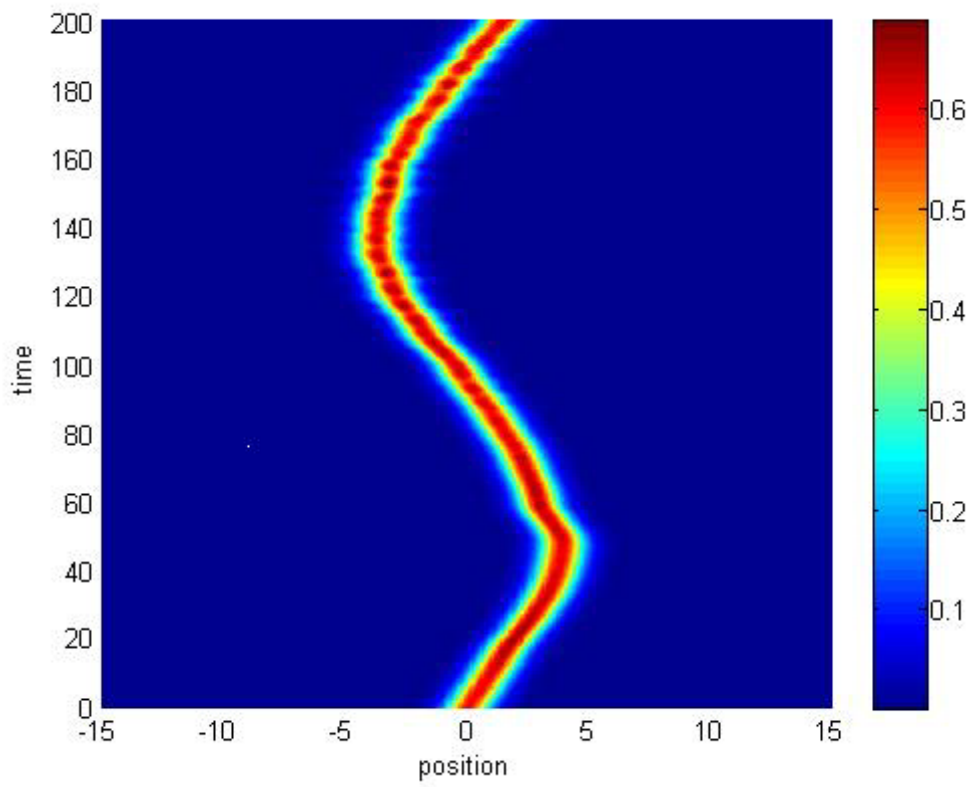
3.1.4.1 Density Profile for  $\lambda_1 = 0$  and  $\lambda_2 = 0.06$



3.1.4.2 Density Profile for  $\lambda_1 = 0.02$  and  $\lambda_2 = 0.06$

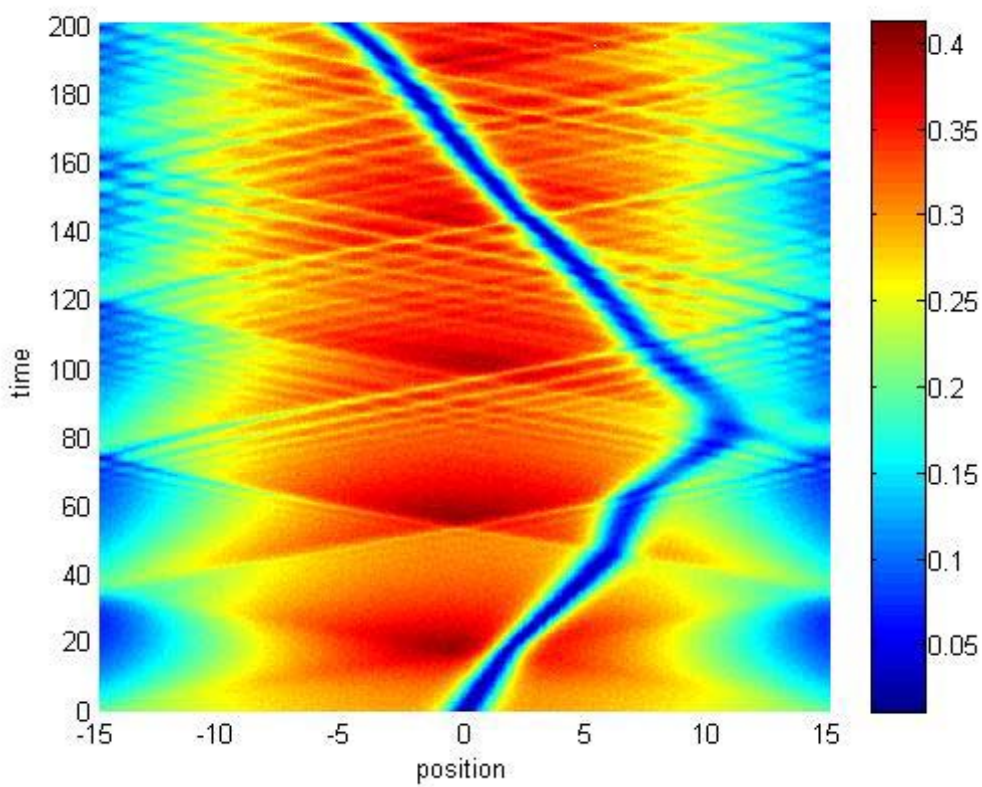
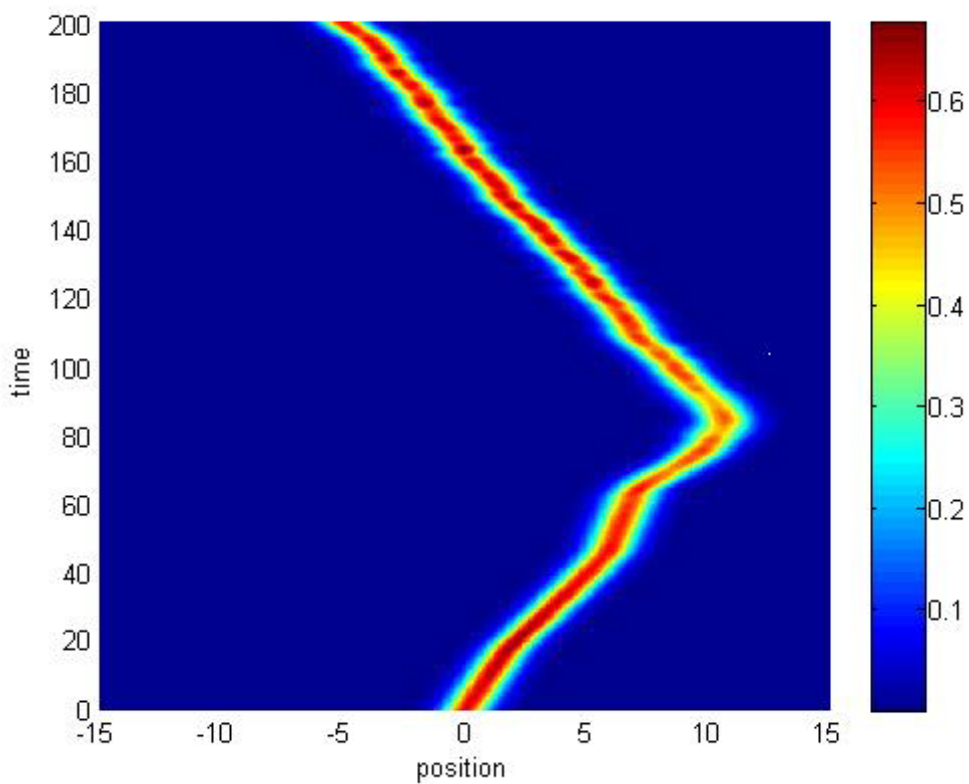


3.1.4.3 Density Profile for  $\lambda_1 = 0.04$  and  $\lambda_2 = 0.06$

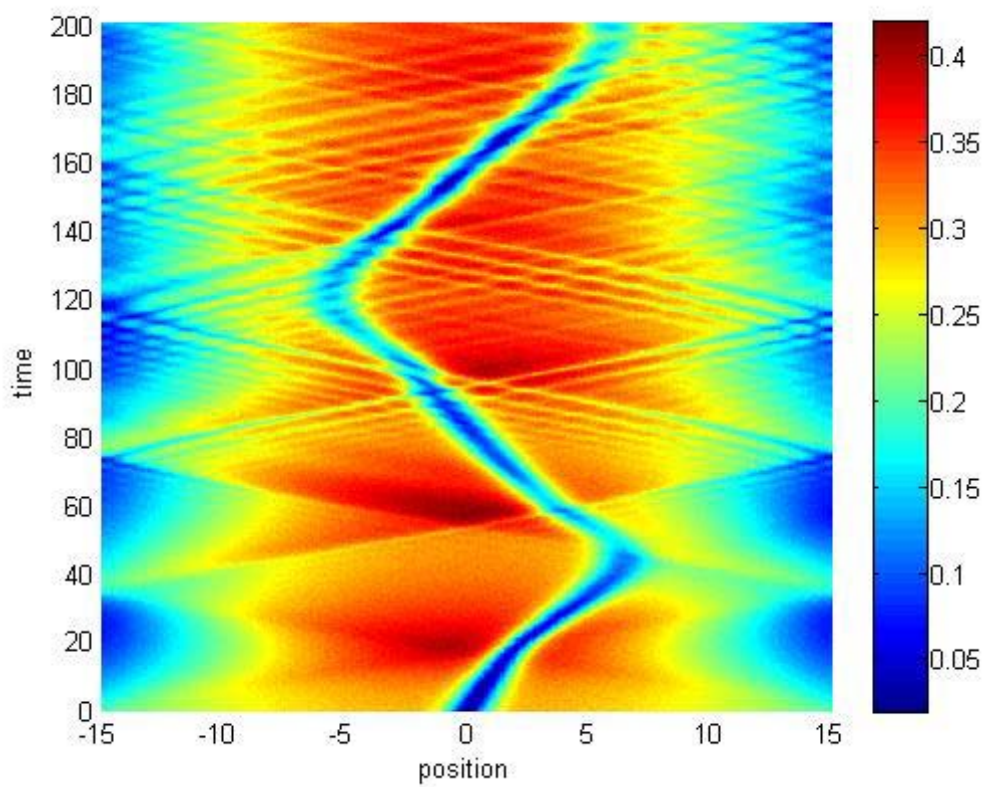
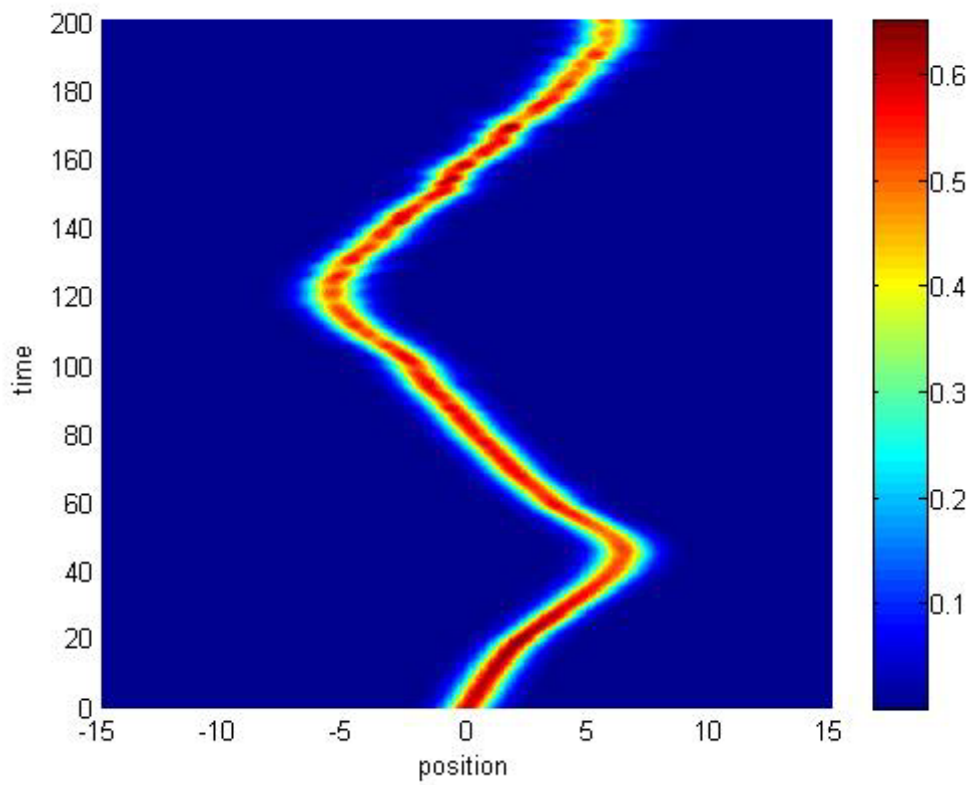


3.1.4.4 Density Profile for  $\lambda_1 = 0.06$  and  $\lambda_2 = 0.06$

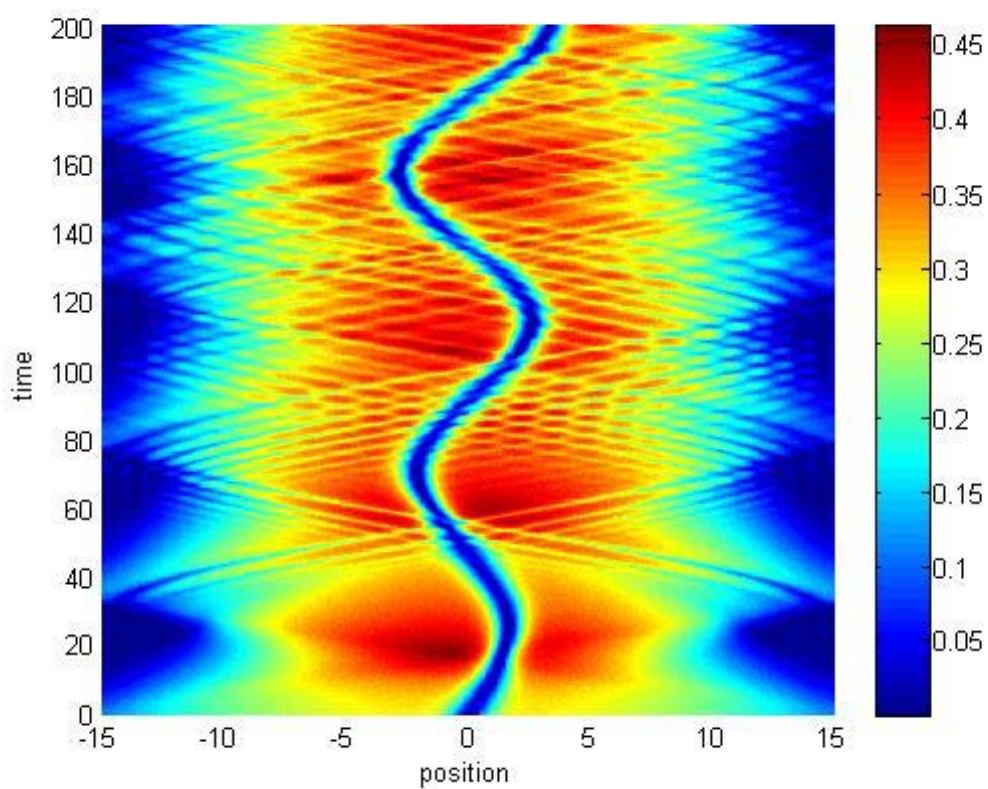
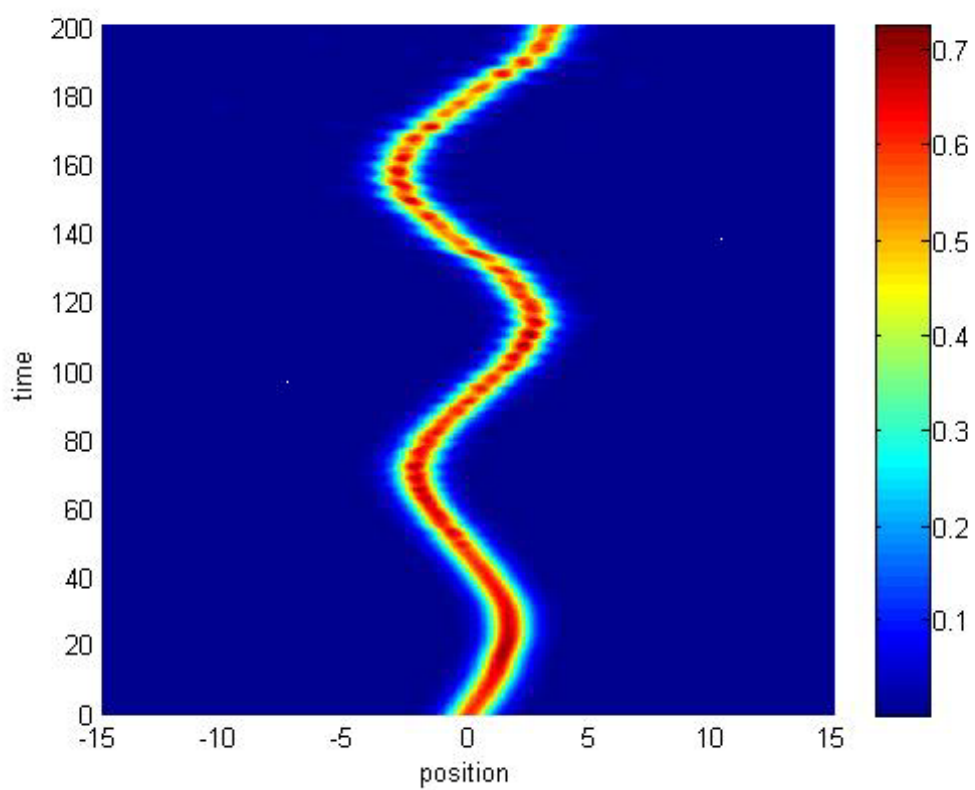




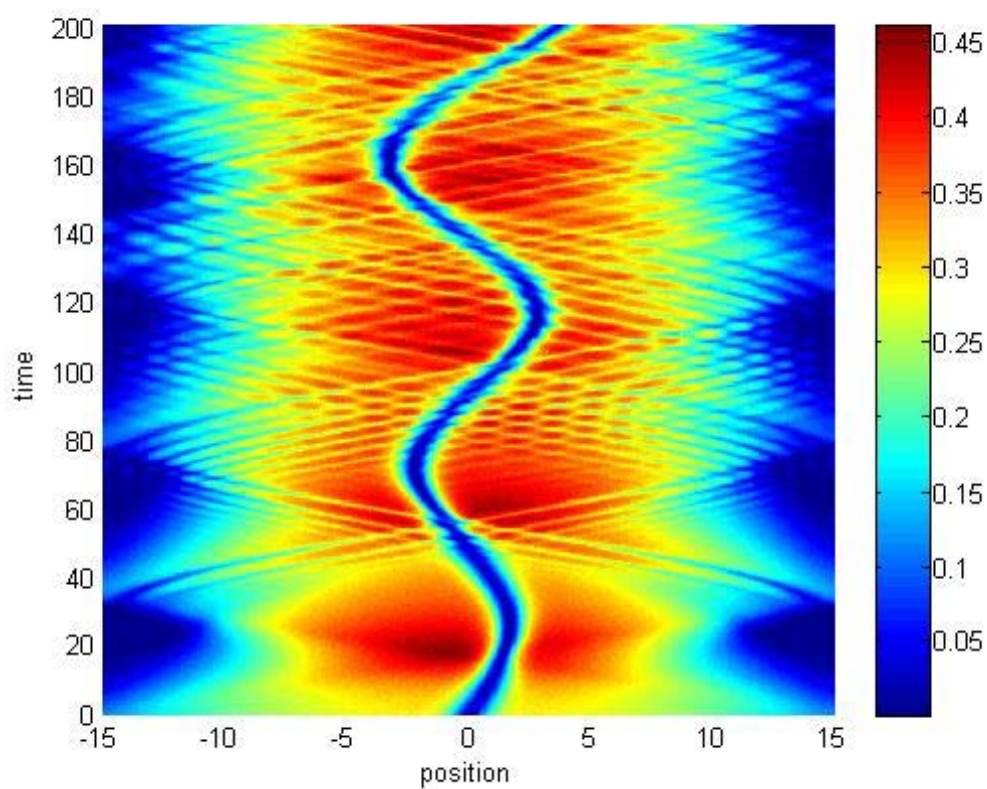
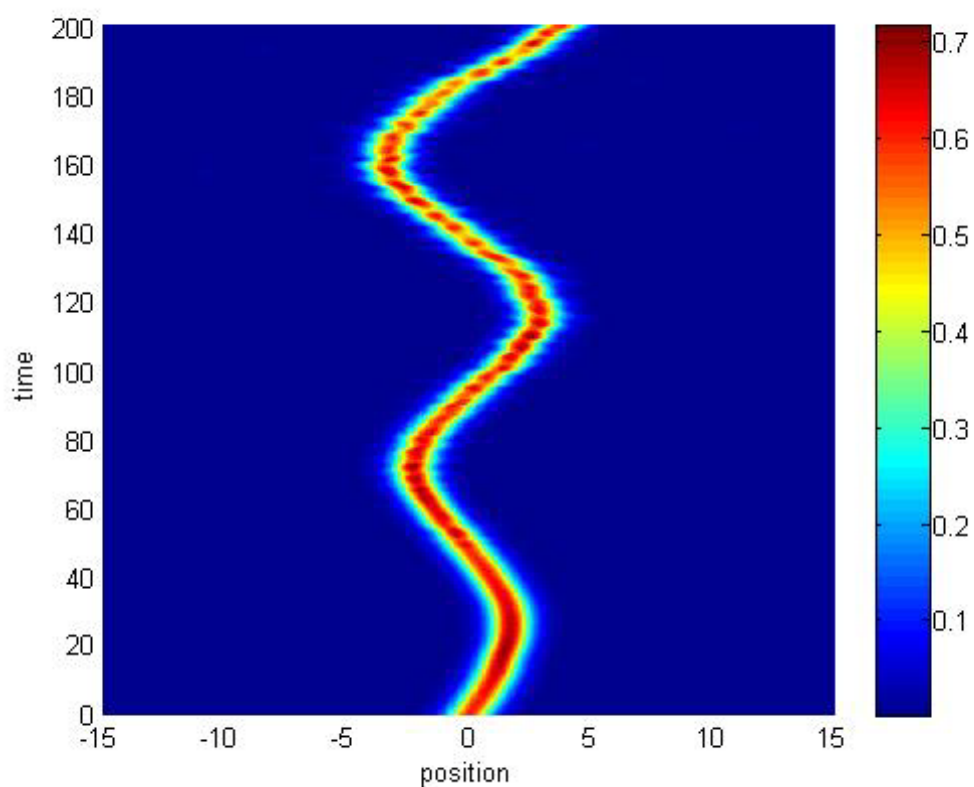
3.1.4.5 Density Profile for  $\lambda_1 = 0.08$  and  $\lambda_2 = 0.06$



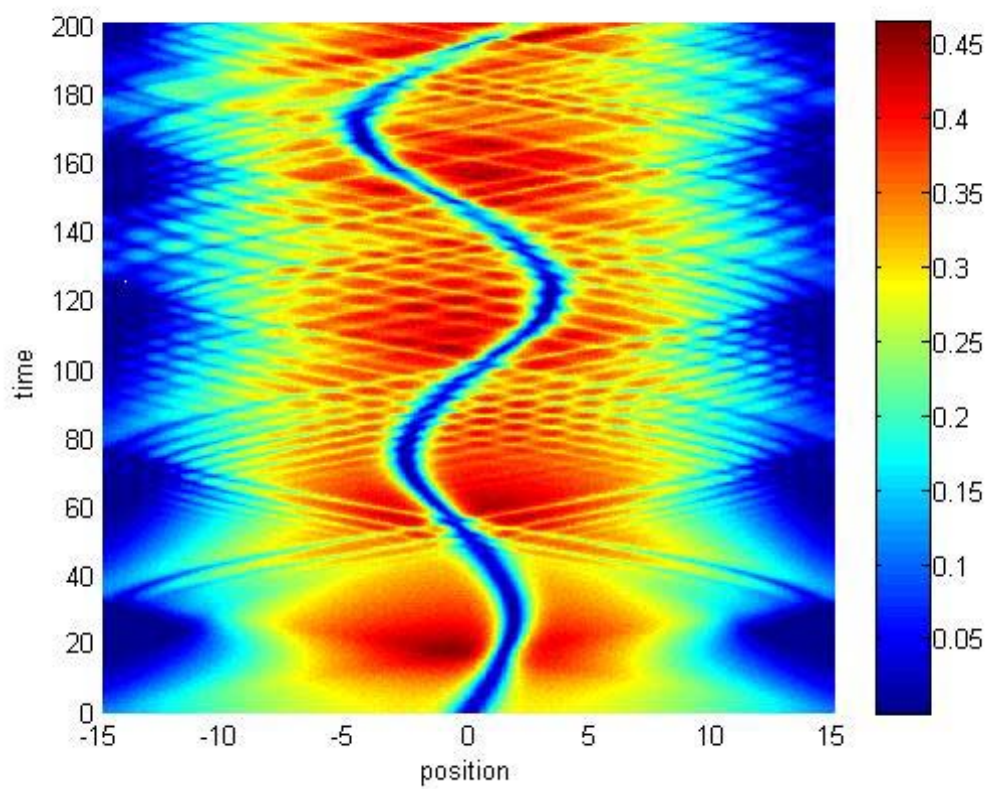
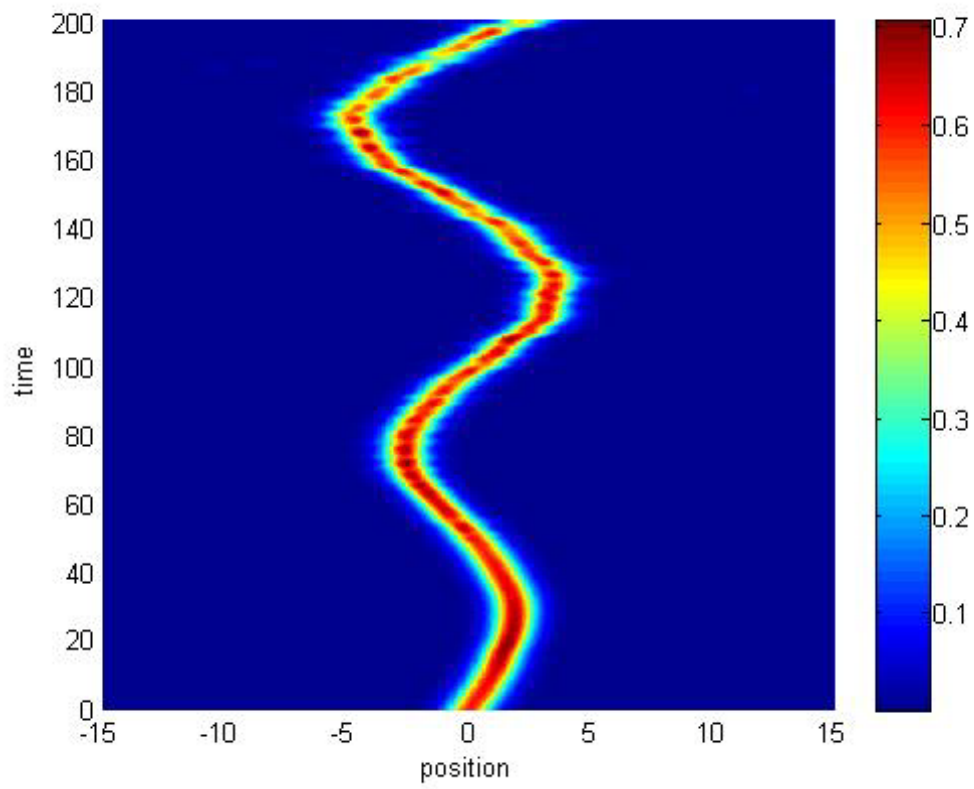
3.1.4.6 Density Profile for  $\lambda_1 = 0.1$  and  $\lambda_2 = 0.06$



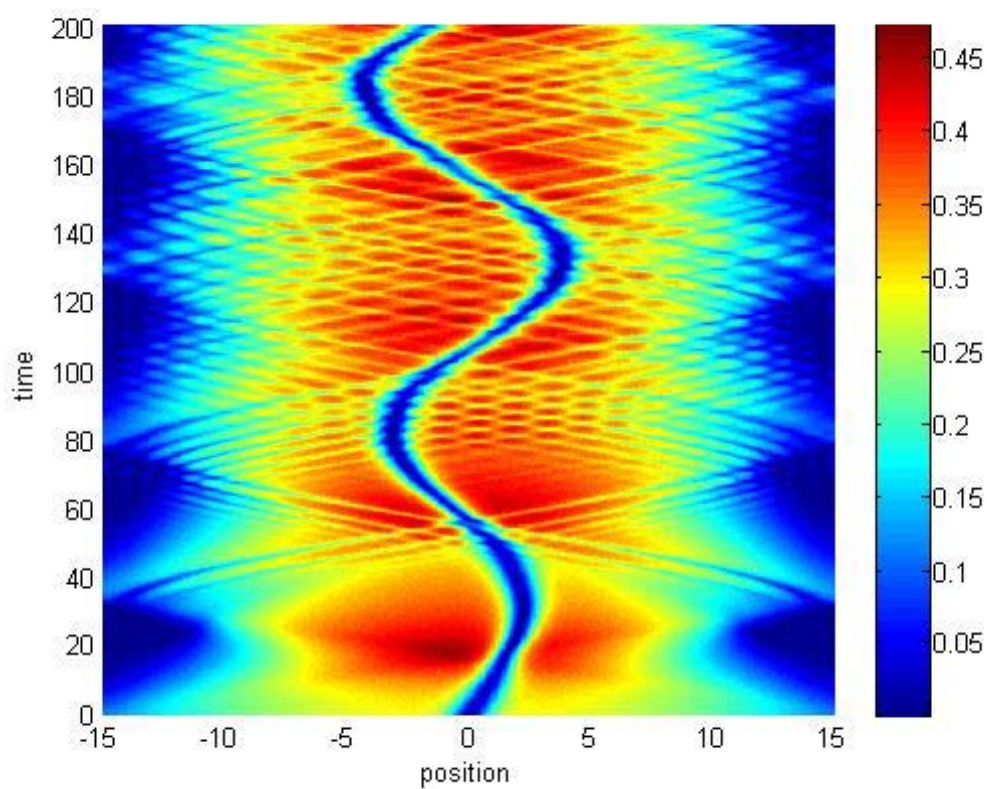
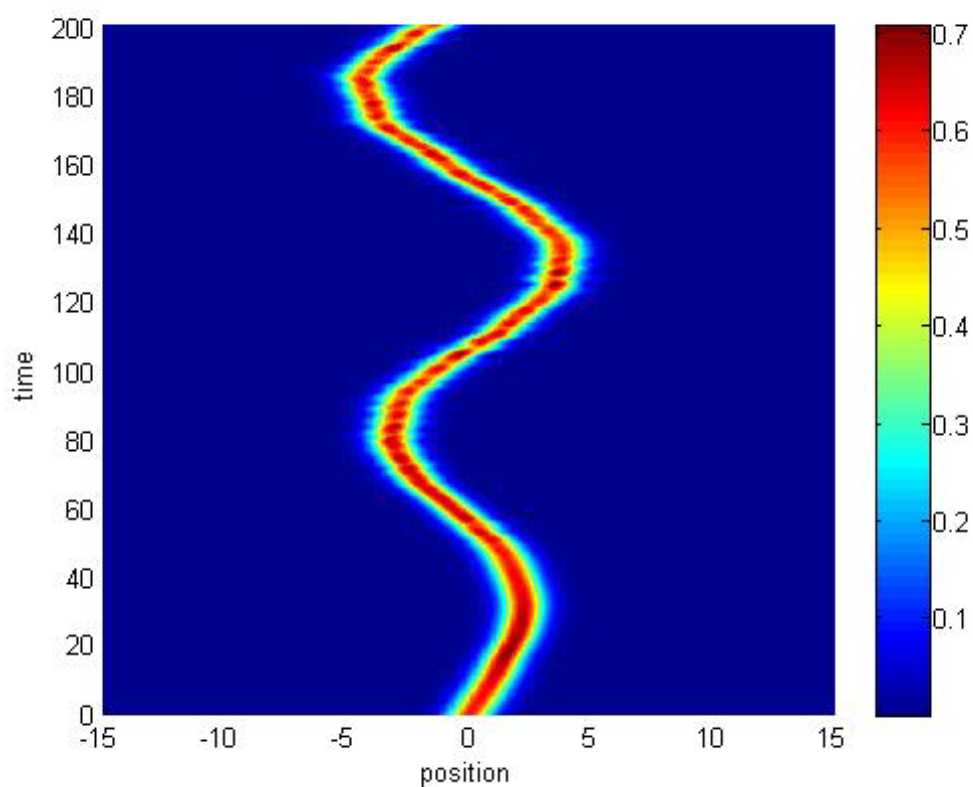
3.1.5.1 Density Profile for  $\lambda_1 = 0$  and  $\lambda_2 = 0.08$



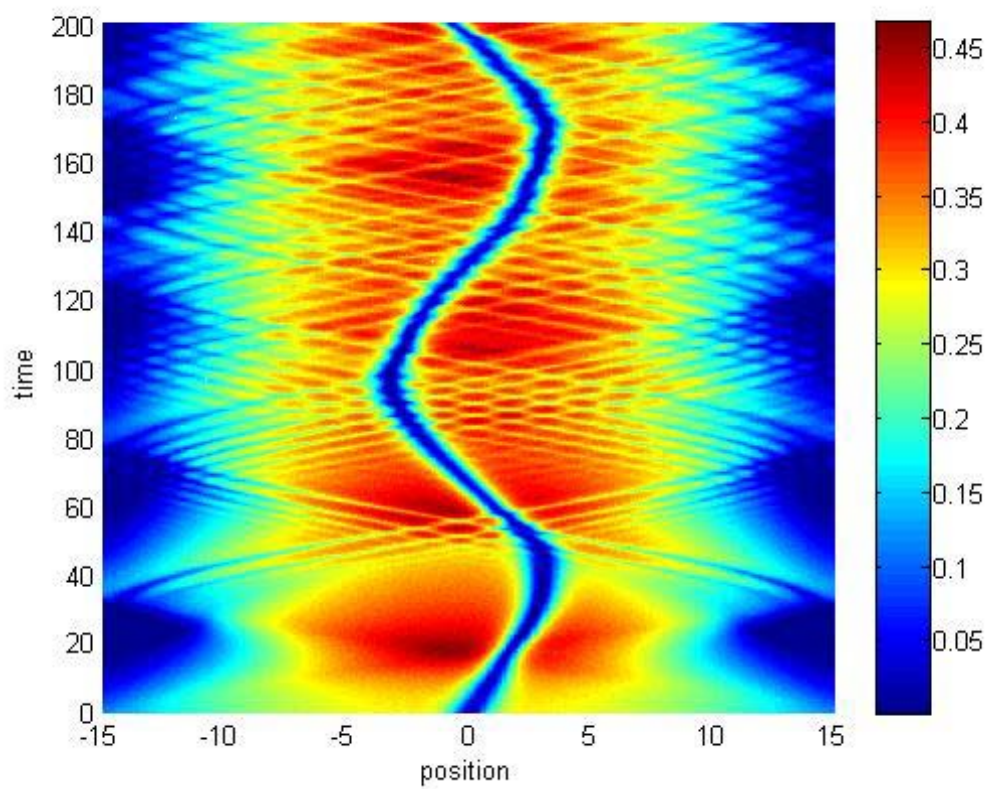
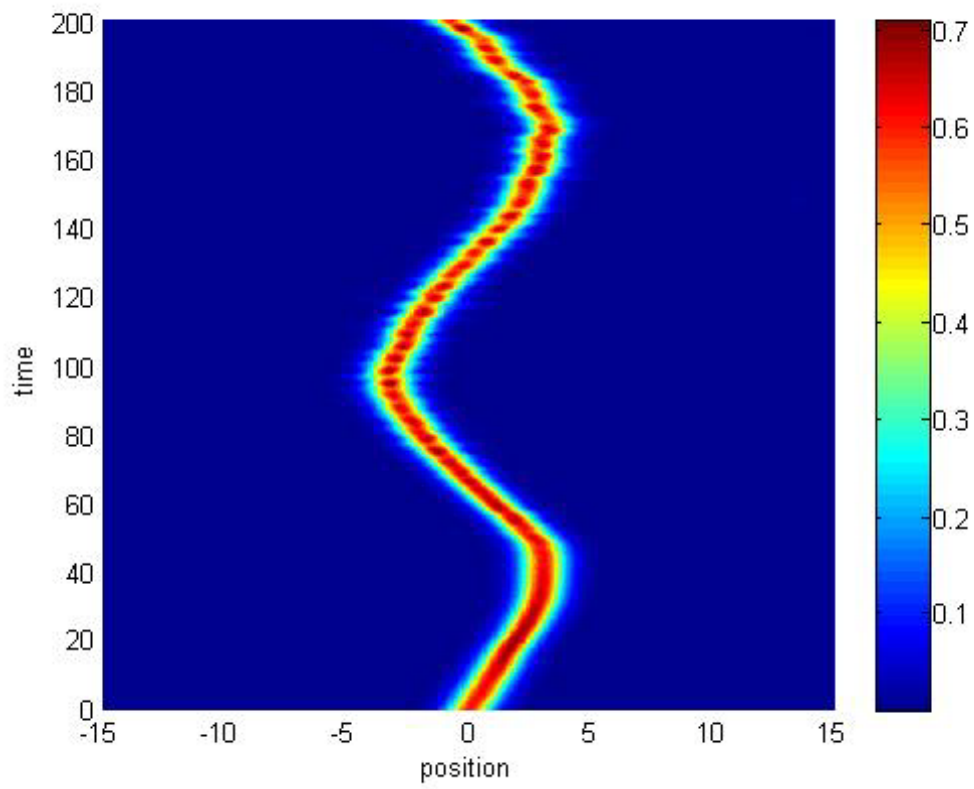
3.1.5.2 Density Profile for  $\lambda_1 = 0.02$  and  $\lambda_2 = 0.08$



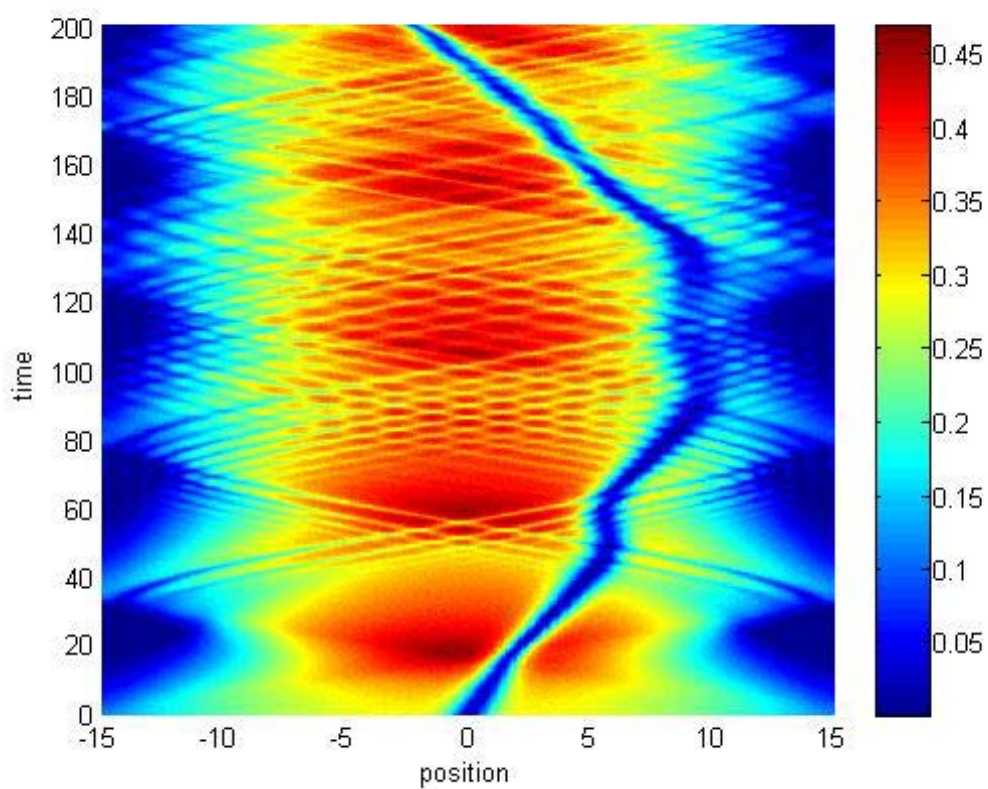
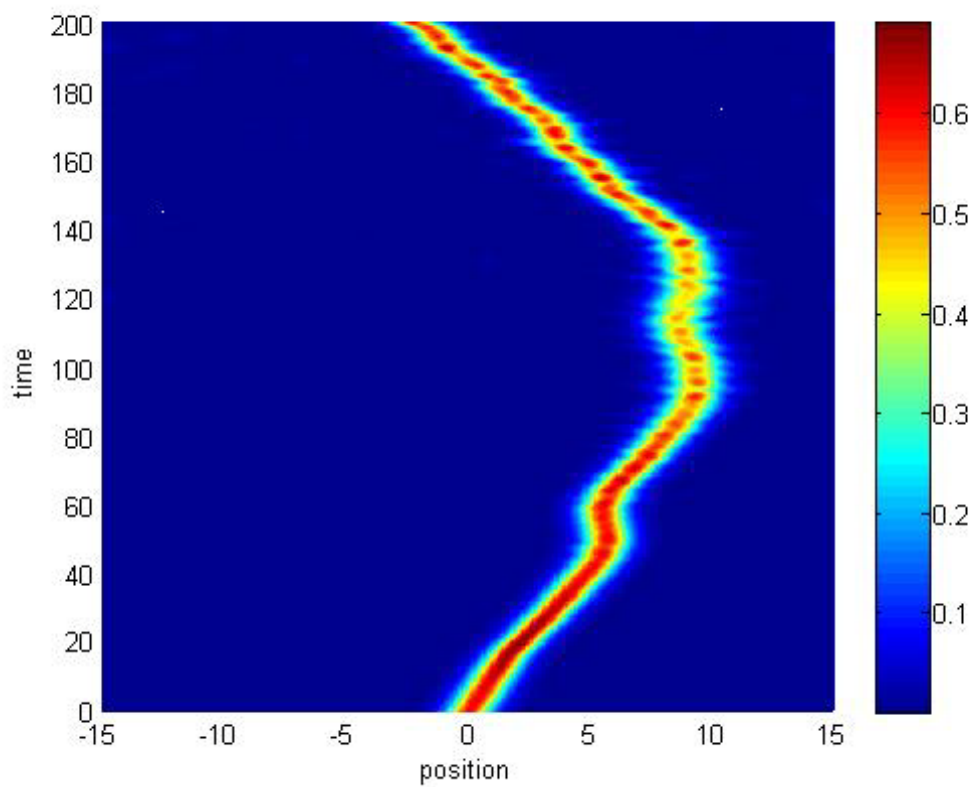
3.1.5.3 Density Profile for  $\lambda_1 = 0.04$  and  $\lambda_2 = 0.08$



3.1.5.4 Density Profile for  $\lambda_1 = 0.06$  and  $\lambda_2 = 0.08$

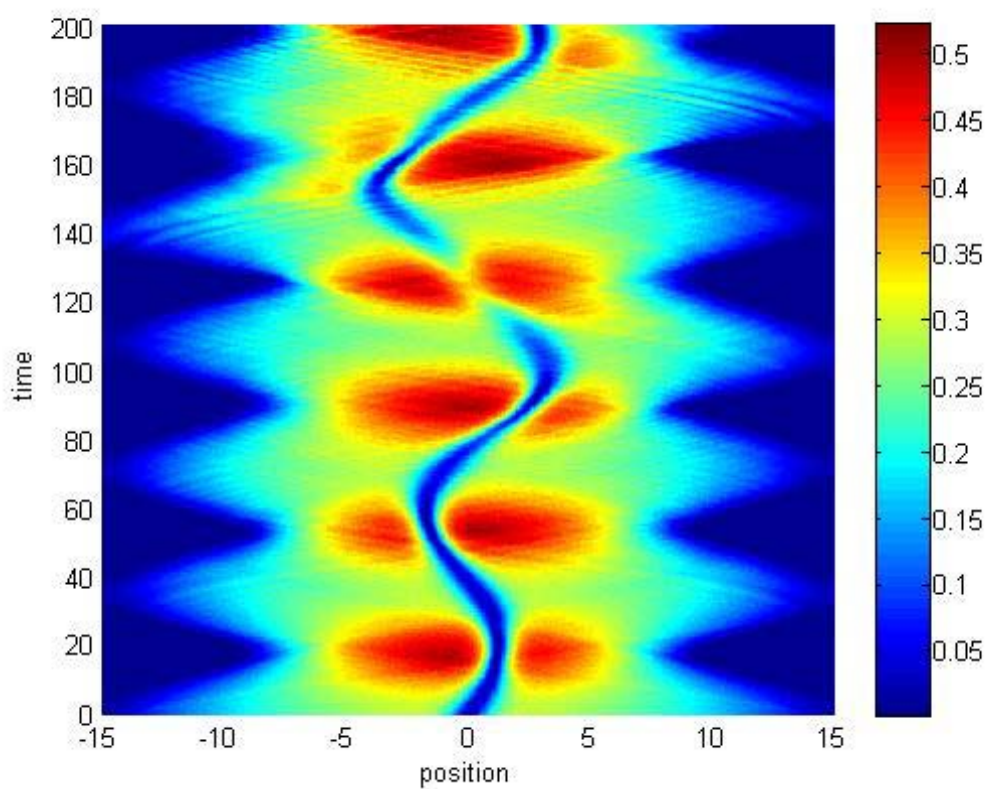
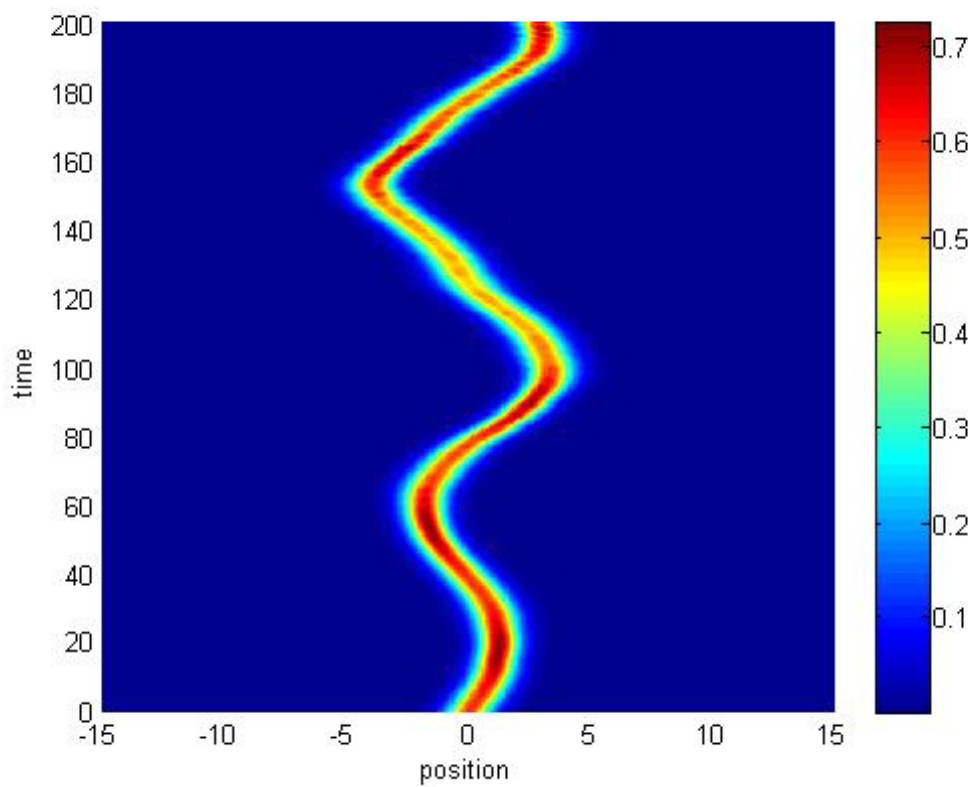


3.1.5.5 Density Profile for  $\lambda_1 = 0.08$  and  $\lambda_2 = 0.08$

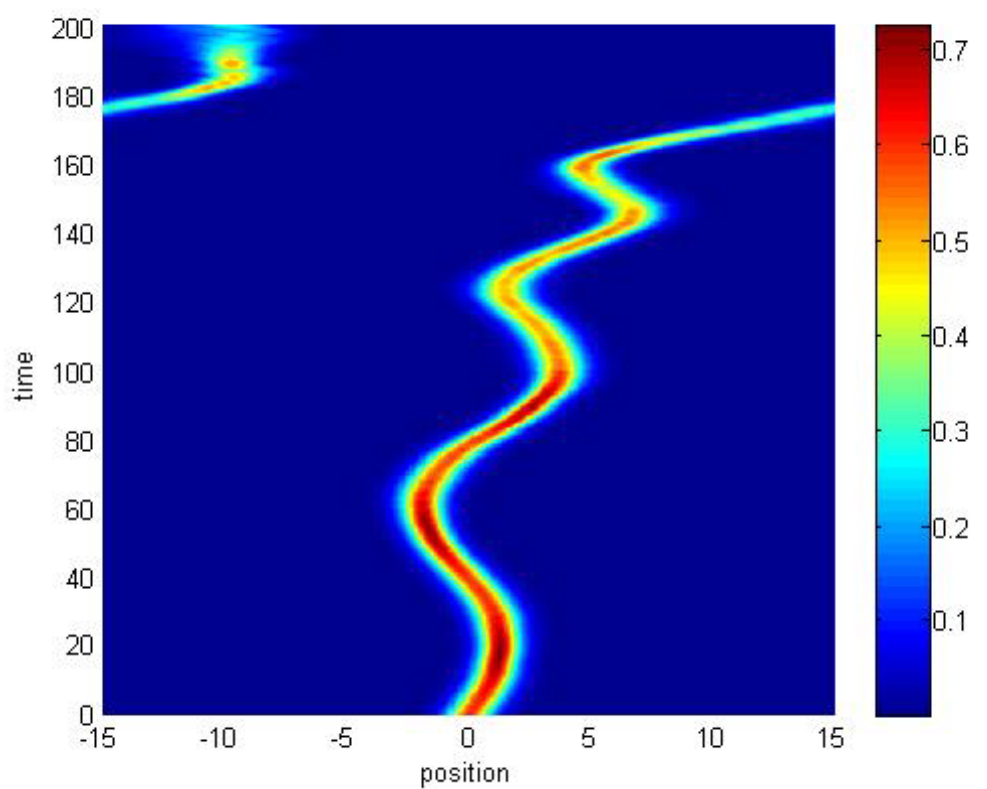
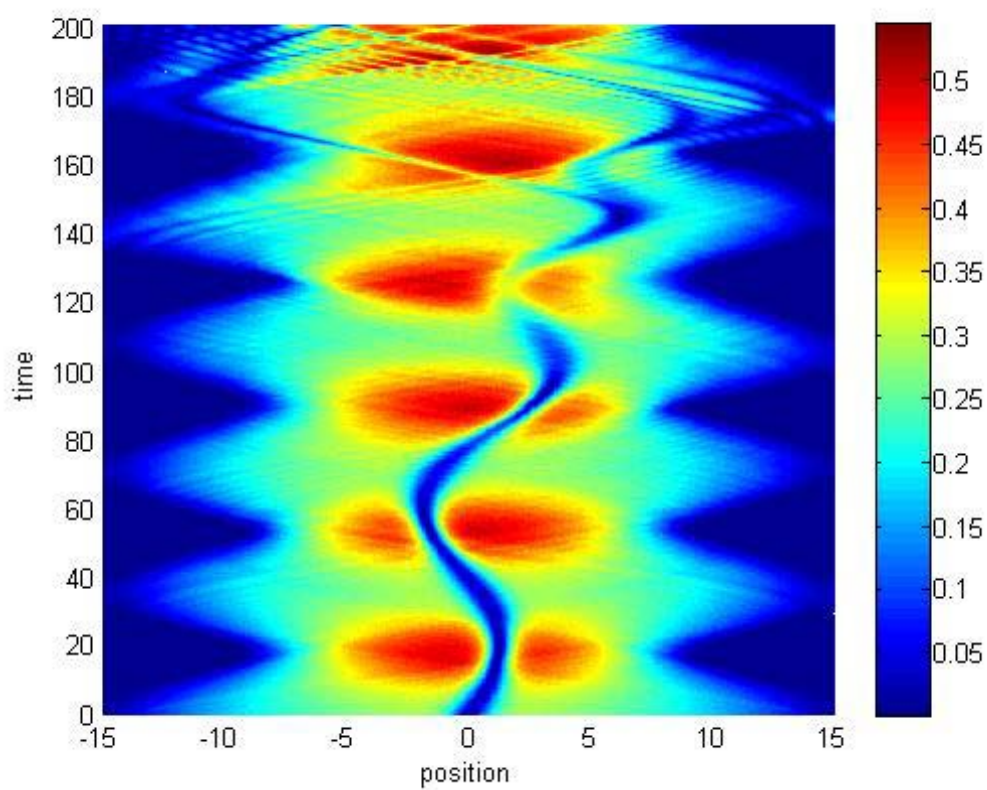


3.1.5.6 Density Profile for  $\lambda_1 = 0.1$  and  $\lambda_2 = 0.08$

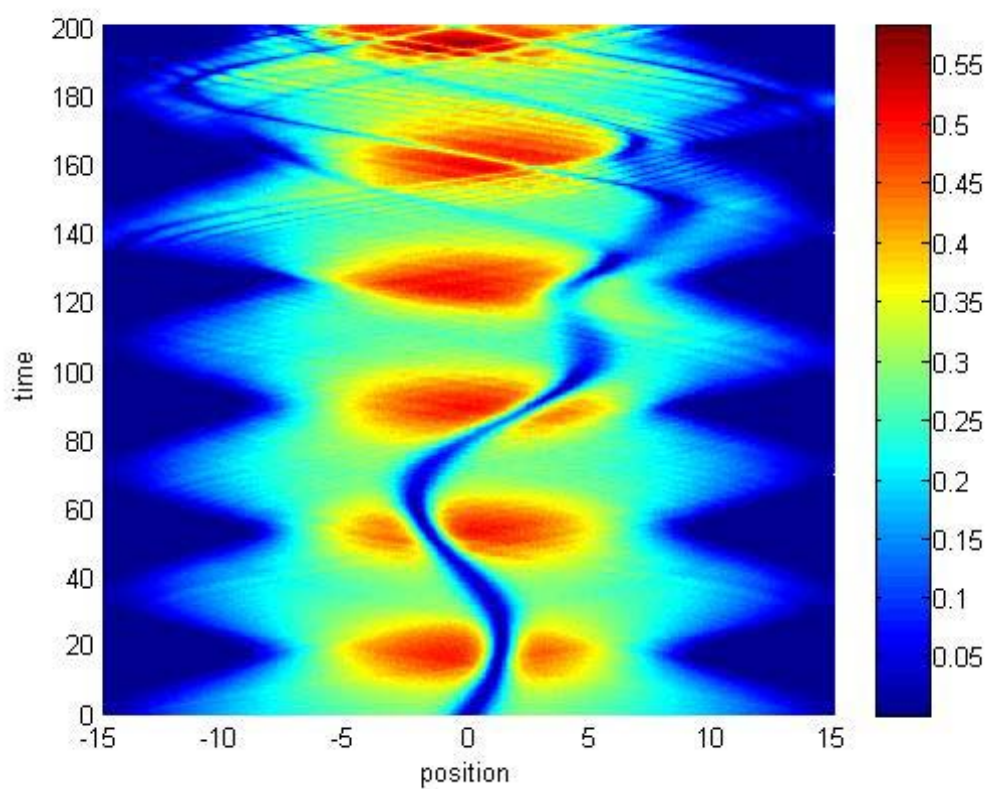
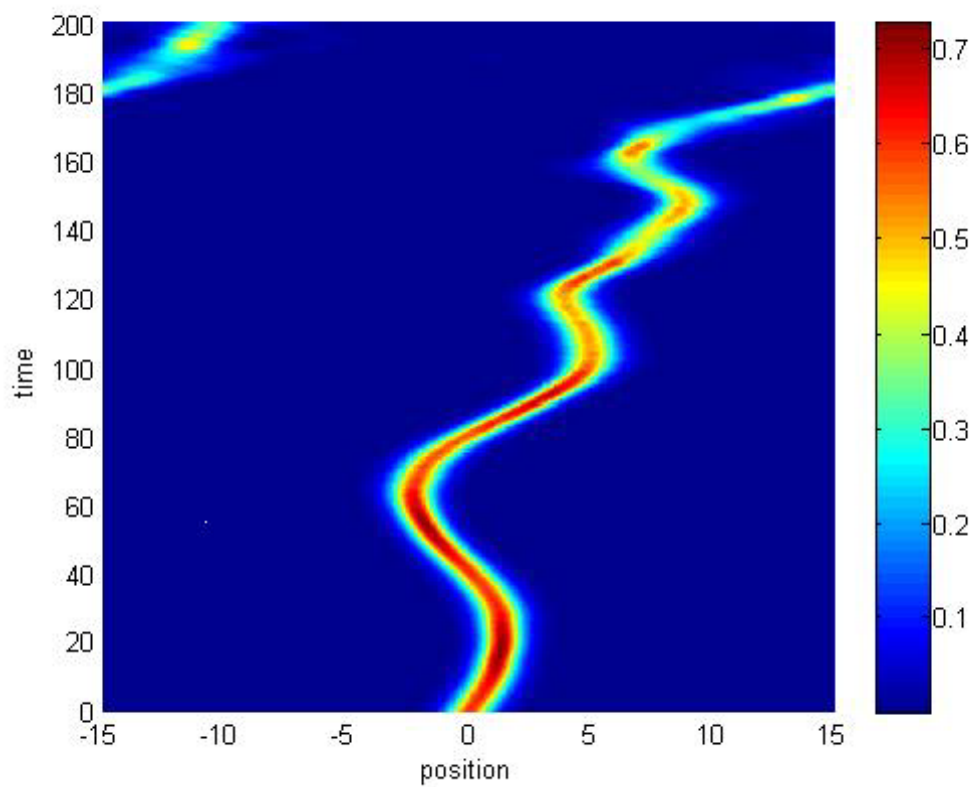




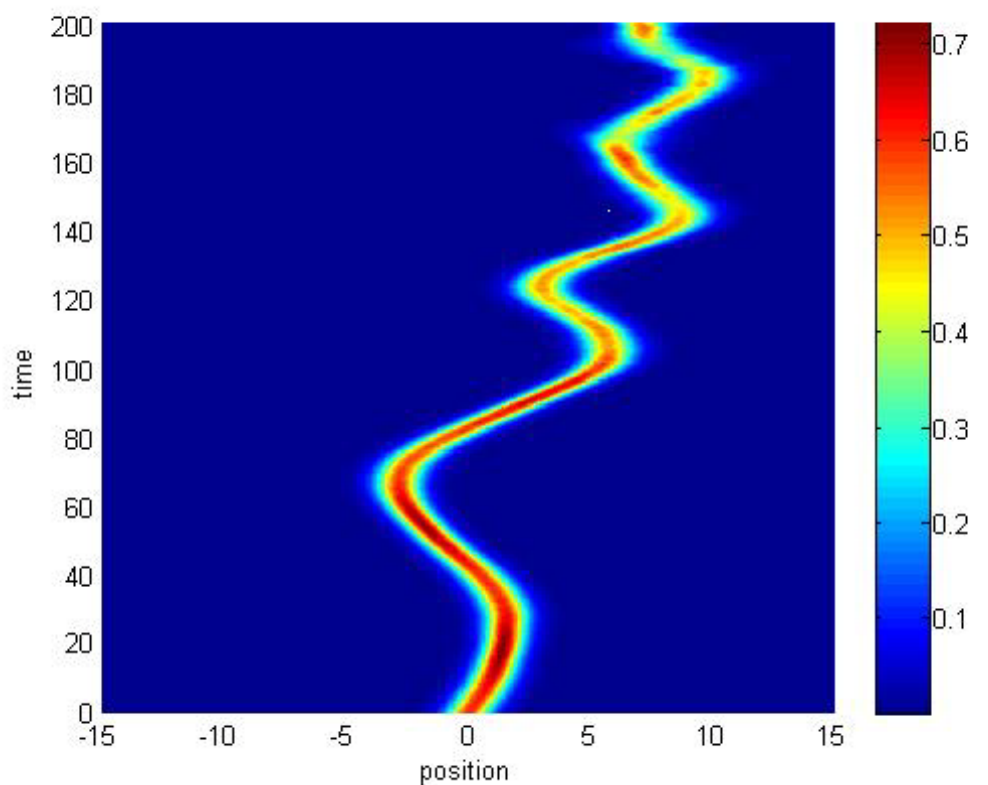
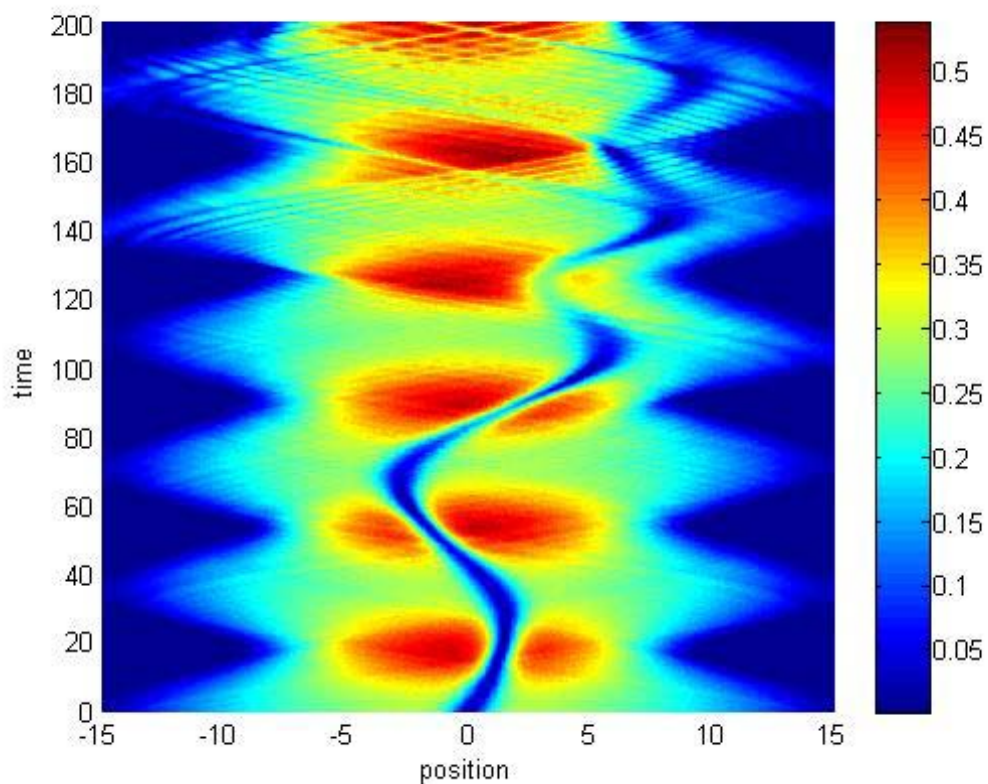
3.1.6.1 Density Profile for  $\lambda_1 = 0$  and  $\lambda_2 = 0.1$



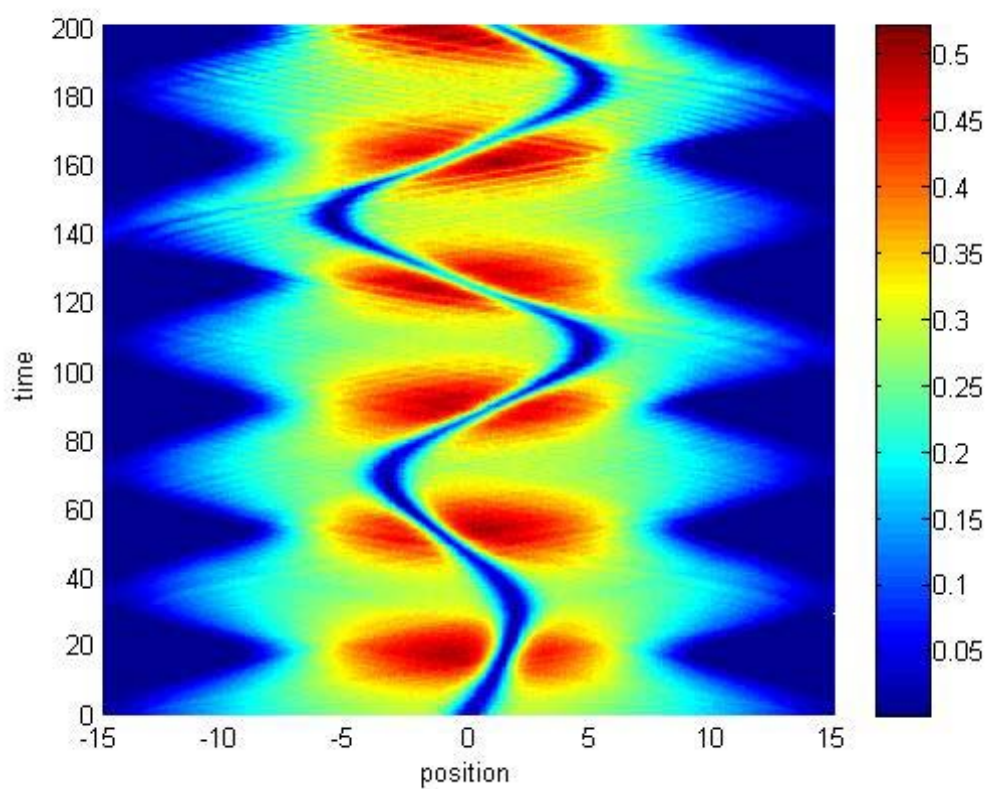
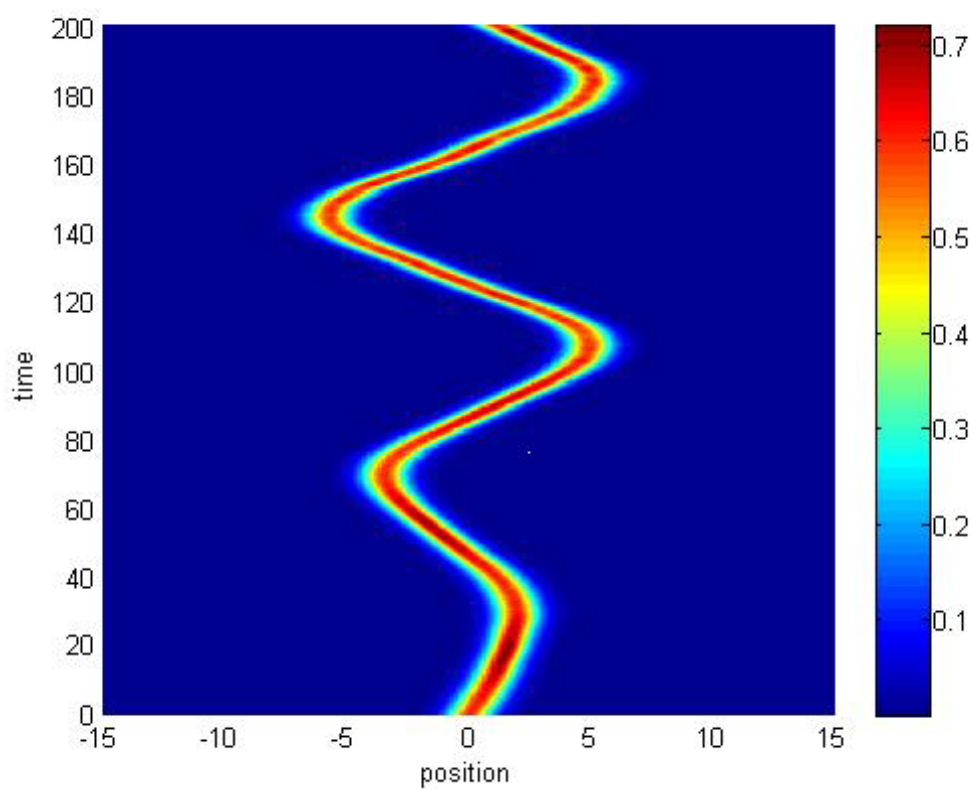
3.1.6.2 Density Profile for  $\lambda_1 = 0.02$  and  $\lambda_2 = 0.1$



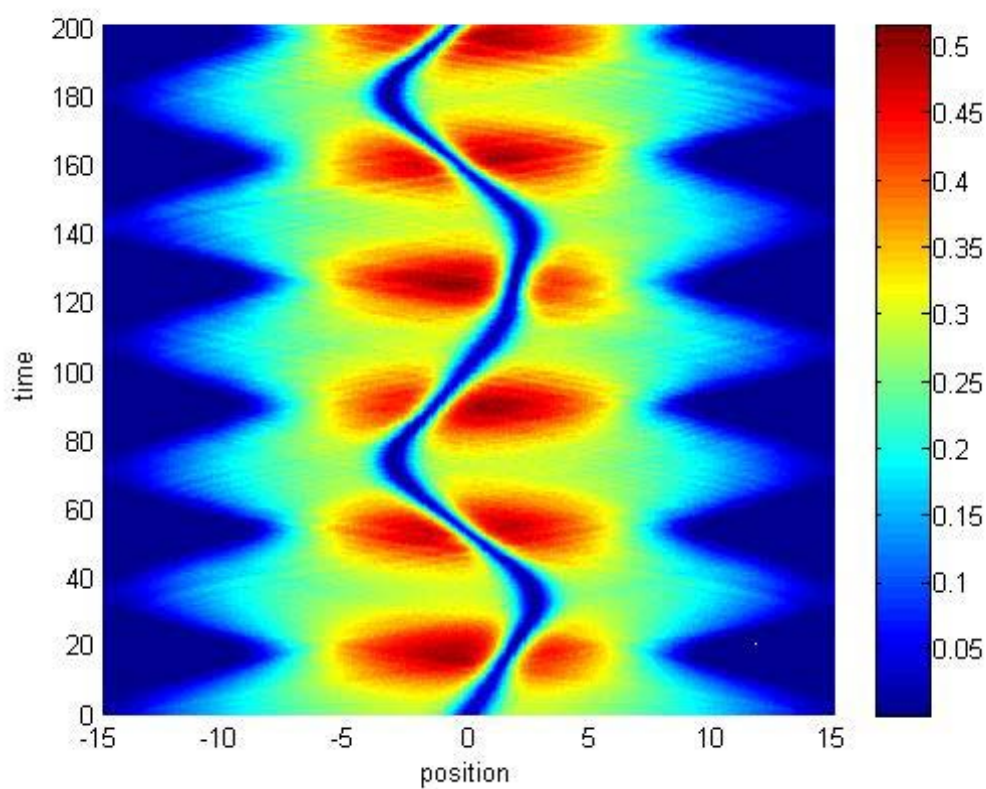
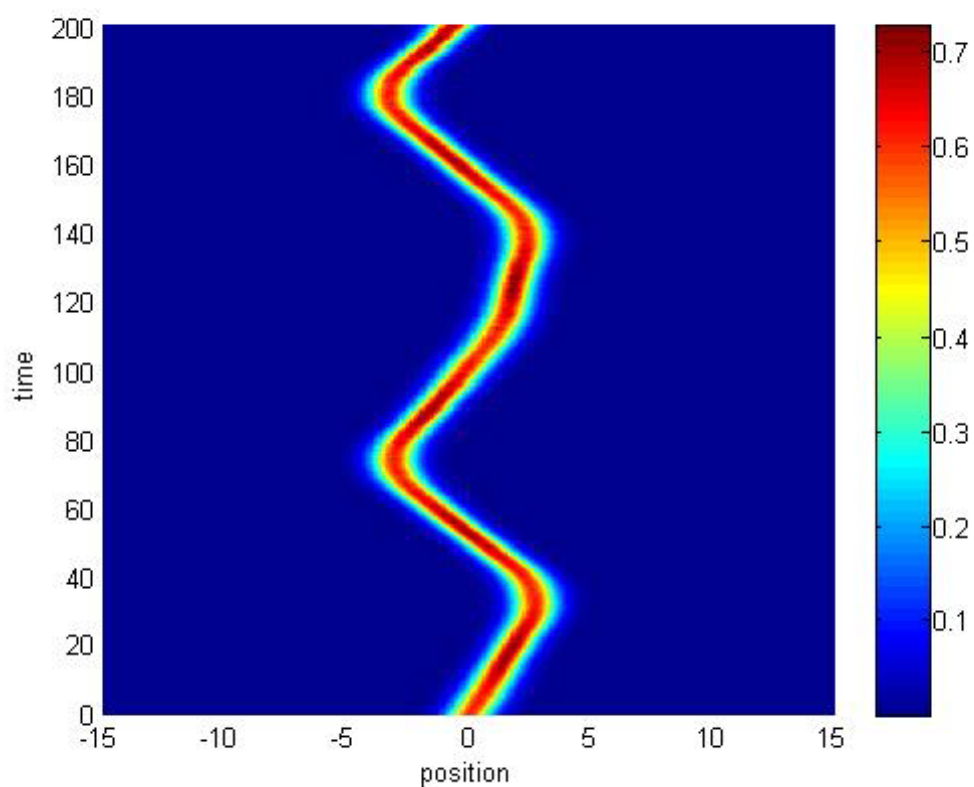
3.1.6.3 Density Profile for  $\lambda_1 = 0.04$  and  $\lambda_2 = 0.1$



3.1.6.4 Density Profile for  $\lambda_1 = 0.06$  and  $\lambda_2 = 0.1$



3.1.6.5 Density Profile for  $\lambda_1 = 0.08$  and  $\lambda_2 = 0.1$



3.1.6.6 Density Profile for  $\lambda_1 = 0.1$  and  $\lambda_2 = 0.1$

Thus, as shown above, we can conclude for different density profiles as following:

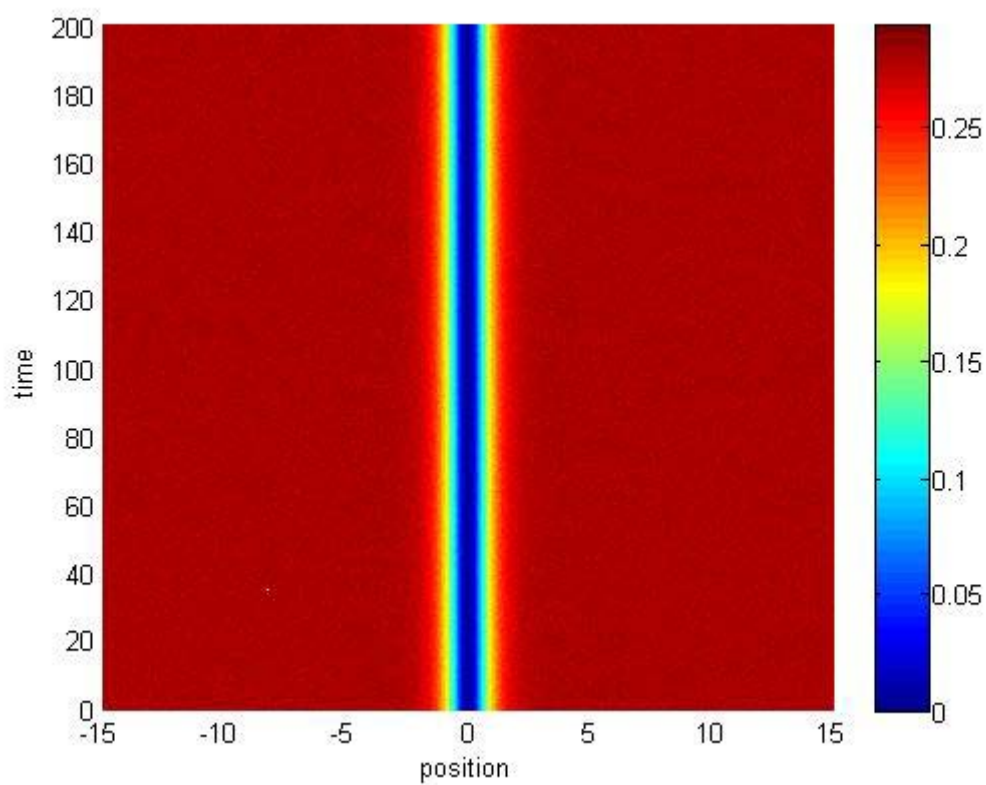
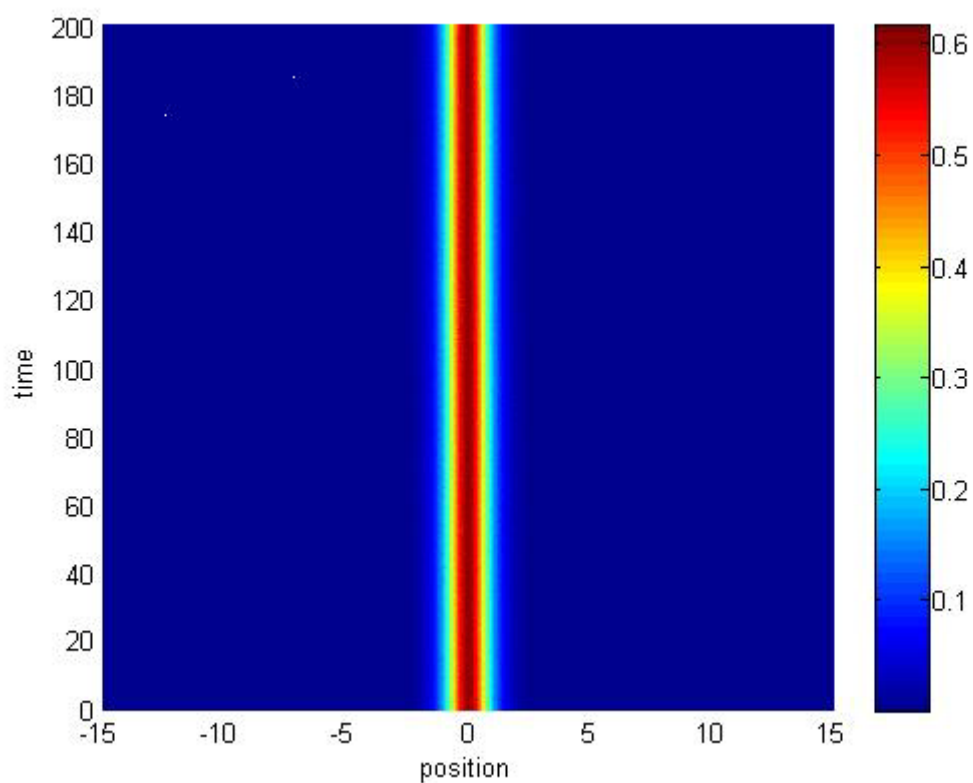
- When  $\lambda_1$  and  $\lambda_2$  are zero, i.e. there is no trapping potentials, there is a small oscillation or soliton is still moving as velocity is not zero. Soliton is moving slowly with constant velocity.
- When  $\lambda_2$  is constant and  $\lambda_1$  is changing,  $\lambda_2$  follows  $\lambda_1$  such that as  $\lambda_1$  increases, we will get periodic oscillations as  $\lambda_1$  approaches form 0 to 1.0.
- When  $\lambda_2 > \lambda_1$  (slightly greater), periodic behaviour does not exist there.

## Part 3.2 : Density profile for Special Cases

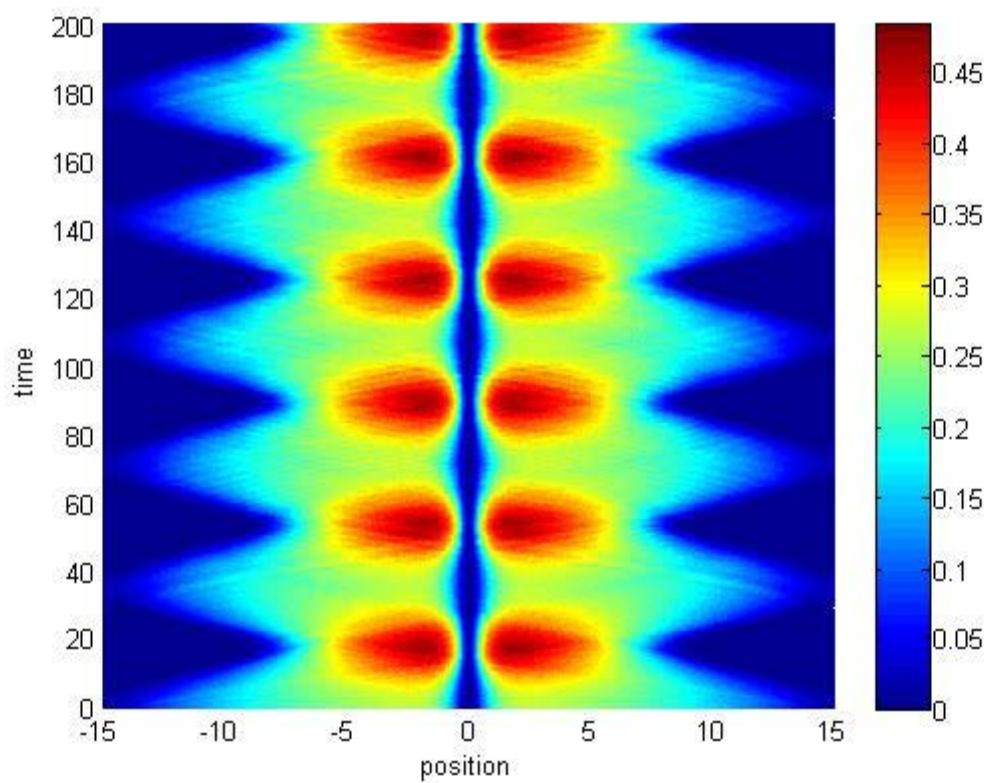
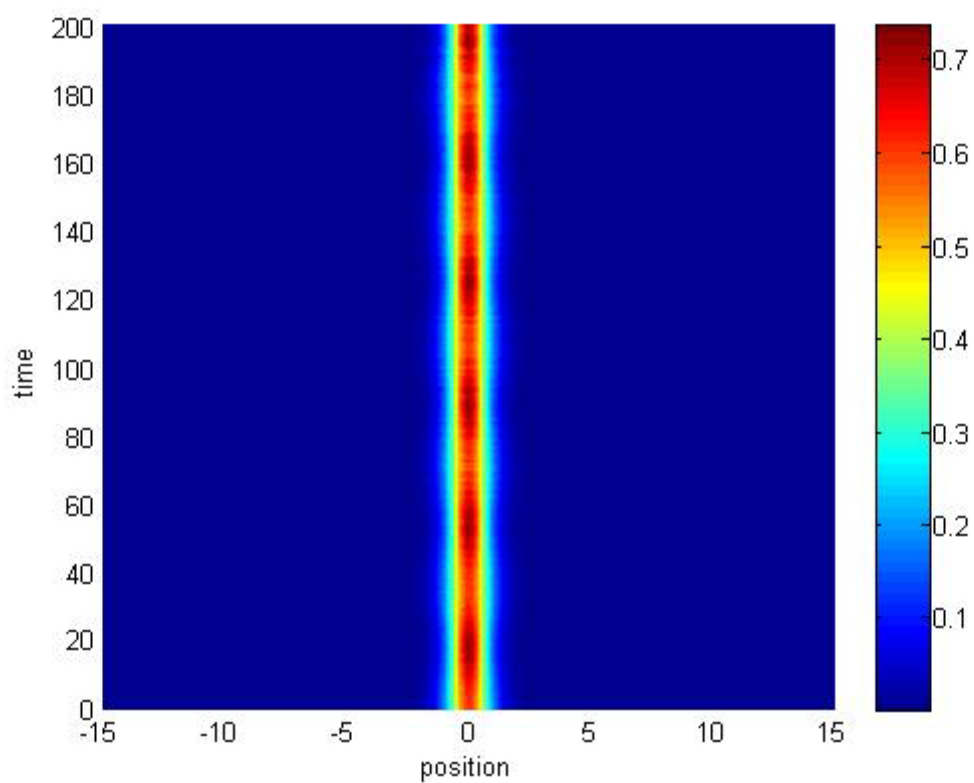
Here we have shown some special cases for Bright and Dark solitons. For example, if velocity  $v$ , trapping potentials  $\lambda_1 = \lambda_2 = 0$  and inter-species Interaction strength  $b_{12} = 0$  then what will be the behaviour of solitons. And we have got interesting results for such cases as following:

- When  $\lambda_1 = \lambda_2 = 0$ ,  $v = 0$  and  $b_{12} = 0$ , in this case, soliton is not moving as velocity is zero.
- When  $\lambda_1 = \lambda_2 = 0.1$ ,  $v = 0$  and  $b_{12} = 2$ , still soliton is stationary.
- When  $\lambda_1 = \lambda_2 = 0.1$ ,  $v = 0.1$  and  $b_{12} = 0$ , small oscillations will be there.
- But when  $\lambda_1 = \lambda_2 = 1.0$ ,  $v = 0.1$  and  $b_{12} = 0$ , [figure 3.7.5] Bright soliton is not moving as trapping potential is quite strong to trap the soliton. In this case, trapping potential is higher than kinetic energy.
- In case of  $\lambda_1 = \lambda_2 = 0.1$ ,  $v = 0.5$  and  $b_{12} = 2$ , i.e., velocity is increased, we will get large oscillations as shown in figure 3.7.6.
- Plots are shown as following:

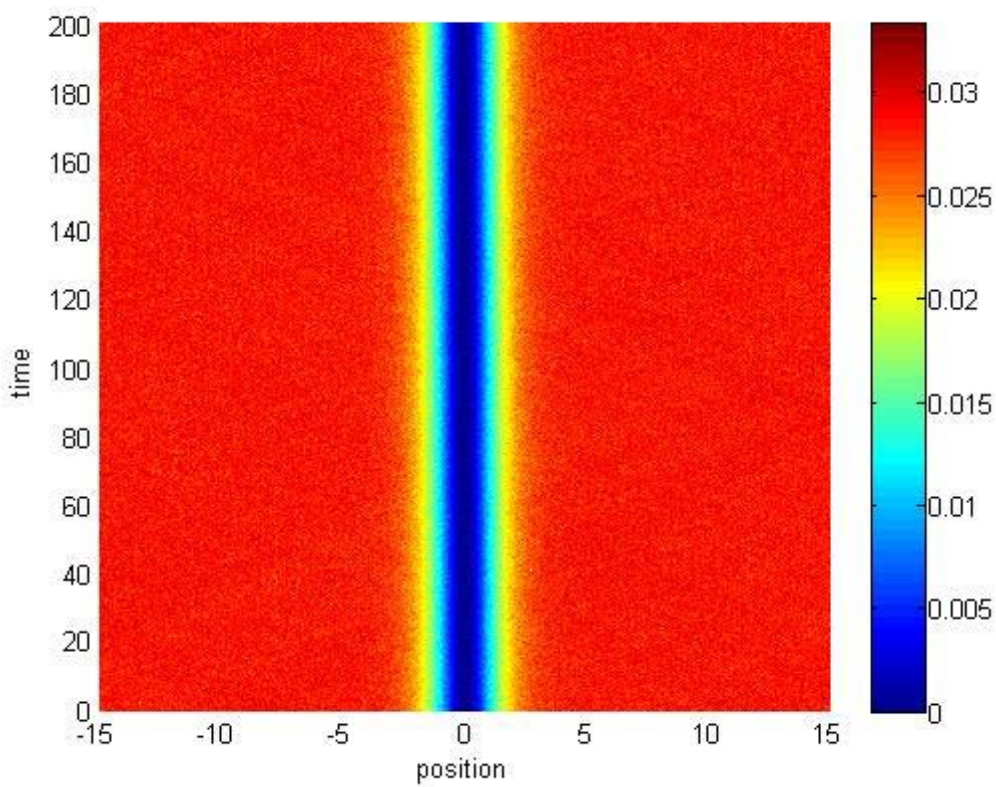
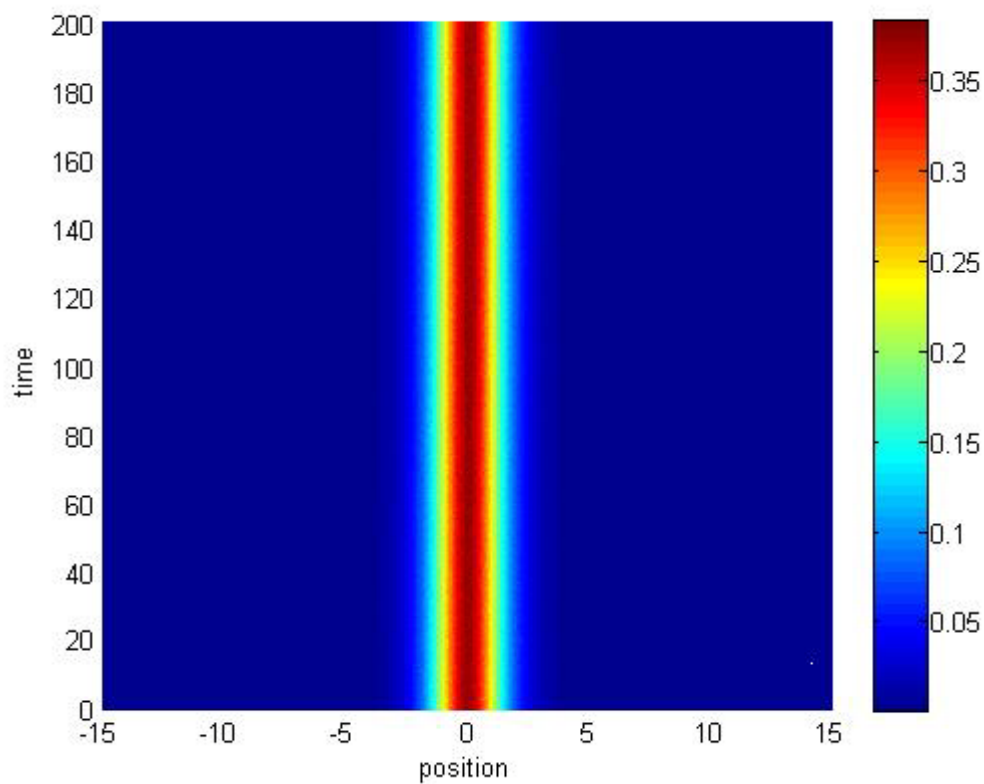




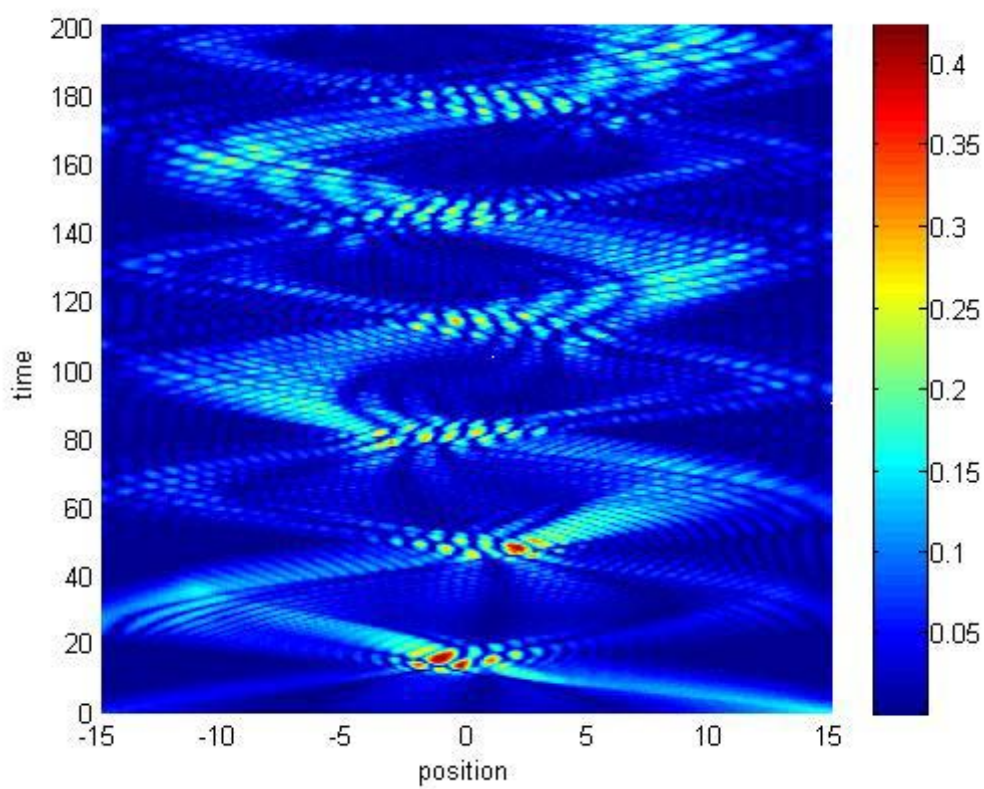
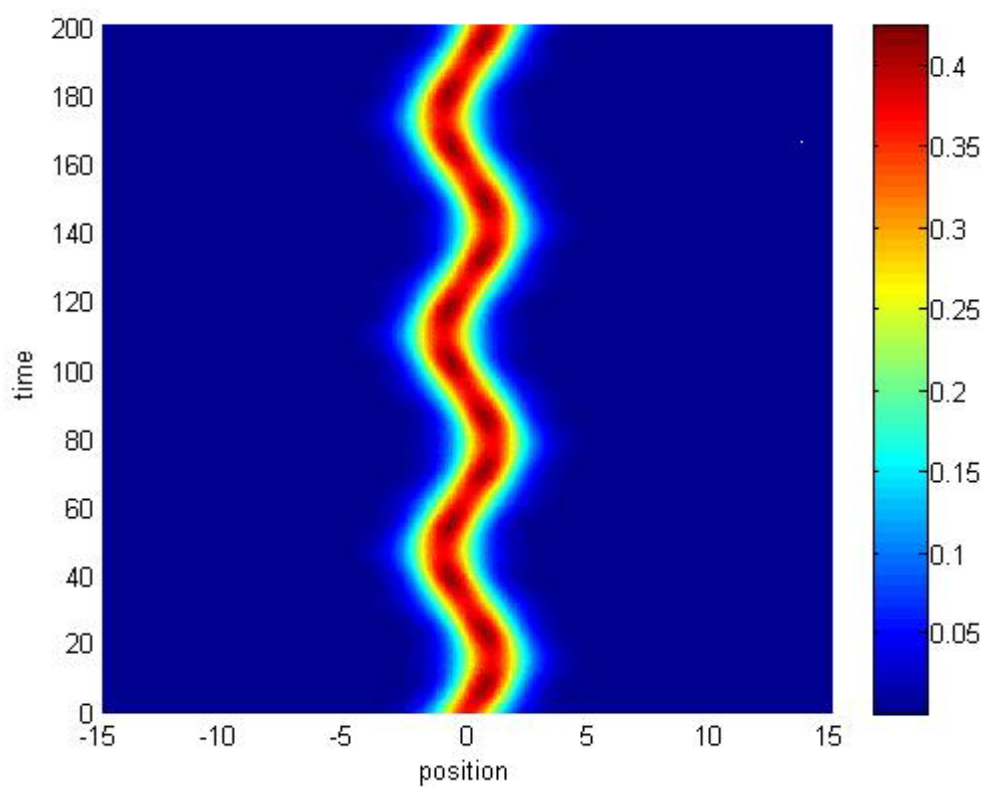
3.2.1 Density profile for  $\lambda_1 = \lambda_2 = 0$  with  $b_{12} = 2$  and  $v = 0$



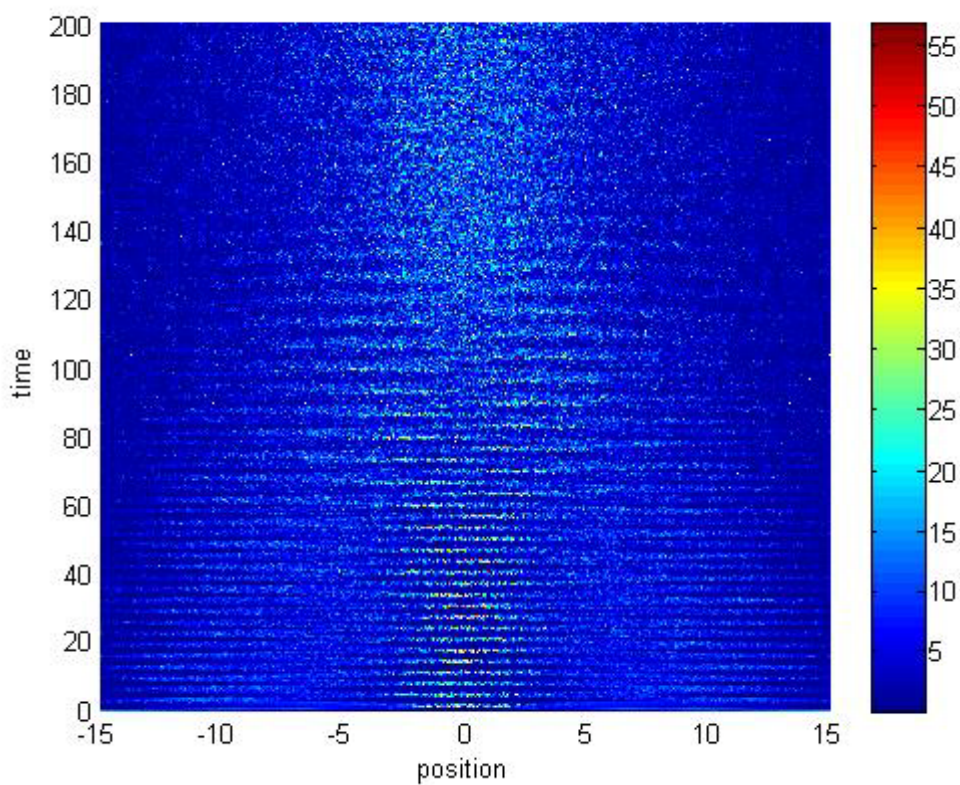
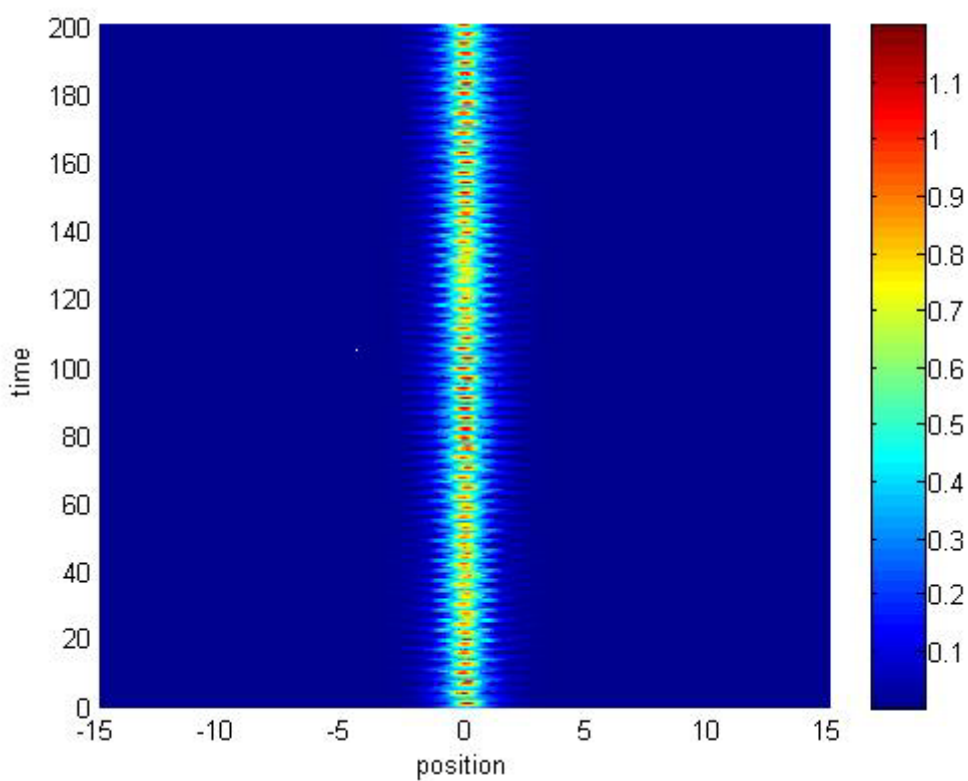
3.2.2 Density profile for  $\lambda_1 = \lambda_2 = 0.1$  with  $b_{12} = 2$  and  $v = 0$



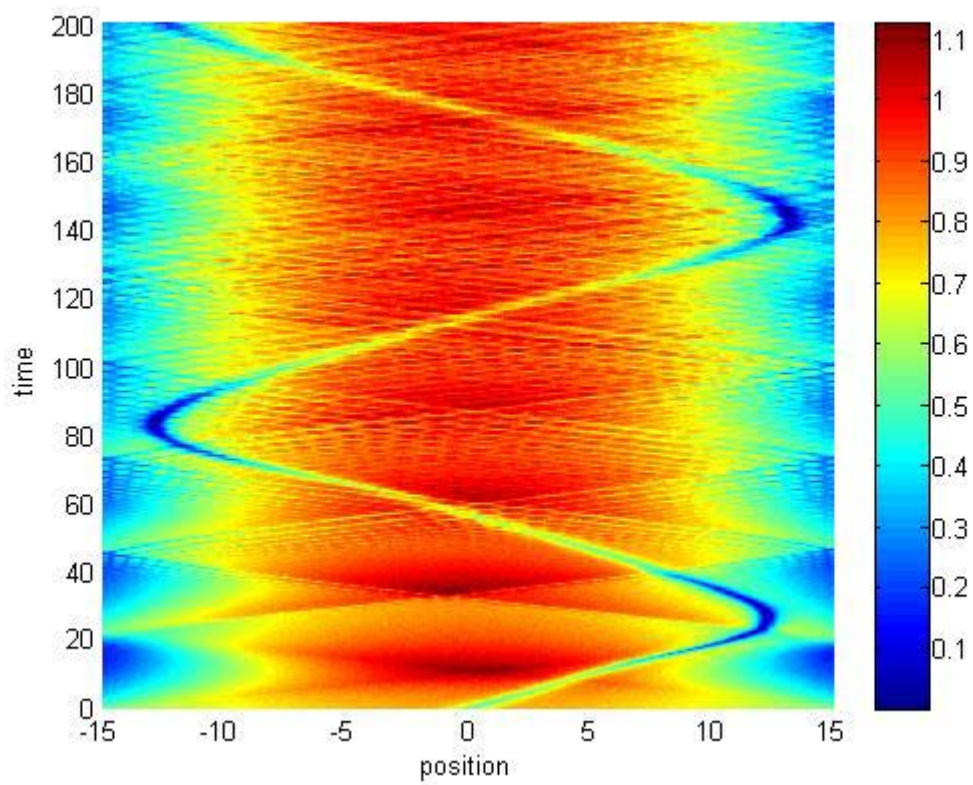
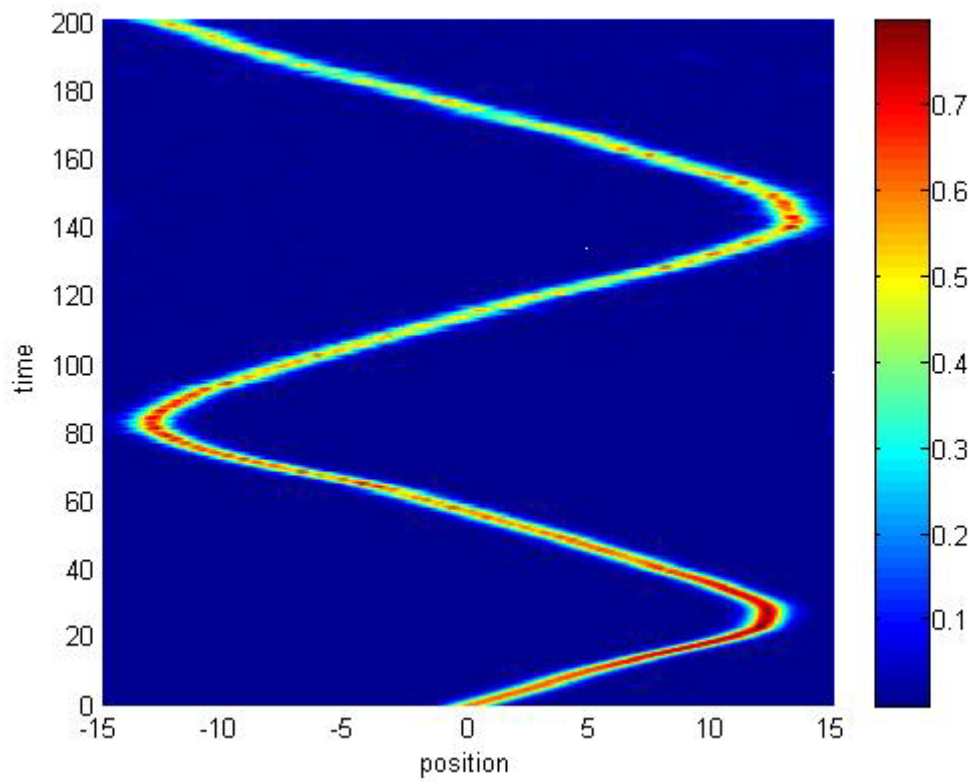
3.2.3 Density profile for  $\lambda_1 = \lambda_2 = 0$  with  $b_{12} = 0$  and  $v = 0$



3.2.4 Density profile for  $\lambda_1 = \lambda_2 = 0.1$  with  $b_{12} = 0$  and  $v = 0.1$



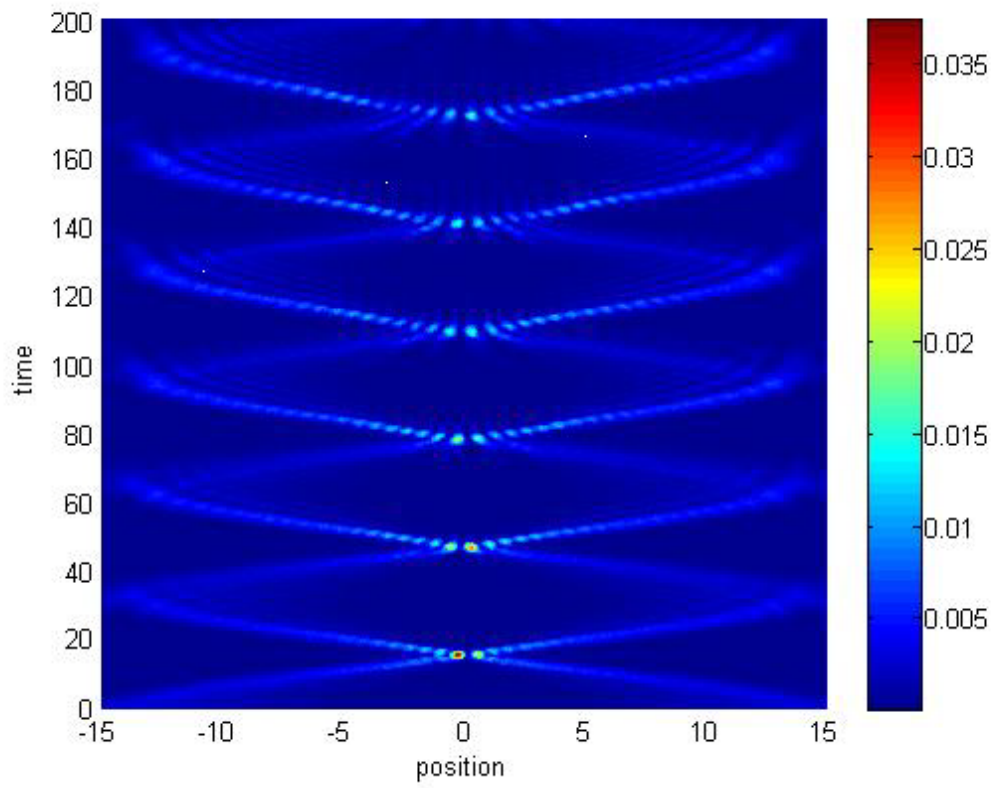
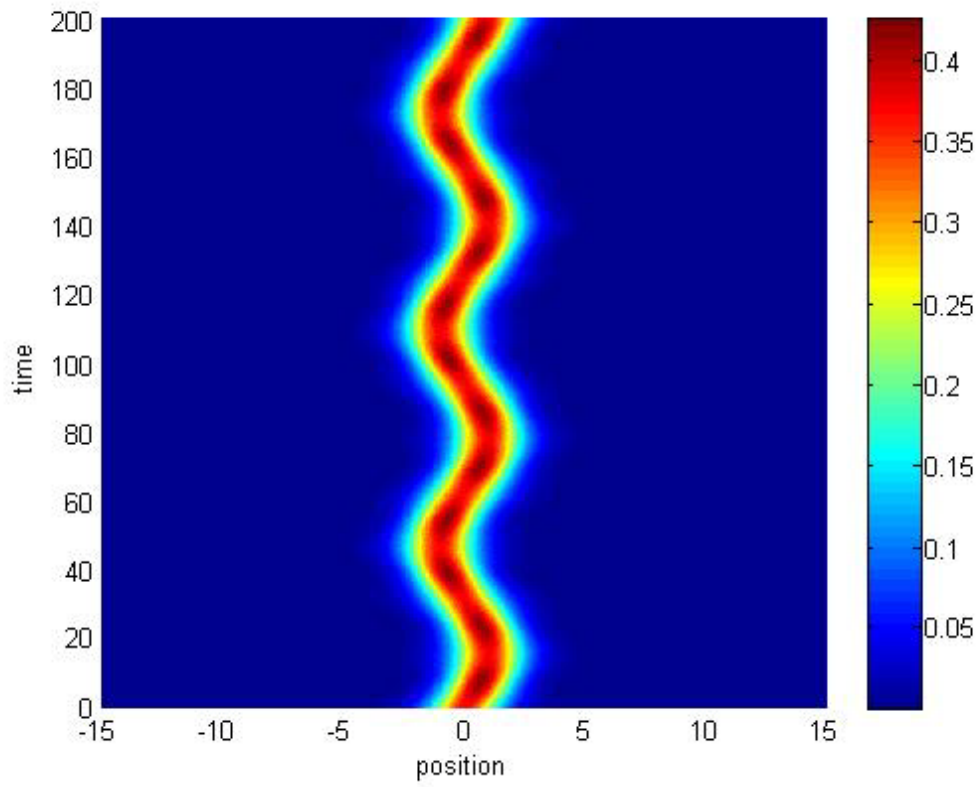
3.2.5 Density profile for  $\lambda_1 = \lambda_2 = 1$  with  $b_{12} = 0$  and  $v = 0.1$



3.2.6 Density profile for  $\lambda_1 = \lambda_2 = .01$  with  $b_{12} = 2$  and  $v = 0.5$

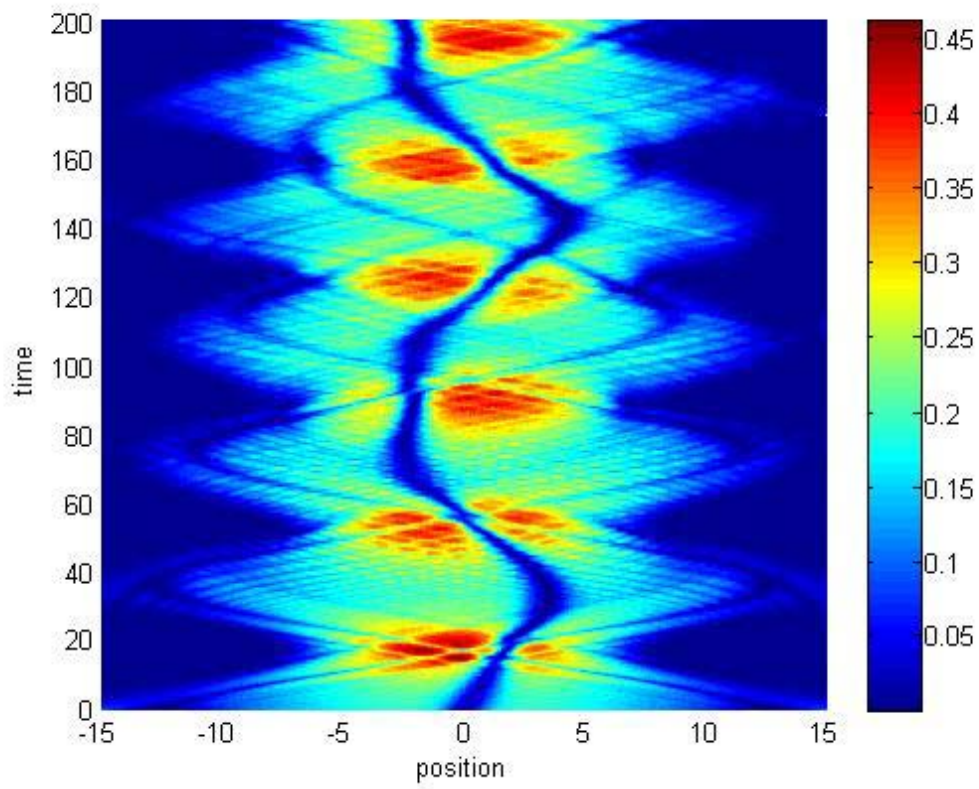
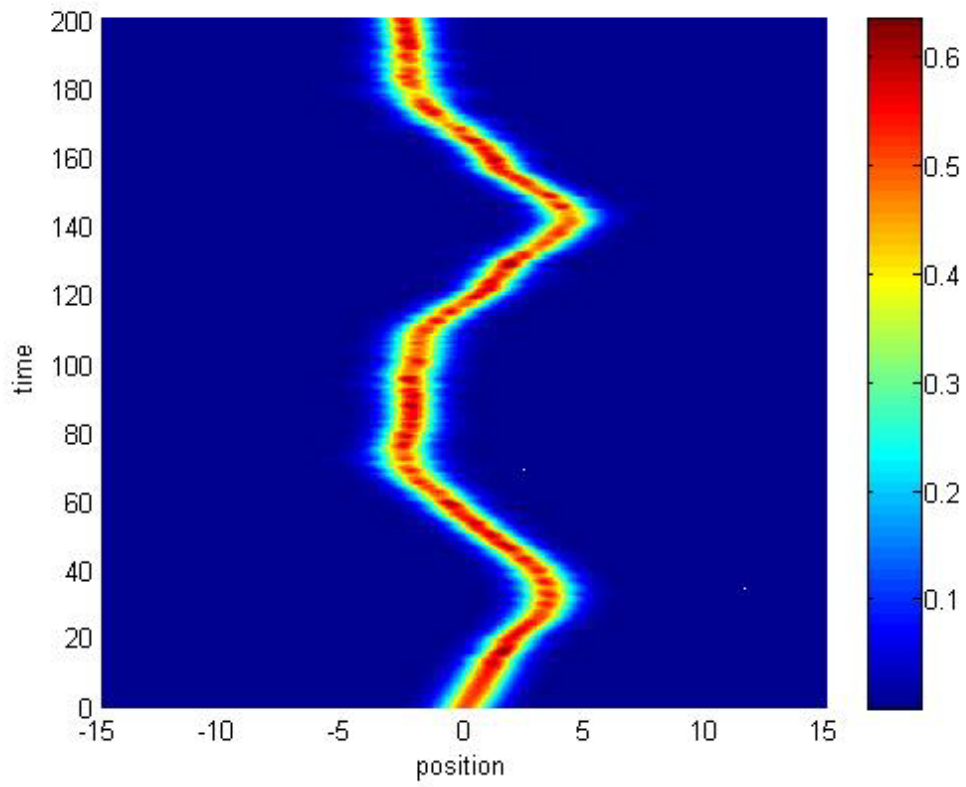
### Part 3: Density Profile for Different $b_{12}$ values

In this part, different values for  $b_{12}$  have been taken to evaluate density profiles. As shown in Phase Diagram in Chapter 2, Bright-Dark solitons exist in the range from -0.45 to 19.35. So to check this criterion, I have taken 10 values for  $b_{12}$  in the range from -0.45 to 19.35 and evaluated density profiles for Bright-Dark solitons as shown in the following figures:

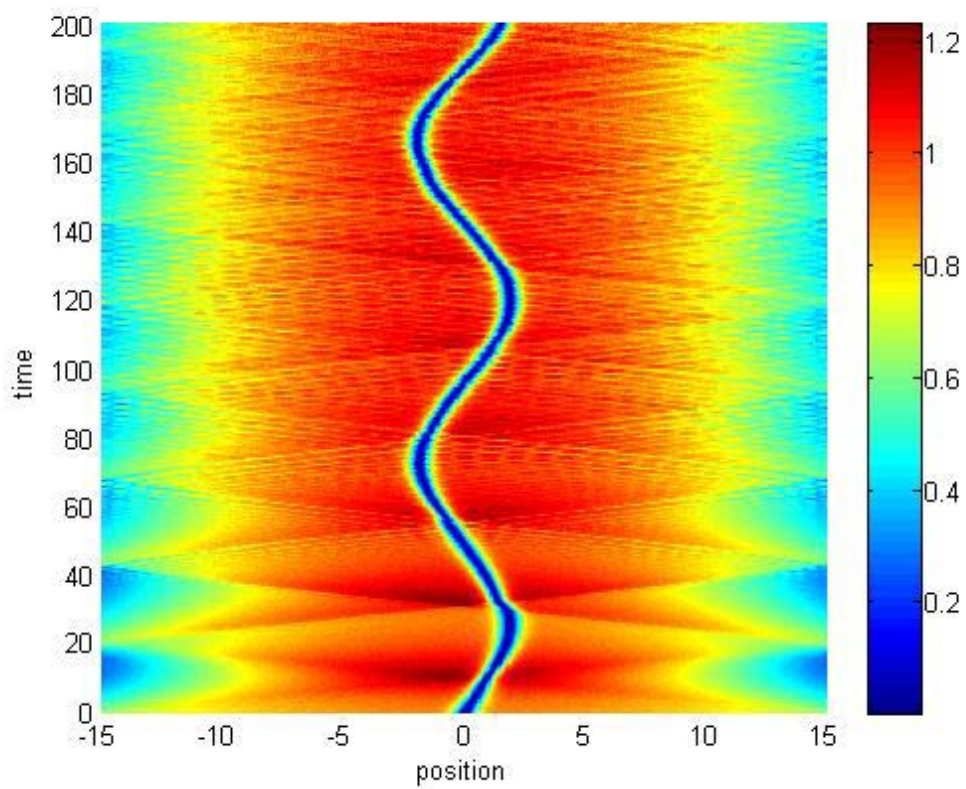
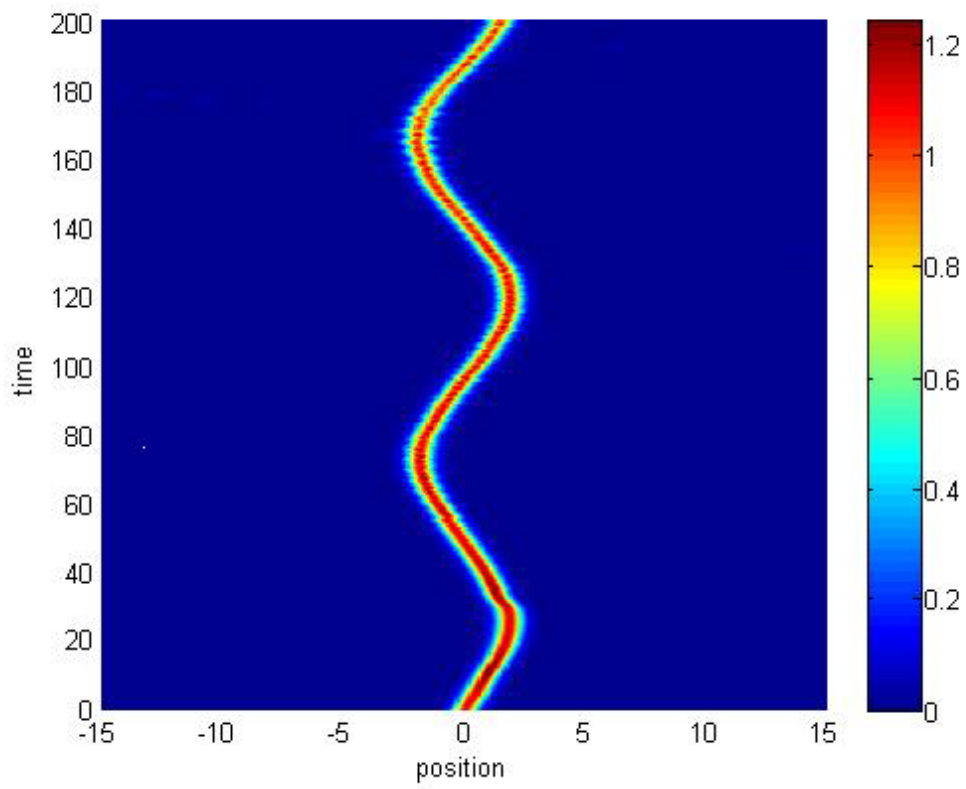


3.3.1 Density profile for  $\lambda_1 = \lambda_2 = 0.1$  with  $b_{12} = -0.45$  and  $v = 0.1$

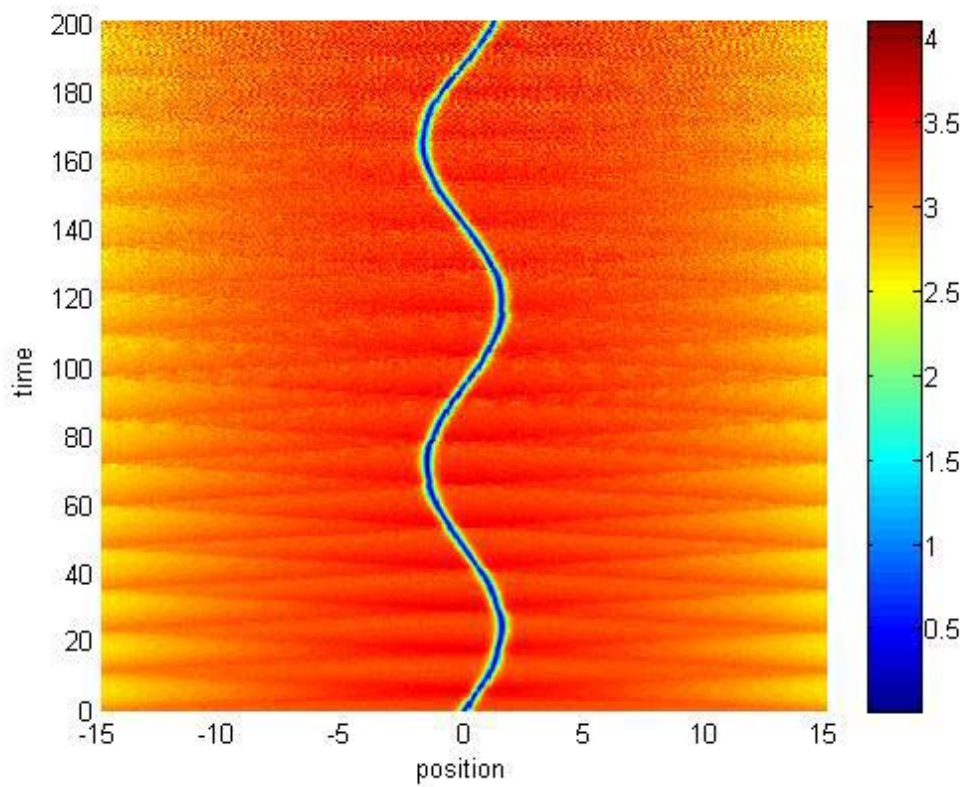
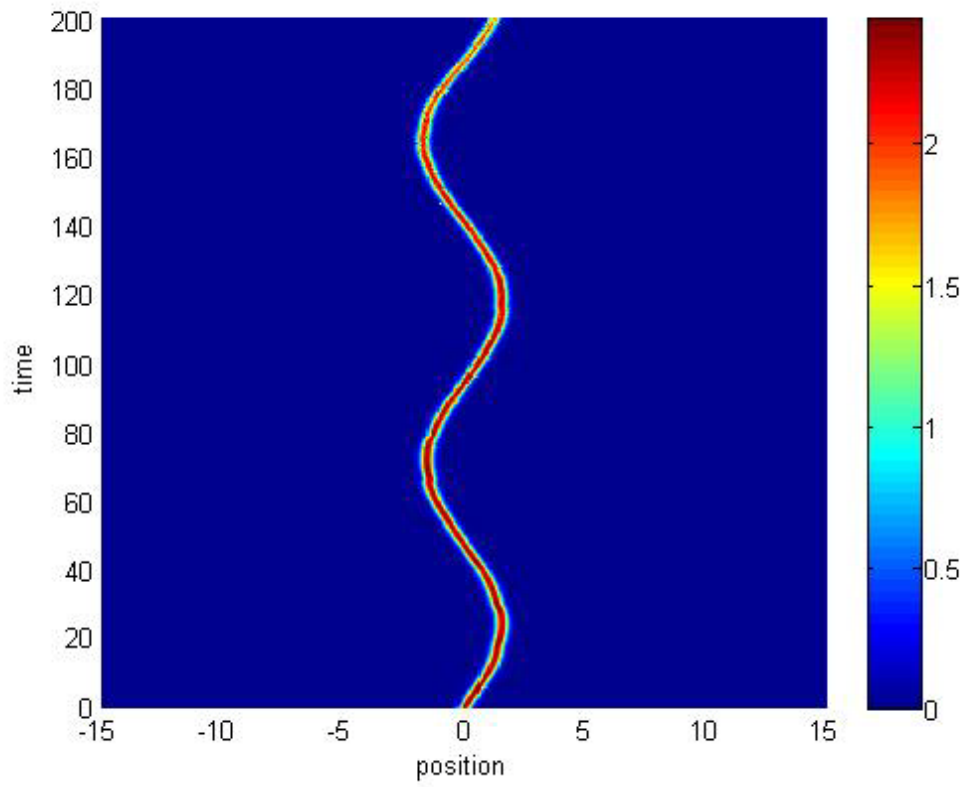




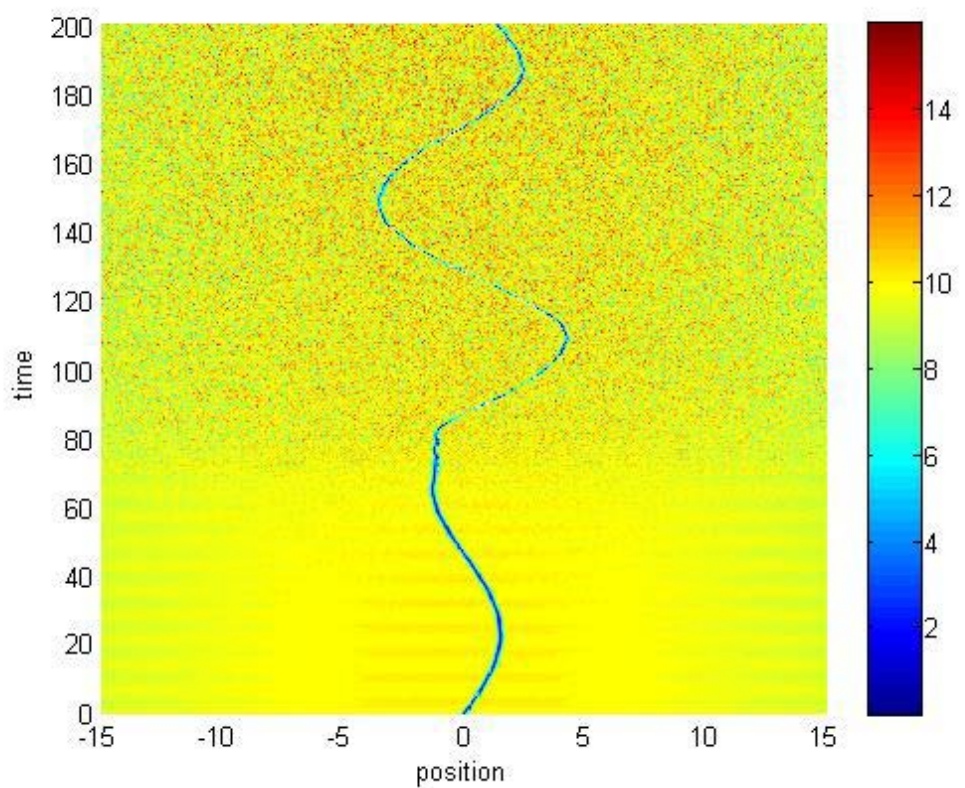
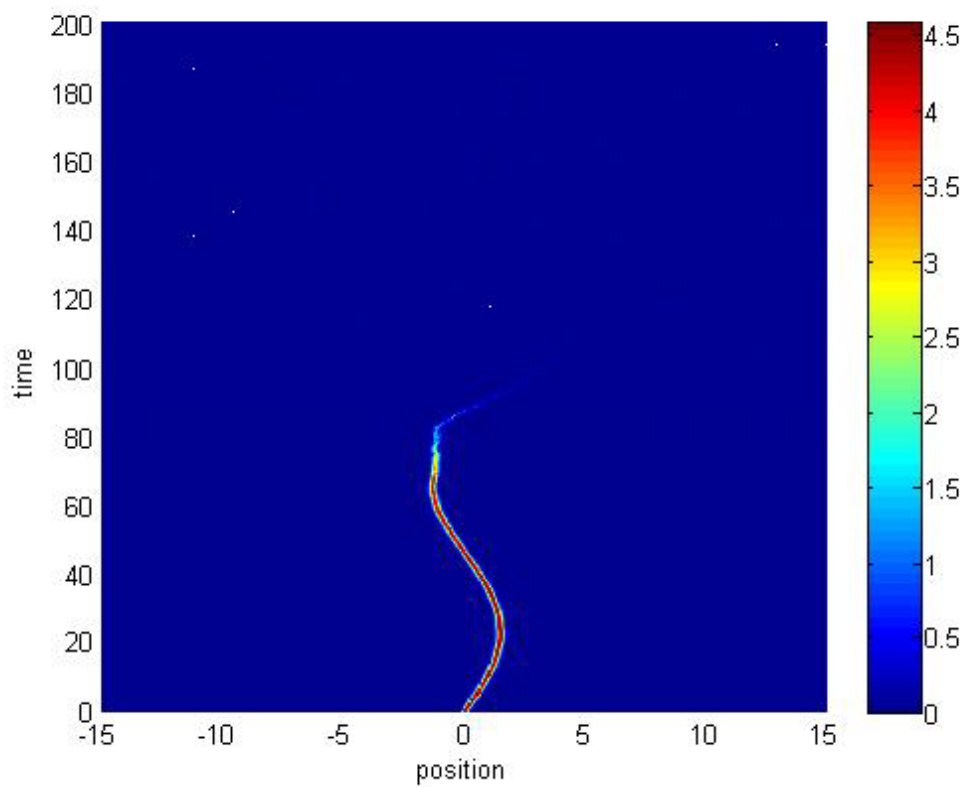
3.3.2 Density profile for  $\lambda_1 = \lambda_2 = 0.1$  with  $b_{12} = 1.53$  and  $v = 0.1$



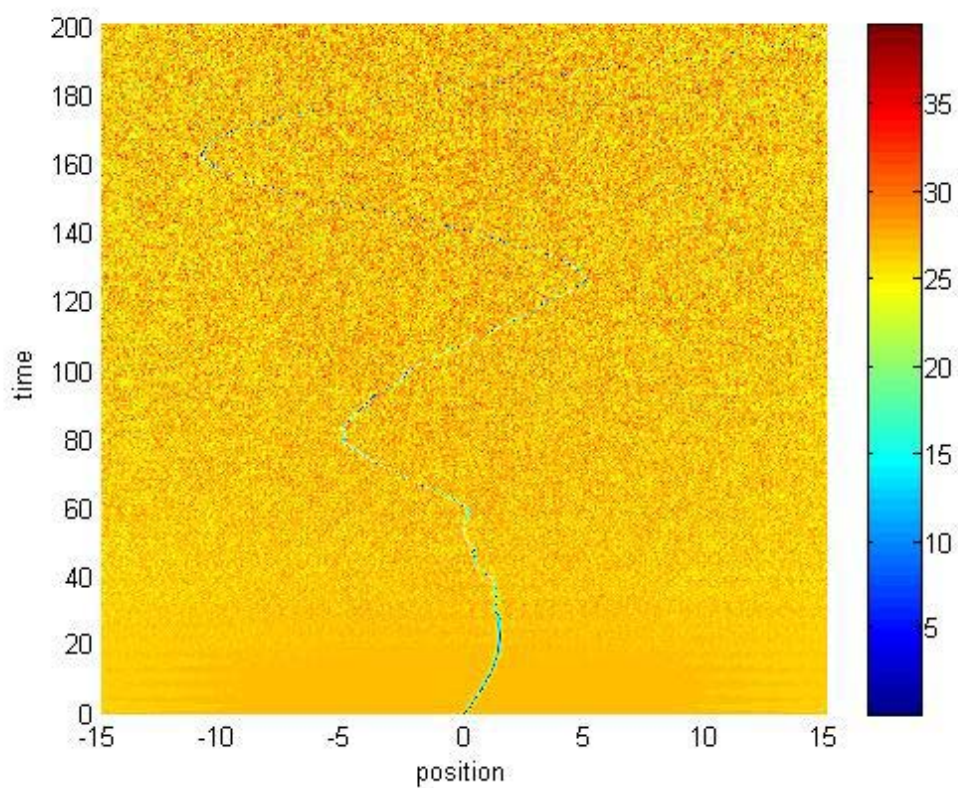
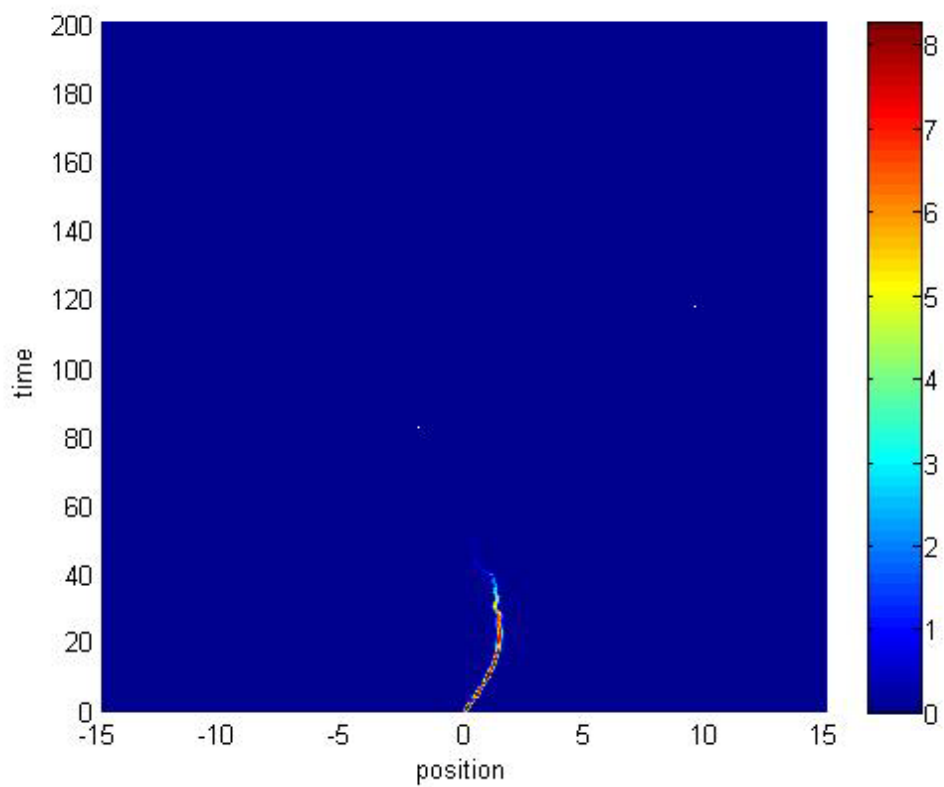
3.3.3 Density profile for  $\lambda_1 = \lambda_2 = 0.1$  with  $b_{12} = 3.51$  and  $v = 0.1$



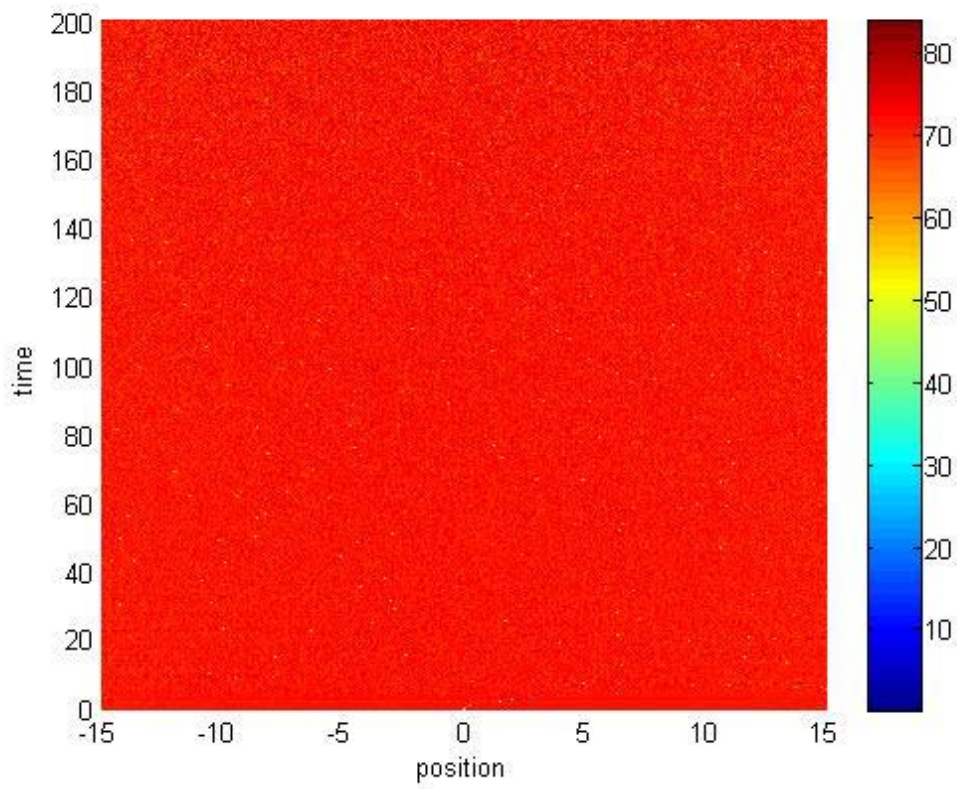
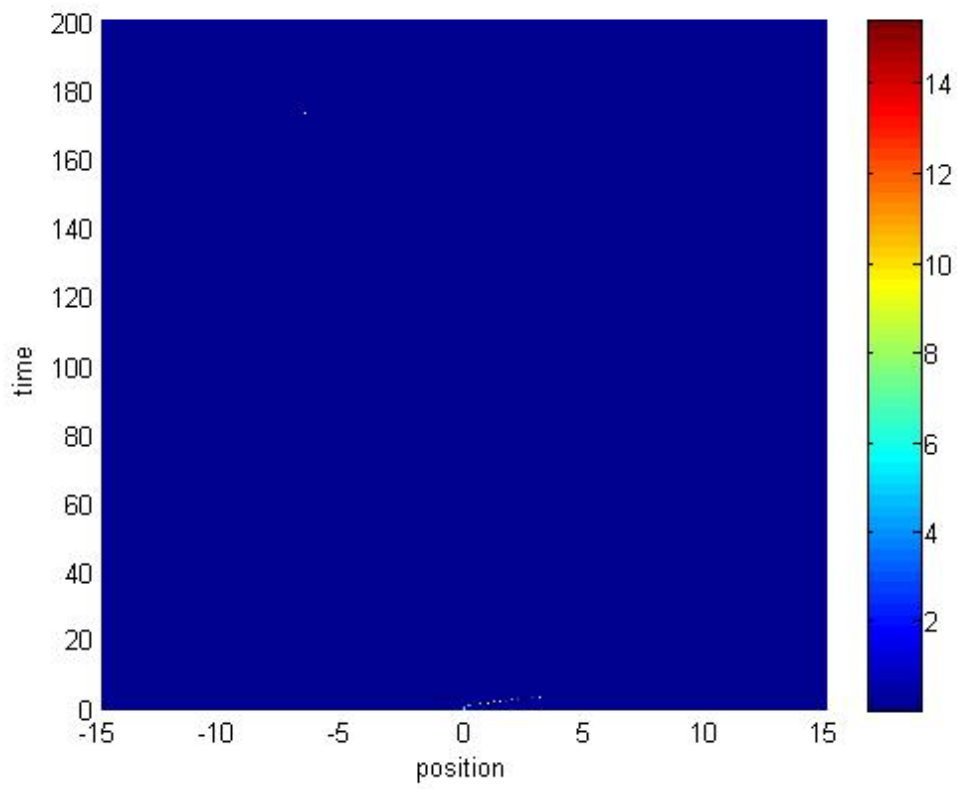
3.3.4 Density profile for  $\lambda_1 = \lambda_2 = 0.1$  with  $b_{12} = 5.49$  and  $\nu = 0.1$



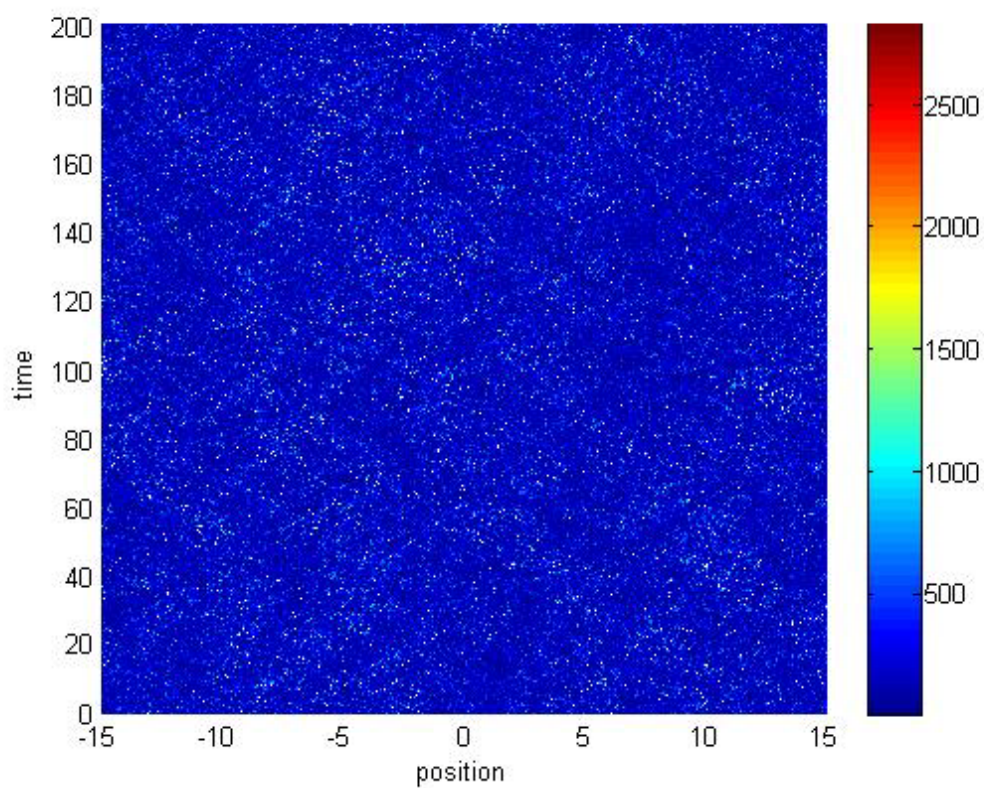
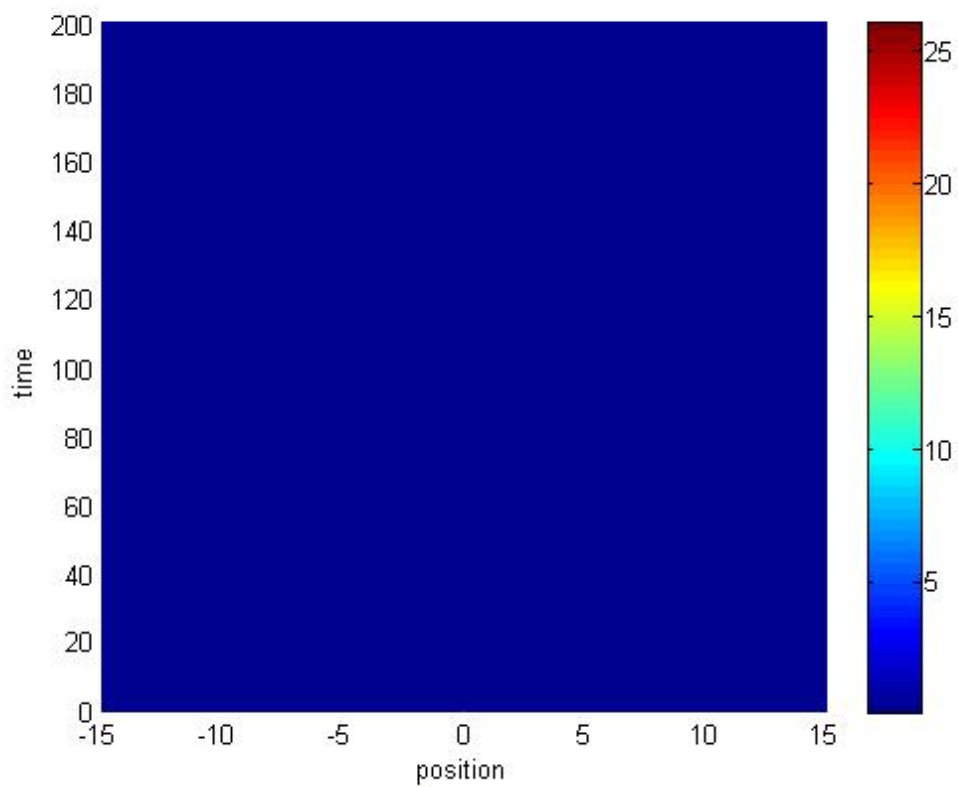
3.3.5 Density profile for  $\lambda_1 = \lambda_2 = .0.1$  with  $b_{12} = 7.47$  and  $v = 0.1$



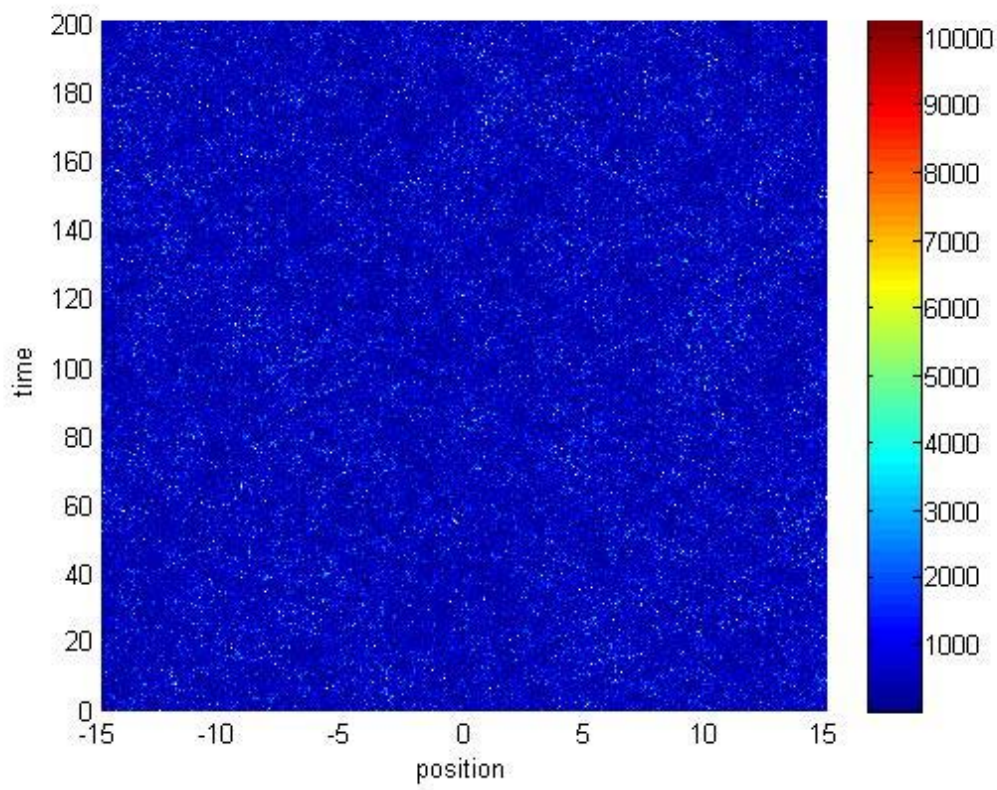
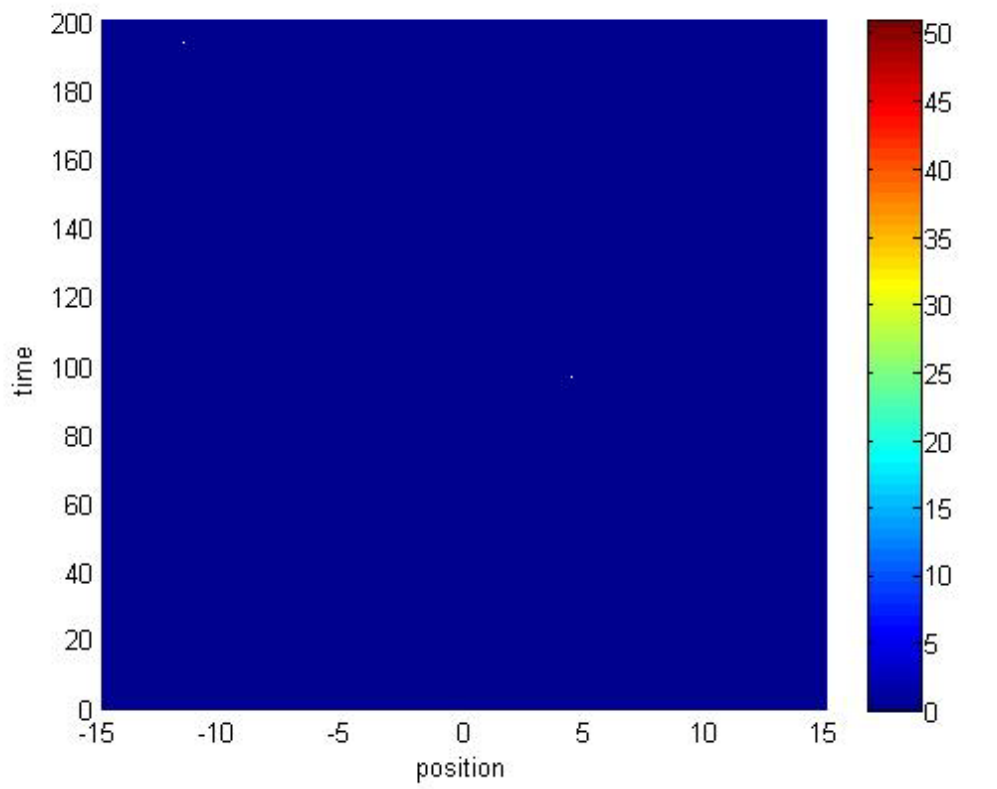
3.3.6 Density profile for  $\lambda_1 = \lambda_2 = 0.1$  with  $b_{12} = 9.45$  and  $v = 0.1$



3.3.7 Density profile for  $\lambda_1 = \lambda_2 = 0.1$  with  $b_{12} = 11.43$  and  $v = 0.1$

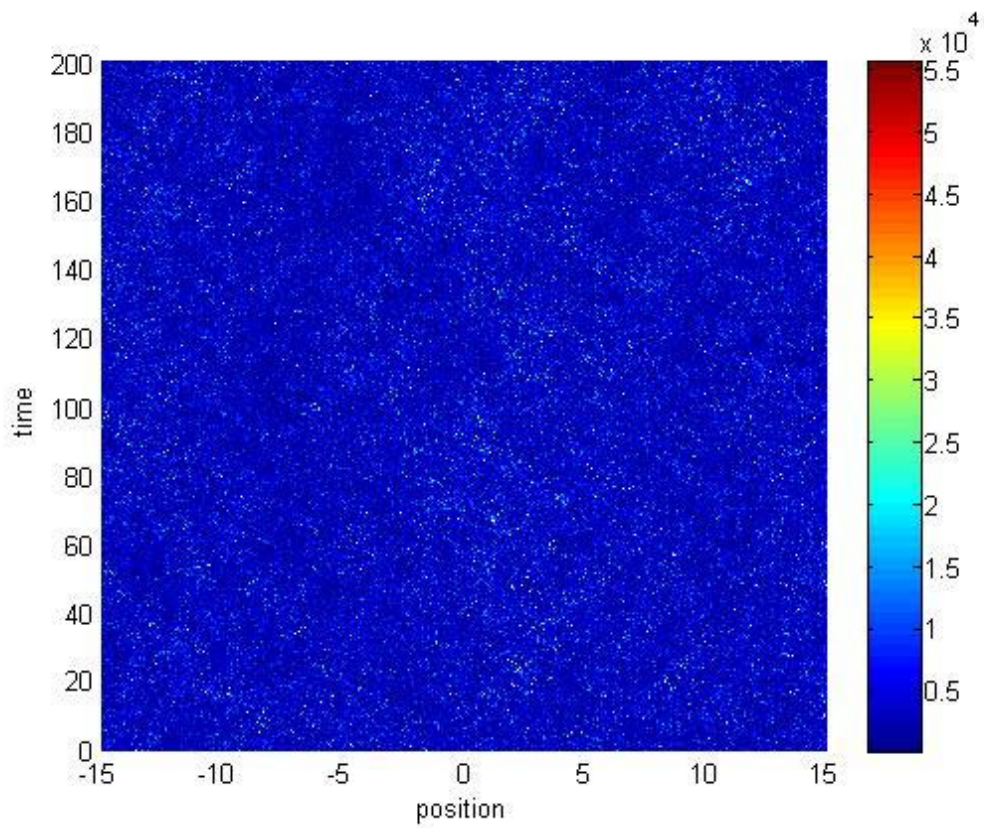
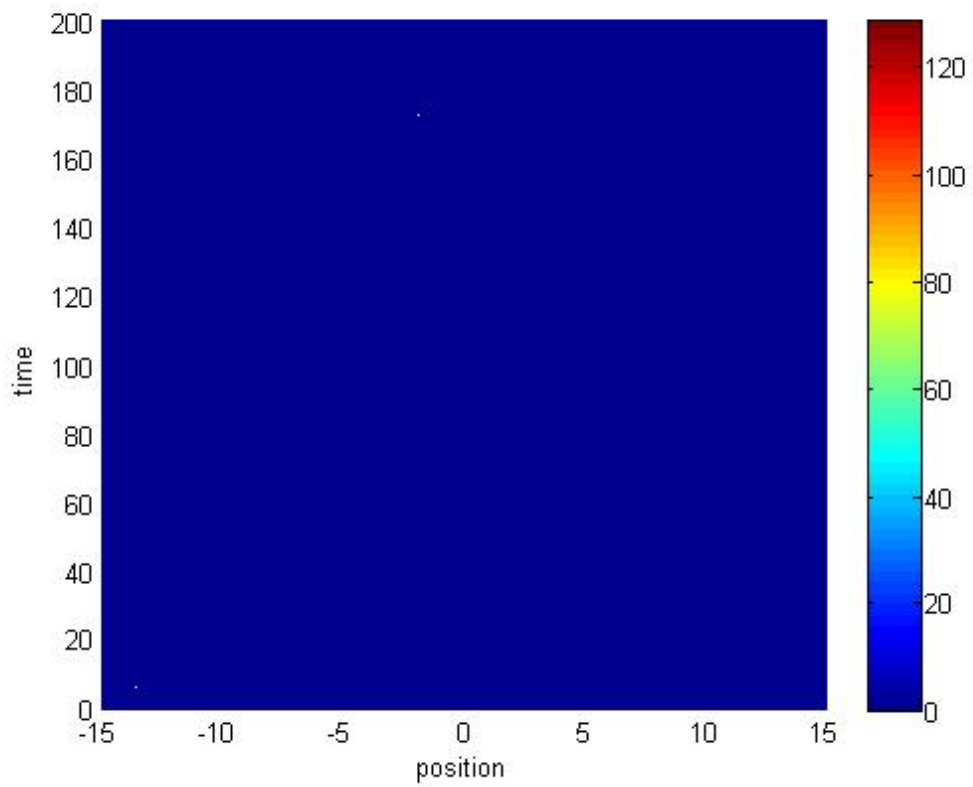


3.3.8 Density profile for  $\lambda_1 = \lambda_2 = 0.1$  with  $b_{12} = 13.41$  and  $\nu = 0.1$

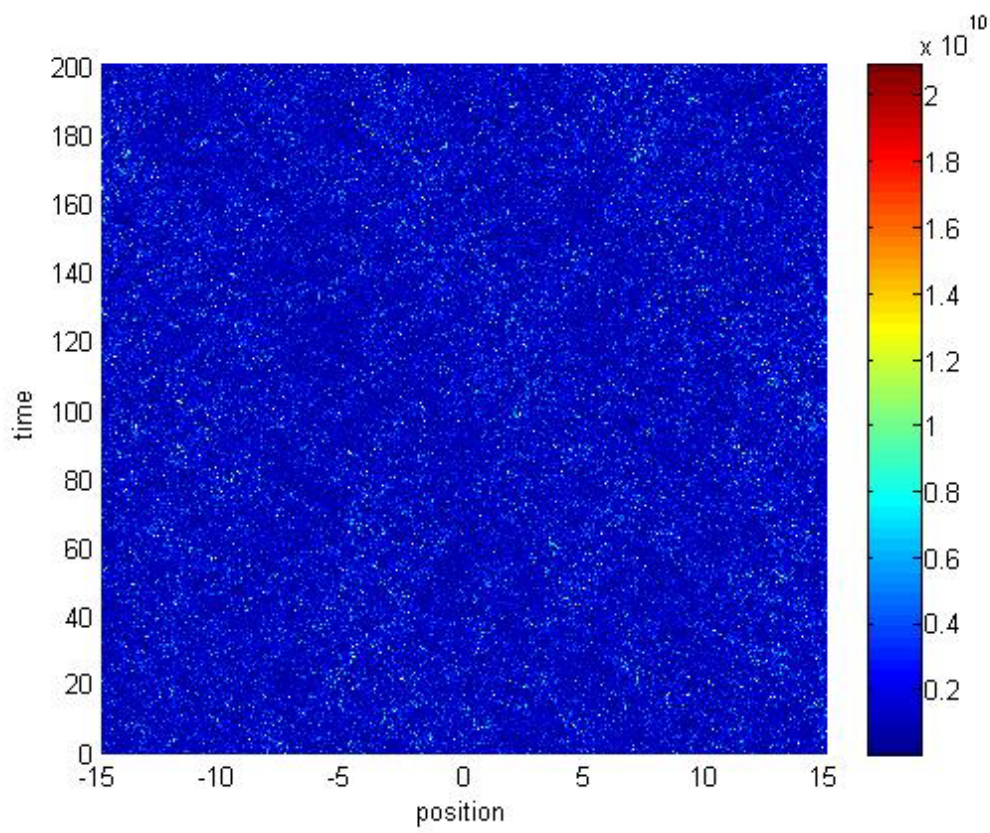
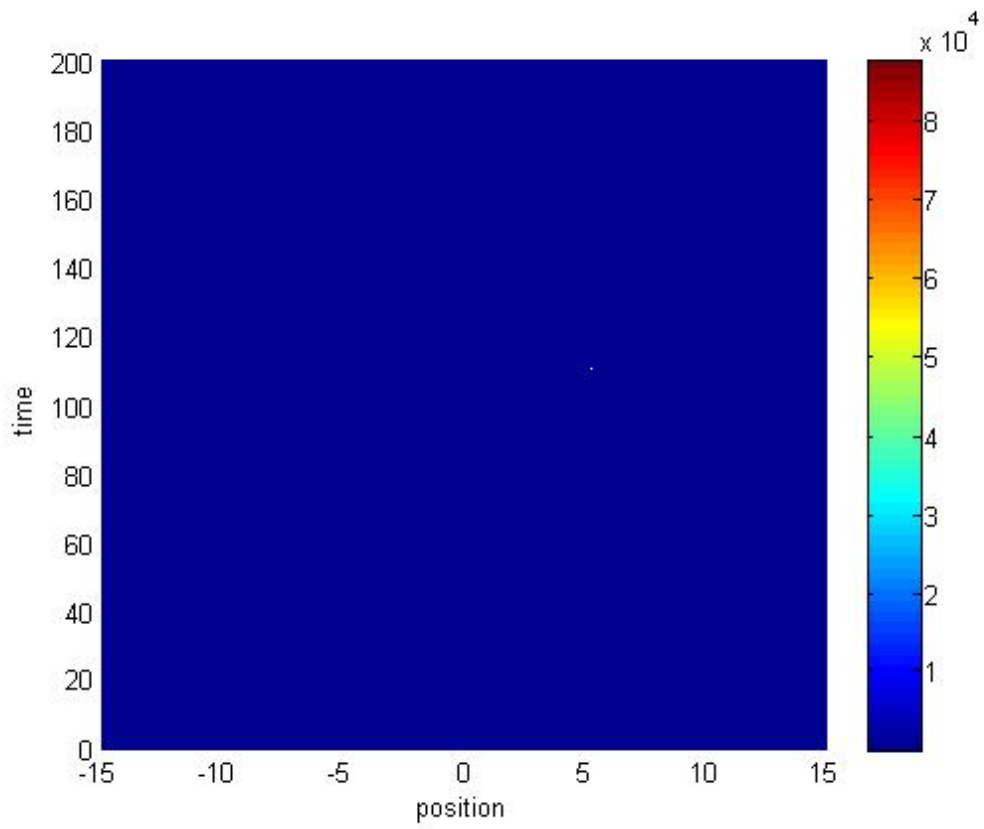


3.3.9 Density profile for  $\lambda_1 = \lambda_2 = 0.1$  with  $b_{12} = 15.39$  and  $v = 0.1$





3.3.10 Density profile for  $\lambda_1 = \lambda_2 = 0.1$  with  $b_{12} = 17.37$  and  $v = 0.1$



3.3.11 Density profile for  $\lambda_1 = \lambda_2 = 0.1$  with  $b_{12} = 19.35$  and  $v = 0.1$

Thus, we can conclude that,

- At  $b_{12} = -0.45$ , there is a Bright soliton with small oscillation but there is no stable Dark soliton at  $b_{12} = -0.45$ .
- As  $b_{12}$  increases and going towards 19.35, there are Bright and Dark solitons but the thickness of oscillations is decreasing as shown in figures from 3.3.3 and 3.3.4.
- But after that the oscillations start disappearing as  $b_{12}$  increases as shown in figures 3.3.5 and 3.3.6.
- And finally for  $b_{12} = 19.35$ , there is no existence of Bright and Dark solitons.
- This part gives the clear proof for  $b_{12}$  values responsible for Bright and Dark solitons.

## Chapter-4

### Conclusion:

- The presence of the weak longitudinal trap causes the vector-soliton to oscillate while maintaining the overall shape as shown in figures for density profiles for Bright and Dark solitons.
- The two coupled cubic nonlinear Schrodinger equations (2.5) and (2.6) in the absence of the trapping potential terms, support a special class of vector-soliton solutions even when the equations are not integrable.
- Trapping potential plays an important role for the stability of Bright and Dark solitons.
- Velocity is also key parameter for solitons to maintain their shapes while oscillating.
- Inter-species interaction strength  $b_{12}$  is responsible for types of solitons. Types of solitons also change if  $b_{12}$  changes. For example, as shown in phase diagram, there are three regions related to  $b_{12}$  values so if it changes, we have Bright-Bright solitons, Bright-Dark solitons and Dark-Dark solitons respectively.

## Scope for the future work:

- Here I have only studied dynamics for Bright-Dark solitons as time is very limited for me to finish my project work.
- I would like to do my further study for stability analysis for Dark-Dark solitons and Bright-Bright solitons.
- Soliton conversion via Feshbach resonance is also very interesting case so I would like to study in this area.

## Appendix A:

### Gross-Pitaevskii Equation:

The Gross-Pitaevskii Equation (GPE) describes the ground state of a quantum system of identical bosons using the Hartree-Fock approximation and the pseudopotential interaction model.

In the Hartree-Fock approximation the total wave function  $\Psi$  of the system of  $N$  bosons is taken as a product of single-particle functions  $\psi$ ,

$$\Psi(r_1, r_2, \dots, r_N) = \psi(r_1) \psi(r_2) \dots \psi(r_N), \quad \text{--- (A.1)}$$

where  $r_i$  is the coordinate of the boson number  $i$ .

The pseudopotential model Hamiltonian of the system is given as,

$$H = \sum_{i=1}^N \left( -\frac{\hbar^2}{2m} \frac{\partial^2}{\partial r_i^2} + V(r_i) \right) + \sum_{i < j} \frac{4\pi\hbar^2 a_s}{m} \delta(r_i - r_j), \quad \text{--- (A.2)}$$

where  $m$  is the mass of the boson,  $V$  is the external potential,  $a_s$  is the boson-boson scattering length and  $\delta(r)$  is the Dirac-Delta function.

If the single-particle wave-function satisfies the GPE,

$$\left( -\frac{\hbar^2}{2m} \frac{\partial^2}{\partial r^2} + V(r) + \frac{4\pi\hbar^2 a_s}{m} |\Psi(r)|^2 \right) \Psi(r) = \mu \Psi(r), \quad \text{--- (A.3)}$$

The total wave-function minimizes the expectation value of the model Hamiltonian under normalization condition  $\int d\mathbf{r} |\Psi|^2 = N$ . Here  $\mu$  is the chemical potential. The chemical potential can be found from the condition that the total number of particles is related to the wavefunction by  $\int d\mathbf{r} |\Psi|^2 = N$ .

It is a model equation for the single-particle wave function in a BEC.

The equation has the form of the Schrodinger equation with the addition of an interaction term. The coupling constant,  $U_0$  is proportional to the scattering length  $a_s$  of two interacting bosons:

$$U_0 = \frac{4\pi\hbar^2 a_s}{m}, \text{ where } \hbar \text{ is the Planck's constant and } m \text{ is the mass of the boson.}$$

So equation (A.3) can be written as,

$$\left( -\frac{\hbar^2}{2m} \frac{\partial^2}{\partial r^2} + V(r) + U_0 |\Psi(r)|^2 \right) \Psi(r) = \mu \Psi(r), \quad \text{--- (A.4)}$$

From the time-independent Gross-Pitaevskii equation, we can find the structure of a Bose-Einstein condensate in various external potentials. For example, a harmonic trap.

The time-dependent Gross-Pitaevskii equation is,

$$i\hbar \frac{\partial \Psi(\mathbf{r})}{\partial t} = \left( -\frac{\hbar^2}{2m} \frac{\partial^2}{\partial r^2} + V(\mathbf{r}) + U_0 |\Psi(\mathbf{r})|^2 \right) \Psi(\mathbf{r}), \quad \text{--- (A.5)}$$

From the time-dependent Gross-Pitaevskii equation we can look at the dynamics of the Bose-Einstein condensate. It is used to find the collective modes of trapped gas.

## Appendix B:

### Thomas-Fermi Approximation:

For sufficiently large clouds, an accurate expression for the ground-state energy may be obtained by neglecting the kinetic energy term in the Gross-Pitaevskii equation (GPE). When the number of atoms is large and interactions are repulsive, the ratio of kinetic to potential (or interaction) energy is small. A better approximation for the condensate wave function for large numbers of atoms may be obtained by solving GPE, neglecting the kinetic energy term. Thus from equation (A.4),

$$(V(\mathbf{r}) + U_0 |\Psi(\mathbf{r})|^2) \Psi(\mathbf{r}) = \mu \Psi(\mathbf{r}), \quad \text{--- (B.1)}$$

This has the solution,

$$n(\mathbf{r}) = |\Psi(\mathbf{r})|^2 = (\mu - V(\mathbf{r})) / U_0, \quad \text{--- (B.2)}$$

in the region where the right hand side is positive, while  $\Psi = 0$  outside this region. The boundary of the cloud is therefore is given by,

$$V(\mathbf{r}) = \mu,$$

The physical content of this approximation is that the energy to add a particle at any point in the cloud is the same everywhere. This energy is given by the sum of the external potential  $V(\mathbf{r})$  and an interaction contribution  $n(\mathbf{r})U_0$  which is the chemical potential of a uniform gas having a density equal to the local density  $n(\mathbf{r})$ . Since this approximation is reminiscent of the Thomas-Fermi approximation in the theory of atoms, it is generally referred to by the same name.

In our case, for dark solitons, the interactions are repulsive, so from equation (2.8b), the bulk density for the dark soliton is,

$$n_D = \eta^2 C_2, \quad \text{--- (B.3)}$$

Now according to Equation (2.8b), performing the Thomas-Fermi (TF) approximation by neglecting the kinetic energy term and the inter-species term, the TF density for species 2 is given by,

$$n_2(x) = \frac{\mu - \frac{\lambda_2^2 x^2}{2\kappa}}{b_{22}} = \frac{\mu}{b_{22}} \left(1 - \frac{\lambda_2^2 x^2}{2\kappa\mu}\right), \quad \text{--- (B.4)}$$

Let  $n_2(0) = n_D$ , leads to  $\mu = \eta^2 C_2 b_{22}$ .

Therefore, we have,

$$n_2(x) = n_D \left(1 - \frac{\lambda_2^2 x^2}{2\kappa\eta^2 C_2 b_{22}}\right), \quad \text{--- (B.5)}$$

Thus, we need to multiply the dark soliton amplitude  $\tilde{\Psi}_{2D}$  with  $\sqrt{1 - \frac{\lambda_2^2 x^2}{2\kappa\eta^2 C_2 b_{22}}}$  to get density profile for dark solitons.



## References:

- [1] Bose-Einstein Condensation in Dilute Gases, C.J.Pethik and H.Smith.
- [2] M. H. Anderson, J. R. Ensher, M. R. Matthews, C. E. Wieman, and E. A. Cornell, *Science* **269**, 198 (1995).
- [3] K. B. Davis, M.-O. Mewes, M. R. Andrews, N. J. Van Druten, D. S. Durfee, D. M. Kurn and W. Ketterle, *Phys. Rev. Lett.* **75**, 3969 (1995).
- [4] C. C. Bradley, C. A. Sackett, J. J. Tollett, and R. G. Hulet, *Phys. Rev. Lett.* **75**, 1687 (1995); C. C. Bradley, C. A. Sackett, and R. G. Hulet, *Phys. Rev. Lett.* **78**, 985 (1997).
- [5] P. G. Kevrekidis, D. J. Frantzeskakis and R. Carretero-Gonzalez, ed. *Emergent Nonlinear Phenomena in Bose-Einstein Condensate* (Springer-Verlag, Berlin, 2008).
- [6] O. E. Alon et al., *Phys. Rev. Lett.* **95**, 030405 (2005).
- [7] T. L. Ho and V. B. Shenoy, *Phys. Rev. Lett.* **77**, 3276 (1996).
- [8] B. D. Esry et al., *Phys. Rev. Lett.* **78**, 3594 (1997).
- [9] H. Pu. and N. P. Bigelow, *Phys. Rev. Lett.* **80**, 1130 (1998); *ibid* **80**, 1134 (1998).
- [10] C. J. Myatt et al., *Phys. Rev. Lett.* **78**, 586 (1997).
- [11] G. Modugno et al., *Science* **294**, 1320 (2001).
- [12] D. S. Hall, in *Emergent Nonlinear Phenomena in Bose-Einstein Condensates* (Ref. [5])
- [13] G. Thalhammer et al., *Phys. Rev. Lett.* **100**, 210402 (2008).
- [14] S. B. Papp, J. M. Pino and C. Wieman, *Phys. Rev. Lett.* **101**, 040402 (2008).
- [15] S. Burger et al., *Phys. Rev. Lett.* **83**, 5198 (1999); J. Denschlag et al., *Science* **287**, 97 (2000).
- [16] K. E. Strecker et al., *Nature* **417**, 150 (2002); L. Khaykovich et al., *Science* **296**, 1290 (2002).
- [17] C. Becker et al., *Nature Phys.* **4**, 496 (2008).
- [18] Yu. S. Kivshar and G. P. Agrawal, *Optical Solitons: From Fibers to Photonic Crystals* (Academic Press, San Diego, 2003).

- [19] Soliton, Wikipedia ( <http://en.wikipedia.org/wiki/Soliton>).
- [20] Xunxu Liu, Han Pu, Bo Xiong, W.M. Liu, and Jiangbin Gong, Phys. Rev. A. **79**, 013423 (2009).
- [21] S. V. Manakov, Sov. Phys. JETP **38**, 248 (1974).
- [22] A. P. Sheppard and Y. S. Kivshar, Phys. Rev. E **55**, 4773 (1997).
- [23] Th. Bushch and J. R. Anglin, Phys. Rev. Lett. **87**, 010401 (2001).
- [24] D. J. Kaup and B. A. Malomed, Phys. Rev. A **48**, 599 (1993).
- [25] Weizhu Bao and Hanquan Wang, Journal of Computational Physics **217**, 612 (2006).
- [26] Yanzhi Zhang, Weizhu Bao and Hailiang Li, Physica D **234**, 49 (2007).